



Conductive polymers for thermoelectric power generation

Meetu Bharti^{a,b,*}, Ajay Singh^{a,*}, Soumen Samanta^a, D.K. Aswal^{a,c}

^a Technical Physics Division, Bhabha Atomic Research Centre, Mumbai 400 085, India

^b All India Jat Heroes' Memorial College, Rohtak 124 001, India

^c CSIR National Physical Laboratory, New Delhi 110 012, India

ARTICLE INFO

Article history:

Received 7 March 2017

Received in revised form 12 May 2017

Accepted 18 September 2017

Available online 14 October 2017

Keywords:

Conducting polymers

Organic thermoelectrics

Energy harvesting

Seebeck effect

Thermal conductivity

Thermoelectric power generators

ABSTRACT

In spite of the fact that conducting polymers, during the past decade, have made inroads into various flexible devices including electronics, supercapacitors, sensors, transistors and memories etc. their exploration in the field of thermoelectric power-generation has not yet been significant. This review provides a comprehensive study regarding thermoelectric performance of various conducting polymers depending upon their specific structural and physico-chemical properties. Recent trends in organic thermoelectrics are discussed as: (i) factors affecting thermoelectric performance; (ii) strategies required for improvement of the power factor (due to inherent low thermal conductivity); and (iii) challenges that still lie ahead. A detailed analysis of electrical and thermal transport-mechanisms suggests that various processes such as stretching, controlled doping and addition of inorganic materials/carbon nanostructures, may be applied for enhancement of the thermoelectric figure-of-merit. The attempts are made for highlighting as to how these conducting polymers can be realized into efficient thermoelectric generators by summarizing various reported architectural-designs. These devices have a tremendous potential for tapping low-temperature heat (e.g. body/appliances' heat, geo-thermal/oceanic heat etc.) to power wearable medical sensors and smart electronic devices. Finally, the efforts are put together to familiarize the reader with the big breakthrough that can be created by light-weight, flexible, non-toxic conducting polymers in thermoelectric domain.

© 2017 Elsevier Ltd. All rights reserved.

Contents

| | |
|---|-----|
| 1. Introduction | 271 |
| 2. Basic insight of transport mechanisms in CPs | 273 |
| 2.1. Electrical conductivity | 273 |
| 2.2. Seebeck coefficient | 275 |
| 2.3. Thermal conductivity | 276 |
| 3. Summary of thermoelectric performance of conducting polymers | 277 |
| 3.1. Polyacetylene | 277 |
| 3.2. Polycarbazole and its derivatives | 277 |
| 3.3. Poly-pyrrole and its composites | 282 |
| 3.4. Poly(3-hexylthiophene) (P3HT) and its composites | 283 |
| 3.5. Polyaniline (PANI) and its composites | 283 |

* Corresponding authors at: Technical Physics Division, Bhabha Atomic Research Centre, Mumbai 400 085, India (M. Bharti).

E-mail addresses: meetubharti@yahoo.com (M. Bharti), asb_barcode@yahoo.com (A. Singh).

| | | |
|--------|--|-----|
| 3.6. | Poly(3–4 ethylenedioxythiophene) (PEDOT) and its composites | 284 |
| 4. | Key issues with conducting polymers | 287 |
| 4.1. | Factors influencing thermoelectric properties | 287 |
| 4.1.1. | Polymer structure | 287 |
| 4.1.2. | Polymer concentration | 287 |
| 4.1.3. | Polymer molecular weight and chain length | 288 |
| 4.1.4. | Temperature | 288 |
| 4.1.5. | Humidity | 288 |
| 4.1.6. | Alignment of the polymer chains | 288 |
| 4.2. | Challenges with the organic materials for thermoelectric applications | 289 |
| 4.2.1. | Long term stability | 289 |
| 4.2.2. | Sample preparations and measurement techniques | 290 |
| 4.2.3. | Adherence of films to substrates | 290 |
| 4.2.4. | Good electrical contacts between the organic/inorganic interface at active thermoelectric region and as well as between the polymer and metallic interconnect for device application | 290 |
| 4.3. | Strategies required for optimizing thermoelectric properties in conducting polymers | 291 |
| 4.3.1. | Doping of polymers | 291 |
| 4.3.2. | Polymers - carbon nanotubes blends | 291 |
| 4.3.3. | Organic-Inorganic composites | 292 |
| 4.3.4. | Nanoscaled organic/inorganic materials | 292 |
| 4.3.5. | Energy filtering effect | 293 |
| 4.3.6. | Bilayer/multilayer approach | 293 |
| 4.3.7. | Externally controlled factors such as device structure, electrode potential during electro polymerization, size of counter-ions, technique of polymerization, calibration of oxidation level | 293 |
| 5. | Designing and development of an organic thermoelectric module | 294 |
| 6. | Unrealized potential in the field of organic thermoelectric power-generation | 304 |
| 7. | Conclusion | 308 |
| | Acknowledgement | 308 |
| | References | 308 |

1. Introduction

The energy conversion technologies that are at present in prevalence bring with them the issues of heat emission and pollution resulting in global warming. Therefore, thermoelectric power generation, converting the thermal gradient into useful electrical energy, can better serve the purpose of providing a clean and green option in this arena. The device used for thermoelectric power generation is termed as a Thermoelectric Power Generator (TEG). Its basic prerequisite is the availability of a large number of p-type and n-type thermoelements (having equivalent thermoelectric figure-of-merit (ZT)) alternately connected electrically in series and thermally in parallel to deliver sufficiently high electrical power for operating small electronic devices, electrical motors etc. TEGs offer many advantages such as (i) silent operation as they work without mechanical movement, (ii) long operating life, (iii) green technology since no harmful by-products are formed during operation and (iv) wide use in remote and unattended places where there is less availability of other energy conversion technologies [1–3]. However, these have still not found enough place in commercial applications due to their low conversion efficiency (of typically less than 6%) and high cost [4,5]. Concerted efforts are being made to search for some alternative materials for TEG applications because a majority of them are based on inorganic materials which involve complex high-cost processing techniques, high raw-material cost (making use of less abundant metals such as Te and Ge) and are also toxic and brittle in nature.

Conducting polymers (CPs) have proved their potential in the field of supercapacitors, sensorics, electronic displays, transistors and memory devices etc. for many years and can therefore, bring major breakthroughs in the field of thermoelectrics. Their ability to emerge as free-standing films, ease of patternizing on various types of large-area flexible substrates, compatibility to blend with inorganic materials can surely carry thermoelectricity towards smart technologies and wearable devices. These days, intense research is being focussed on enhancing the thermoelectric (TE) performance of CPs. As a result, many research-groups [3,6–12] have compiled the on-going trends in organic thermoelectrics. The very first review that came as a guiding force for organic thermoelectrics was by Olga et al. and it provided basic concepts of charge-transport along with a few earlier versions of organic thermoelectric generators [7]. The importance of fill-factor (i.e. ratio of the area of active conductive-polymer layer to the total area occupied by the substrate holding it) for device optimization has been shown by Je-Hyeyong [9]. On the other hand Chen et al. [10] suggested the integration of photovoltaic and thermoelectricity for enhancing energy-output. Moreover, the latest two reviews by Muller et al. [11] and Segelman et al. [12] focus on the structural-property association among CPs as the basis of their thermoelectric performance. The significance of these researches apart, the full journey from the initial stage of material synthesis to device development has, however, not been compiled under a single roof as of now. This review provides an exhaustive summary of thermoelectric performance of popular conducting polymers based on their particular molecular design. So far, to the best of our knowledge no article has

placed an emphasis on device designing and fabrication. The present article, therefore, tries to move one step ahead and discusses the realization of highly efficient thermoelectric materials into useful power devices for practical applications. The key issues with CPs such as stability of n-type (electron donor) polymers, adherence to substrates, contact resistances as well as the strategies required for efficient thermoelectrics are also summarized. Many factors determine the efficiency of a TEG which include accessibility of n- and p-type (electron acceptor) organic thermoelectric materials with significant stable figure-of-merit, highly conducting interface between thermoelements/interconnects and effectual heat flow through the device [13]. These aspects for inorganic materials have already been covered in an article [13] by Aswal et al.

Thermoelectric efficiency (η) is directly related to the material characteristic known as dimensionless figure-of-merit (ZT) through the relation:

$$\eta = \frac{T_h - T_c}{T_h} \left[\frac{\sqrt{1 + ZT_{avg}} - 1}{\sqrt{1 + ZT_{avg}} + T_c/T_h} \right] \quad (1)$$

Here T_h and T_c are respective temperatures of hot and cold ends of thermoelectric material and T_{avg} is the average temperature of T_h and T_c . The ZT_{avg} is estimated by integrating all peak ZT s at a particular temperature lying within the specific temperature-range defined from T_c to T_h . While peak ZT of a material, at a particular temperature T , is defined as:

$$ZT = \alpha^2 \sigma T / \kappa \quad (2)$$

Here α is the Seebeck coefficient, σ is the electrical conductivity and κ is the thermal conductivity of material. Thermal conductivity (κ) has two components i.e. contribution from charge-carriers (k_e) and lattice (k_l).

To achieve high figure-of-merit (ZT) and conversion efficiency (η) the following criteria should be followed: (i) Material should exhibit high α to have high voltage output; (ii) high σ to have large short-circuit current and low Joule heating; and (iii) low κ to have a large temperature difference [13–15]. Extremely low κ in case of CPs has already shifted the strategy towards enhancing the power factor rather than lowering κ even in the case of organic/inorganic composites (where the inorganic part can certainly contribute towards enhancement of κ) to have high ZT . Electrical conductivity (σ) depending on charge-carrier density and carrier mobility can be enhanced through doping, but since charge carrier transport takes place in energy levels close to the Fermi level, doping leads to a decrease in the difference between transport and Fermi levels and thus reduces α [14,48]. Therefore, enhanced ZT for high TE efficiency can be realized through optimization of both σ and α without affecting κ by various methods discussed later. However, the structure-property correlation (i.e. influence on α , σ , κ due to anisotropy and loss of solution processability due to various methods of optimization of TE parameters [11]) in the case of CPs needs proper consideration at each and every step of the process from compatible material-synthesis to device fabrication.

As seen from Eq. (1), the efficiency of conversion depends on Carnot efficiency (which depends on temperature difference (ΔT)) and figure-of merit. Also $\Delta T/T$ ratio, being smaller near room-temperature applications, shows that the use of CP-based TEGs can be more practical as compared to the presently existing expensive TE modules in order to harness thermal energy at such temperatures [11,12]. Using Eq. (1) and different values of ZT (i.e. 0.05, 0.1, 0.2, 0.3, 0.5 and 1) the variation of calculated efficiency as a function of hot-end temperature is plotted in Fig. 1. Considering the stability of CPs up to 150 °C and assuming hot-end temperature of 100 °C with cold-end at ambient temperature (~ 27 °C) along with $ZT_{avg} \sim 1$ as depicted in Fig. 1, it can be expected that futuristic organic thermoelectric generators (OTEGs) will exhibit the efficiency of $\sim 4\%$.

Recently, the highest ZT values of 0.42 [72] and 0.20 [91] have been achieved for p- and n-type CPs respectively near room-temperature. It suggests that CPs-based thermoelectric materials hold a very good promise for commercial applica-

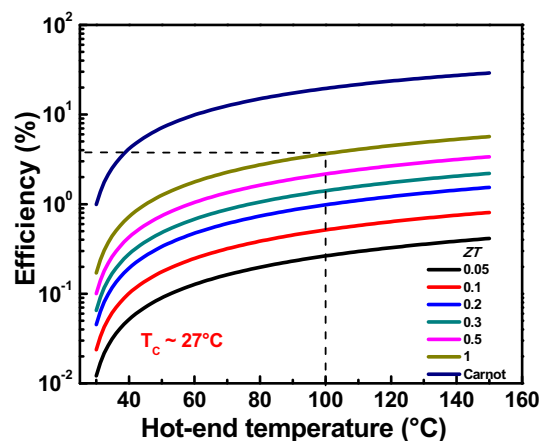


Fig. 1. Variation of efficiency as a function of hot-end temperature calculated by using Eq. (1) and different ZT values (0.05, 0.1, 0.2, 0.3, 0.5, 1) for conducting polymers.

tions in the low temperature heat-recovery programmes. The basic overview of electrical and thermal transport mechanisms in CPs has been given in order to understand and identify the various approaches required to optimize their thermoelectric performances.

2. Basic insight of transport mechanisms in CPs

Understanding the transport mechanism in CPs is essential for basic insight of their thermoelectric properties. Saturated insulating polymers consist of covalently-bonded atoms (similar to Si) with sp^3 hybridized carbons, where the shared electrons are localized in the low energy orbitals of chain molecule, thus resulting in poor electrical conductivity. However, in conjugated polymers, the carbon atoms are sp^2 hybridized. In simple terms, the three electrons from the outer shell of each carbon atom form three “sigma” (σ)-bonds (forming the skeleton of the polymer chain) and one 2p electron, which consequently becomes delocalized in “pi” (π)-orbitals with an electronic density dominant in the plane perpendicular to the σ skeleton. These p_z orbitals of sp^2 hybridized successive carbon atoms, due to overlapping, result in facile movement of the delocalized electrons along the backbone of the polymer [2,7]. In such alternately σ and π -bonded C-atoms, due to Peierls instability (i.e. a consequence of coupling between electronic and elastic properties), the π -band is divided into π - (i.e. filled) and π^* (i.e. empty) bands with an opening of a gap (E_g) in the electronic excitation spectrum [2]. In comparison with the traditional semi-conductor, the bonding orbital (π) corresponds to the valence “band” of the semi-conductor and the anti-bonding orbital (π^*) corresponds to the conduction “band”. This band-like energy distribution among electronic density of states with energy gap (E_g) between Highest Occupied Molecular Orbital (HOMO) and Lowest Unoccupied Molecular Orbital (LUMO) in conjugated parts of a molecule of polymer resembles that of an intrinsic semi-conductor [2,7]. Conjugated polymers due to having poor electrical conductivity in this form indicate that just conjugation is not enough for electrical conductivity. However, electrical conductivity of polymers can be enhanced by doping. But the doping mechanism has its own side-effects due to substantial structure-property relationships of CPs [11] which have been discussed later in Section 4.

2.1. Electrical conductivity

Usually the polymers can be doped by either electro-chemical or chemical methods. Infact regarding the term doping Bredas et al. [22] has well explained that “doping” is a misnomer term in case of polymers. Actually “doping” in case of CPs is a type of redox reaction through which a non-conducting pristine polymer is transformed into an ionic complex made up of a polymeric cation/anion and a counterion which is the reduced/oxidized form of oxidizing/reducing agent [22]. Such types of reactions are much favoured by π -bonded unsaturated polymers having π - electrons that are easy to delocalize without disruption of sigma bonds that are responsible for keeping the polymer intact [22]. Detailed mechanism of doping i.e. creation of charge carriers (be it electrochemical/chemical) includes: (i) Oxidation/reduction of monomer that begins with the removal/acceptance of electron from the π -system of the backbone chain resulting in production of a free radical and a spinless positive/negative charge. The reduced/oxidized dopants transform into negative counterions and neutralize the positive/negative charge introduced in the π - electron system; (ii) The local resonance of the charge (i.e. lattice distortion) and the radical (having spin $\frac{1}{2}$) results in coupling of the charge site with the radical and this coupling is termed as polaron; (iii) This formation of polaron which can be either radical cation or radical anion creates new localized electronic states in the gap, with the lower energy states being occupied by single unpaired electrons; (iv) Removal/addition of an electron from the polaron can further, give rise to new spinless defect known as bipolaron which is a radical ion pair linked with polaronic distortion and can be influenced over three to four monomers depending upon the polymer’s chemical structure [2]. The creation of a bipolaron is thermodynamically more favourable than creation of two distinct polarons and therefore, at higher doping levels there lies higher probability of combination of two polarons to form a bipolaron [22]. Schematic shown in Fig. 2 displays the creation of polaron, bipolaron and bipolaron bands as a function of doping level in case of various CPs. At low doping levels polarons with spin $\frac{1}{2}$ are formed but with increase in doping they recombine to form spinless bipolarons. With further enhancement in doping levels, the bipolaron levels overlap and eventually form continuous bands. As shown in Fig. 2a, band gap between conduction and valence bands also increases because states at both the conduction and valence bands’ edges come forward to create these bipolarons bands/states [22]. This bipolaron model as well as widening of band gap has been well described by Bredas and Street [22] for doped polypyrrole, though similar kind of behaviour has also been observed in case of polythiophenes and polyparaphenylene [22]. However, at very high doping levels in case of many CPs both upper and lower bipolaron bands merge with the conduction and the valence bands respectively (shown in Fig. 2b) to produce partially filled bands similar to metals [7,22]. It should be noted that for a polypyrrole with band gap ~ 3.2 eV, this merging of bipolaron bands can only be made possible with extremely high doping levels i.e. one dopant per every other monomer unit [22]. Whereas polythiophenes with band gap ~ 2.0 eV [22] can readily show the merging of bipolaron bands with conduction and valence bands to produce partially filled states for having electrical conductivities similar to metals.

The conduction mechanism in conjugated polymers with a degenerated ground state such as polyacetylene can be explained by slightly different mechanism [20,21]. In addition to polarons, the solitary wave defects known as solitons exist as charge carriers [22]. The soliton can move along the chain freely by pairing with the adjacent electron. However, solitons

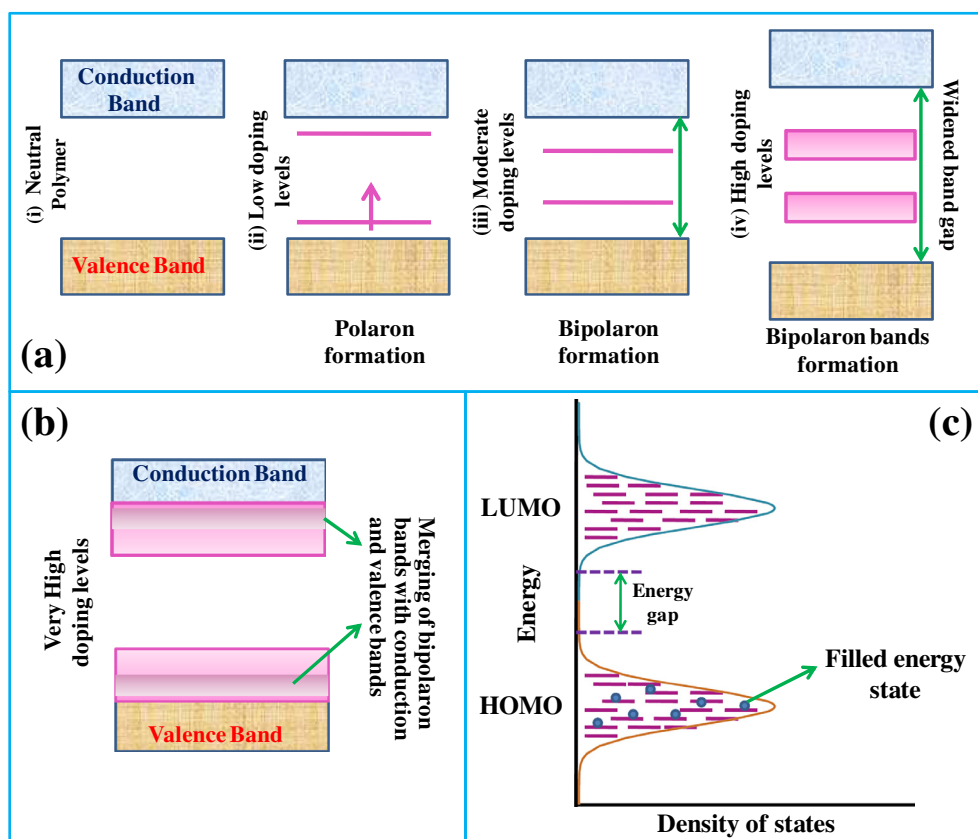


Fig. 2. Schematic showing (a) Formation of polaron, bipolaron and bipolaron bands as a function of doping for CPs; (b) Merging of bipolaron bands with conduction and valence bands at very high doping levels; (c) Gaussian distribution of localized states in HOMO and LUMO orbitals of CPs.

created by doping are more significant than those generated as a result of the bond alternation defects [28] in conduction mechanisms. As a result of doping, the two charges that can form a bipolaron are weakly bound and can easily separate owing to degenerated state of a CP. Since the energy in between these two charges as well as at both of their sides is identical, they resemble like a solitary wave which propagates without any distortion or energy loss [22]. Particularly in case of pristine *trans*-polyacetylene, a soliton is called neutral when there are odd numbers of conjugated carbons which result to an unpaired electron [22,28]. When another unpaired electron is added to it, the charged soliton is called negative whereas removal of this unpaired electron results into a positive soliton. Schematic shown in Fig. 3a displays the formation of two charged solitons on a chain of *trans*-polyacetylene. The formation of a soliton results in the creation of new localized states in the middle of the energy gap (shown in Fig. 3b) which is half-occupied in case of a neutral soliton and empty/doubly occupied in the case of a positive/negative soliton [22]. With increase in doping levels, the charged solitons too interact with each other (like bipolarons shown in Fig. 2a and b) to form a soliton band, which can eventually merge with the valence/conduction band edges and results in metallic conductivity [22,23].

This conductivity/conduction mechanism is affected by the two types of disorders namely energetic and spatial which exist in CPs. Extra charge carriers introduced via doping in the polymer get trapped in the chain due to electrostatic attraction with the counter ions (dopant) [27,86]. The trapping issue is very significant in lightly doped organic materials due to their low dielectric constant (~ 3) and that results in large size of the trap. These traps reduce the charge carrier mobility, however with increase in doping level such charge traps overlap and the energy barrier between them tends to reduce [11]. Such a reduction of energetic disorder in π -orbitals results in huge enhancement of charge carrier mobility [11,20]. Whereas the spatial disorder can affect charge transport at atomic as well as at microscopic scale such as counter ions position, interchain distance, configuration of chains, size of crystalline and amorphous domains, orientation of crystallite etc. Because of spatial disorder, a conjugated polymer cannot have well defined energy bands as shown in Fig. 2a and b. Instead a charge carrier, electron/hole will be localized within conjugated segments with varying energy levels [7]. Usually the distribution of energy levels in HOMO and LUMO bands is approximated by a Gaussian function as shown by the schematic given in Fig. 2c.

The charge transport in CPs takes place by hopping process [2,11,12]. In undoped/lightly doped polymers the polaron hops to the adjacent neutral portion of the polymer chain due to external electric field. On the other hand, in case of doped

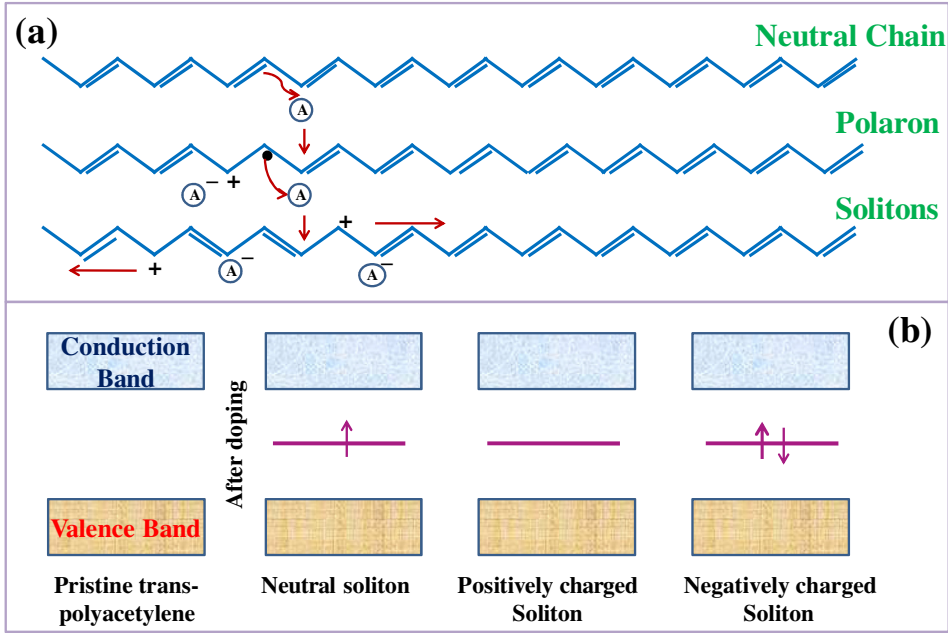


Fig. 3. Schematic showing (a) Formation of two charged solitons on a chain of *trans*-polyacetylene; (b) Band structure of *trans*-polyacetylene consisting of a neutral soliton, a positively charged soliton and a negatively charged soliton.

disordered polymers the charge carriers (pair of polaron and counter ion) hop from one polaronic site to another without any distortion of the polymer chain. The temperature dependence of electrical conductivity in disordered or amorphous CPs is mostly described by variable range hopping (VRH) conduction model assuming constant density of states [11,12]. According to VRH model, temperature dependence of σ can be expressed as:

$$\sigma(T) = \sigma(0) \exp[-(T_0/T)^\lambda] \quad (3)$$

where $\lambda = 1/(d + 1)$, d is dimensionality of hopping process, T_0 is the characteristics Mott temperature and given as:

$$T_0 = \frac{18}{L_c^3 N(E_F) k_B} \quad (4)$$

where L_c is the localization length, $N(E_F)$ is the density of states at the Fermi energy, k_b is the Boltzmann's constant. Whereas, moderately doped and structurally ordered CPs can display insulator to metal transition as a consequence of better chain to chain connectivity [112] with increase of inter-chain localization length. For example, highly doped and highly ordered CPs such as PANI doped with camphor sulfonic acid exhibited metallic temperature dependence with lowering of temperature [7,107].

2.2. Seebeck coefficient

Seebeck coefficient is the ratio of open circuit voltage which is obtained between hot and cold ends of material to the temperature difference between these two ends. Seebeck coefficient can arise from three different contributions namely electronic, phonon and electron-phonon [7,14]. In metallic systems which have large number of free electrons, the electronic contribution to Seebeck coefficient dominates. The migration of thermally excited electrons of the hot-end towards cold-end creates the voltage difference, thus, originates the electronic contribution. In this case Seebeck coefficient is linearly proportional to the temperature [14]. Phonon contribution to Seebeck coefficient known as "Phonon drag" is usually observed at low temperature (<200 K) where phonon mean free path is large [7]. When mean free paths for both the electron and phonon become comparable, electron-phonon scattering becomes significant [7,11]. Highly conducting polymers with good crystalline structure at low temperature may exhibit significant electron-phonon scattering [11,12]. The heavily doped polymers such as polyacetylene, polyaniline, polypyrrole exhibit small positive Seebeck coefficient (<14 $\mu\text{V}/\text{K}$ near room temperature) with linear decrease in its value with temperature [7]. However, deviation from linearity can sometimes be caused due to electron-phonon interactions. In case of lightly doped CPs, the Seebeck coefficient has larger magnitude than heavily doped ones [7,12]. For such CPs, Seebeck coefficient either decreases or increases non-linearly with temperature [7]. Sometimes the non-linear decrease of Seebeck coefficient follows $T^{1/2}$ dependence and can be explained using Mott's variable range hopping transport between localized states [7]. The nearest neighbour hopping within the localized states gives rise to $1/T$ depen-

dence of Seebeck coefficient. Whereas, in case of heavily doped CPs, Seebeck coefficient shows linear dependence with temperature [12,24].

2.3. Thermal conductivity

Unlike inorganic materials, where electronic part of thermal conductivity is coupled with the electrical conductivity, this synergy in CPs is often invalid (Violation of Wiedemann-Franz law) because of stronger charge-lattice coupling. In addition, due to low σ in comparison to that of inorganic solids, the electronic contribution to κ is very small [16,17]. Therefore, in CPs majority of the heat is transported by the phonons (i.e. quantized lattice vibrations) rather than by charge carriers i.e. $\kappa_l > \kappa_e$. And the κ in CPs not only depends on their molecular weight/shape, but also on the difference in their chain structure. Four main structures of polymers (i) Linear polymers, (ii) Branched polymers, (iii) Crosslinked polymers and (iv) Network polymers are shown in Fig. 4a. Polymer chains having so varied structures layout in different fashions to result in amorphous and semi-crystalline polymer structures (Fig. 4b). These different structures lead to anisotropy in thermal conduction and diffusion [18,19]. Such anisotropy is more when the chains are more ordered for a particular CP.

Moreover, this anisotropy exists even for the polymers with an amorphous structure despite being the characteristic of aligned and ordered polymer chains and its existence can be ascribed to the variation in thermal transport mechanism along two different directions [18]. Higher value of in-plane thermal conductivity than its transverse counterpart is attributed to the more efficient transport of thermal energy that occurs due to strong C—C covalent bonding along the polymer chain rather than transfer of thermal energy through weak van der Waals molecular interaction in perpendicular direction [19] (shown in Fig. 5).

Anisotropic thermal conduction can also be introduced in a polymer material due to mechanical deformation experienced by the polymer due to stretching force and deposition of polymer onto a substrate via different modes like spin coating and screen printing. Centrifugal force applied during spin coating aligns the polymer chains in the in-plane direction of the films while in case of curing process volume contraction of the polymer molecules plays the same role of enhancing the orientation. Alignment of higher number of molecules along in-plane direction of films (having thicknesses of few microns order) is the main cause behind anisotropic nature of thermal conductivity exhibited along in-plane and out-of-plane directions [18]. It is interesting to note that for wide variety of CPs, even with a three order of magnitude enhancement of σ there is a minor variation in κ values (i.e. from 0.1 W/m K to 1.0 W/m K). Due to low κ values of CPs, the specific efforts are needed for κ measurement. In addition, during measurements its anisotropic aspect should also be considered [18,19]. When σ increases (≥ 100 S/cm) it can lead to increase in κ_e which becomes equally prominent with κ_l and sometimes exceeds also and demands proper attention while estimation [11]. So far, not many systematic studies are available on thermal conductivity of CPs. Depending on the crystallinity of CPs temperature dependence of their κ may vary. For example in case of low crystalline CPs, thermal conductivity increases monotonically up to their glass transition temperature [11]. On the other hand for highly crystalline polymers, thermal conductivity is high and it increases with temperature up to 100 K and subsequently drops [11]. Occasional rise of thermal conductivity at low temperatures can be attributed to the suppression of phonon-phonon scattering which results in the enhancement of phonon mean free path [11].

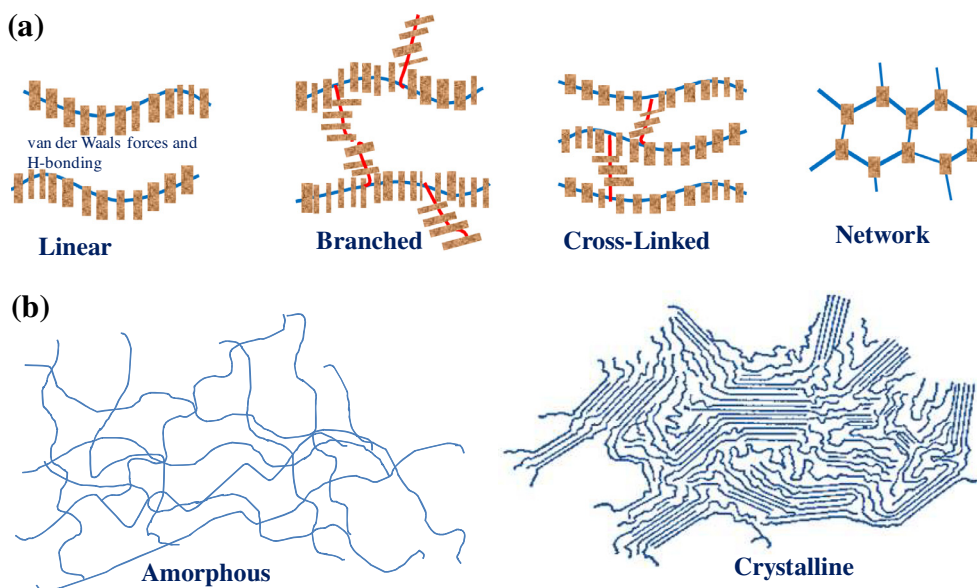


Fig. 4. Schematic showing (a) molecular structures of polymers; (b) alignment of polymer chains showing Amorphous and Crystalline (usually semi-crystalline) structures.

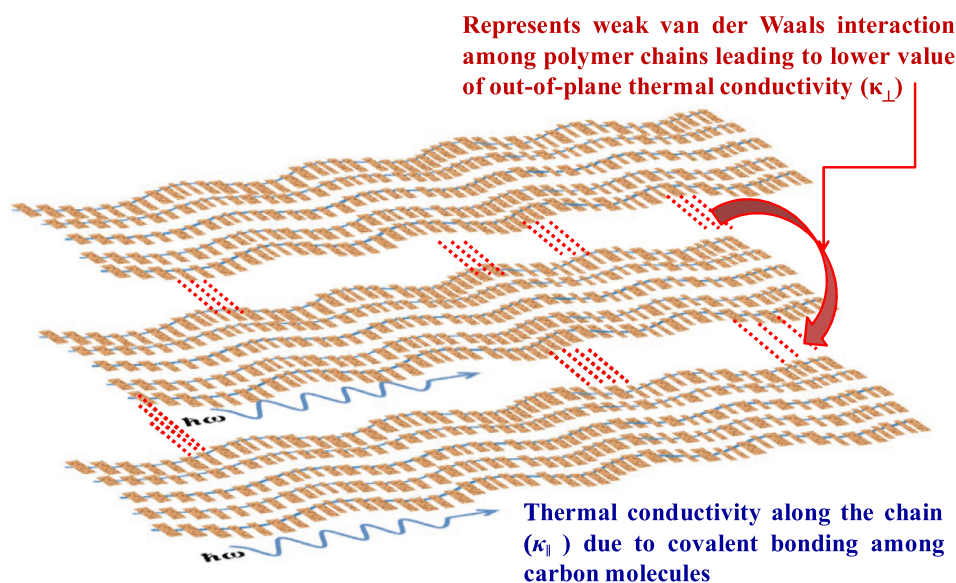


Fig. 5. Schematic depicting the anisotropic thermal conduction in CPs.

3. Summary of thermoelectric performance of conducting polymers

To realize the ideas of smart technology and wearable electronics, thermoelectric research on conducting polymers should be converged accordingly. High average figure-of-merit (ZT_{avg}), as a prerequisite for highly efficient devices, needs to be achieved through optimization of α , σ and κ . Less stability of CPs at higher temperatures restricts the limit of maximum operational temperature up to ≤ 150 °C. However, maximum ZT of 0.42 [72] obtained in case of PEDOT:PSS films at room temperature can surely motivate towards organic TEGs, because this ZT is near to the value (~ 1), achieved in case of the best conventional inorganic material so far (Bi_2Te_3 [11,13]). These Bi_2Te_3 based compounds though, have exhibited the highest $ZT \sim 1.86$ (at 47 °C) due to κ achieved as low as ~ 0.7 W/m K, but still this κ is nearly 4–5 times higher as compared to CPs [13,24]. Thus, CPs have removed an extra burden of taking concern of κ (which is already low [8]) while decoupling the essential three parameters of thermoelectrics to achieve high ZT . Many studies [48,81] have been focussed on hybrid materials to combine the features of both the organic and inorganic realms. Structural manipulation has also been emphasized (through stretching [112] as well as by multilayer approach in case of polymer composites [113] of PEDOT:PSS and PANI) as a tool to bring improvement in TE parameters and this can be extended to other polymer hybrid systems [113]. Binding agents [77] and fillers also [80], when added to the polymer matrix brought dramatic improvements in thermoelectric properties by facilitating the charge transport [112] through better chains connectivity. The Table 1 given here extensively investigates and compares the thermoelectric performance of many CPs so that strategies leading to commercial organic TEGs can be identified as well as devised.

3.1. Polyacetylene

Polyacetylene (PA) when doped with halogens chlorine, bromine or iodine and with arsenic pentafluoride (AsF_5) displayed tremendous enhancements in σ up to eleven orders of magnitude (given in Table 1) i.e. covering a full range from insulator to semiconductor to metal [23]. For instance, $\sigma \sim 20,000$ S/cm was observed in iodine doped free-standing PA films at room temperature and even when the temperature and pressure were 0.48 K and 10 kbar respectively, σ retained to 9000 S/cm [25]. Stretching also caused two times enhancement in conductivity i.e. from 3000 to 6000 S/cm in Iodine doped films [26]. Electrical conductivity and Seebeck coefficient were also studied for PA doped with other metal halides like FeCl_3 , ZrCl_4 , NbCl_5 and highest $\sigma \sim 28,500$ S/cm was achieved in case of FeCl_3 doped PA [28]. Despite being the first polymer showing huge $\sigma \sim 44,247$ S/cm resulting in the highest power factor of 9.9×10^{-4} after doping [29], instability of PA in air and insolubility in solvents discourage its use for practical thermoelectric applications. If tools of polymer science can seek some remedial measures, PA can be a good option for thermoelectric applications. Development of other relatively more stable polymers with due course of time has shifted the interest of the researchers towards many other polymers.

3.2. Polycarbazole and its derivatives

Interesting electroactive and photo-physical properties of Polycarbazoles (PCz) and advancements in synthesis techniques have encouraged their use as electrochromic devices, electronic nanodevices, electrochemical transistors, micro-

Table 1
Electrical and thermal transport properties of various conducting polymers.

| Polymer | Dopant | Conduction Type | σ (S/cm) | α (μ V/K) | κ (W/m K) | PF (W/m K ²) | ZT | Ref. |
|--|--------------------------------------|-----------------|-----------------|-----------------------|------------------|--|------------------------------------|---------|
| Polyacetylene (PA) | Iodine | p | 20,000 | – | – | – | – | [25,26] |
| PA | Iodine | p | 7000 | 17 | – | 2×10^{-4} | – | [26] |
| PA | MoCl ₅ | p | 9580 | 11.4 | – | 1.2×10^{-4} | – | [27] |
| PA | Iodine | p | 18,400 | – | – | – | – | [28] |
| PA | FeCl ₃ | p | 28,500 | – | – | – | – | [28] |
| PA | ZrCl ₅ | p | 4990 | – | – | – | – | [28] |
| PA | MoCl ₅ | p | 6400 | – | – | – | – | [28] |
| PBPMV | Iodine | p | 350 | – | – | – | – | [28] |
| PA | Iodine | p | 44,247 | 15 | – | 9.9×10^{-4} | – | [29] |
| PA | Iodine | p | 7490 (RT) | 19 | – | 2.4×10^{-4} | – | [30] |
| PA | FeCl ₃ | p | 10,200 (RT) | 9 | – | 8.3×10^{-5} | – | [30] |
| Polycarbazole (PCz) | FeCl ₃ | p | 160 | 70 | – | 19×10^{-6} | – | [35] |
| Polypyrrole (PPy) | Benzene-sulphonate | p | 120 | 5 | – | 0.3×10^{-6} (RT) | – | [40] |
| PPy | ClO ₄ ⁻ | p | 120 | 10 | – | 1.2×10^{-6} (RT) | – | [40] |
| PPy | BF ₄ ⁻ | p | 126 | 6 | – | 0.45×10^{-6} (RT) | – | [41] |
| PPy | <i>p</i> -toluene sulphonate (PPpTS) | p | 26 | 5 | – | 0.09×10^{-6} (200 K) | – | [41] |
| PPy | PPpTS | p | 27.58 | 20.02 | – | 1.1×10^{-6} | – | [42] |
| PPy | PF ₆ ⁻ | p | 150 | 7.14 | – | 0.7×10^{-6} | – | [43] |
| PPy | – | p | 9.8 | 17.5 | 0.17 | 4.1×10^{-7} | 7.84×10^{-4} (370 K) | [44] |
| PPy | – | p | 15 | 51 | 0.17 ± 0.02 | 3.9×10^{-6} | 6.8×10^{-3} (300 K) | [45] |
| PPy/rGO composite | – | p | 75.1 ± 6.6 | 33.8 ± 0.3 | – | $8.57 \pm 0.76 \times 10^{-6}$ | – | [47] |
| P3HT/Bi ₂ Te ₃ nanocomposite | FeCl ₃ | p | 17 | 100 | 0.86 | 13.6×10^{-6} | – | [48] |
| P3HT | NOPF ₆ | p | 1 | 25 | – | 0.14×10^{-6} | – | [50] |
| P3HT | Fetf | p | 75 | 50 | 0.2 | 20×10^{-6} | 0.04 (340 K) | [51] |
| P3HT/SW-CNT composites | FeCl ₃ | p | 8 ± 2 | 29 | 0.5 | $95 \pm 12 \times 10^{-6}$ | 0.015 ± 0.004 (RT) | [52] |
| P3HT/MW-CNT composites | – | p | 24 | 12 | 0.16 ± 0.04 | $0.2 \pm 0.1 \times 10^{-6}$ | $(2 \pm 1) \times 10^{-5}$ (RT) | [52] |
| P3HT/SW-CNT composites | – | p | 275 | 32 | 0.13 ± 0.03 | $18 \pm 4 \times 10^{-6}$ | $(7 \pm 2) \times 10^{-4}$ (RT) | [52] |
| P3HT/SW-CNT composites (60% wt) and 4 mg/mL as solid concentration of inks (wire-bar coated) | – | p | 524 ± 56 | 40.3 ± 1.5 | 0.38 | $86.6 \pm 16.2 \times 10^{-6}$ (RT) | – | [53] |
| P3HT/SW-CNT composites (60% wt) and 4 mg/mL as solid concentration of inks (drop casted) | – | p | 383 ± 47 | 32.7 ± 3.8 | – | $41.7 \pm 12.5 \times 10^{-6}$ (RT) | – | [53] |
| P3HT/SW-CNT composites with ink conc. 2 mg/ml (wire-bar coated) | SW-CNT (60 wtn%) | p | 501 ± 32 | 37.5 ± 1.1 | – | $(71.8 \pm 5.2) \times 10^{-6}$ | – | [53] |
| P3HT/SW-CNT composites with ink conc. 2 mg/ml (wire-bar coated) | SW-CNT (30 wt%) | p | 24.8 ± 9.9 | 60.7 ± 2.4 | – | $(8.99 \pm 3.16) \times 10^{-6}$ | – | [53] |
| P3HT | AgClO ₄ | p | 18.3 ± 1.5 | 61.1 ± 2.0 | 0.80 | $6.84 \pm 0.64 \times 10^{-6}$ | 0.0026 (RT) | [54] |
| P3HT | PCBM (30%) | p | – | – | 0.212 ± 0.02 | 34.8×10^{-6} | 0.5 (420 K) | [55] |
| PCBM | P3HT (30%) | n | – | – | – | – | – | – |
| P3OT/Carbon fibre composites | – | p | 3.8 | 136 | – | 7.05×10^{-6} | – | [56] |
| Polyaniline/Graphene composites (50 wt%) | HCl | p | 123 | 33.8 | 3.3 | 14×10^{-6} | – | [57] |
| Polyaniline/Au nanoparticles (PANI) | – | p | 330 | 15 | – | – | – | [59] |

Table 1 (continued)

| Polymer | Dopant | Conduction Type | σ (S/cm) | α (μ V/K) | κ (W/m K) | PF (W/m K ²) | ZT | Ref. |
|-------------------------------|---|-----------------|------------------------------|---------------------------|---|--|--|------|
| Polyaniline | CSA (0.1 M) | p | 5.4×10^{-4} (300 K) | 21 (300 K) | 0.5–0.7 (300 K) | 1.1×10^{-2} (40 K) | 0.77 (45 K) | [61] |
| | | | | 0.58×10^6 (40 K) | | | 2.17 (0.2 M & 17 K) | |
| Polyaniline | Protonic Acid (HCl) | p | 0.03 | 35.7 (RT) | – | – | – | [62] |
| Polyaniline | Protonic Acid (HCl) | n | 32 | –1.1 (RT) | – | – | – | [62] |
| Polyaniline | Iodine | p | 10^{-2} | 55 (RT) | – | – | – | [63] |
| PEDOT | Fe(III) tosylate-pyridine | p | 4500 | – | – | – | – | [65] |
| PEDOT | FeCl ₃ | p | 2000 | – | – | – | – | [65] |
| PEDOT:PSS | H ₂ SO ₄ | p | 3065 | – | – | – | – | [66] |
| PEDOT:PSS | H ₂ SO ₄ | p | 4380 | – | – | – | – | [67] |
| PEDOT single crystal nanowire | FeCl ₃ | p | 8797 | – | – | – | – | [68] |
| PEDOT | ClO ₄ | p | 753 | 9 | 0.35 ± 0.02 | – | – | [69] |
| PEDOT | ClO ₄ (Hydrazine treated for 25 s) | p | 230 | 35 | 0.35 ± 0.02 | 41×10^{-6} (hydrazine treatment for 11 s) | – | [69] |
| PEDOT | PF ₆ | p | 1000 | 11 | 0.22 ± 0.02 | – | – | [69] |
| PEDOT | PF ₆ (Hydrazine treated for 25 s) | p | 312 | 34 | 0.22 ± 0.02 | 60×10^{-6} (hydrazine treatment for 11 s) | – | [69] |
| PEDOT | BTFMSI | p | 2074 | 14 | 0.19 ± 0.02 | – | – | [69] |
| PEDOT | BTFMSI (Hydrazine treated for 25 s) | p | 708 | 42 | 0.19 ± 0.02 | 147×10^{-6} (5 s) | 0.22 (RT) | [69] |
| PEDOT (Pure) | – | p | 123 | 24 | – | 7.15×10^{-6} | 1.0×10^{-2} (323 K) | [59] |
| PEDOT/Au NPs | DT | p | 241 | 22 | – | 11.68×10^{-6} | 1.63×10^{-2} (323 K) | [59] |
| PEDOT/Au NPs | TSH | p | 104 | 21 | – | 4.48×10^{-6} | 0.62×10^{-2} (323 K) | [59] |
| PEDOT:PSS (PH750) | DMSO 5% | p | 570 | 13.5 ± 1.0 | 0.34 | $10.4 \pm 2.1 \times 10^{-6}$ | 9.2×10^{-3} (RT) | [70] |
| PEDOT:PSS (PH500) | DMSO 5% | p | 330 | 14.6 ± 1.0 | 0.32 | $7.0 \pm 1.0 \times 10^{-6}$ | 6.6×10^{-3} (RT) | [70] |
| PEDOT | Tos | p | 300 | 40 | 0.37 | 38×10^{-6} | 0.25 (RT) | [71] |
| PEDOT:PSS | DMSO Mixed | p | 620 ± 37 | 33.4 ± 2.2 | 0.30 (κ_{\perp}) 0.42 (κ_{\parallel}) | 69×10^{-6} | – | [72] |
| PEDOT:PSS | DMSO Mixed and EG post treated | p | 880 | 73 | 0.22 (κ_{\perp}) 0.31 (κ_{\parallel}) | 469×10^{-6} | 0.42 (RT) (computed using κ_{\parallel}) | [72] |
| PEDOT:PSS | EG Mixed | p | 639 ± 21 | 27.3 ± 1.9 | 0.32 (κ_{\perp}) 0.52 (κ_{\parallel}) | 47.6×10^{-6} | – | [72] |
| PEDOT:PSS | EG Mixed and EG post treated | p | 885 | 63 | 0.23 (κ_{\perp}) 0.37 (κ_{\parallel}) | 351×10^{-6} | 0.28 (RT) (computed using κ_{\parallel}) | [72] |
| PEDOT:PSS | – | p | 1.53 | 10.3 | – | 0.016×10^{-6} | – | [73] |
| EDOT:PSS | Sorbitol | p | 722.06 | 8.5–10.0 | – | 7.26×10^{-6} | – | [73] |
| PEDOT:PSS | Sorbitol + TDAE | p | 722.06 | 24.78–27.47 | 0.17–0.52 | 22.28×10^{-6} | 0.013–0.039 (RT) | [73] |
| PEDOT:PSS | DES | p | 620.6 | 29.1 | 0.17 | 24.08×10^{-6} | 0.042 (300 K) | [74] |

(continued on next page)

Table 1 (continued)

| Polymer | Dopant | Conduction Type | σ (S/cm) | α (μ V/K) | κ (W/m K) | PF (W/m K ²) | ZT | Ref. |
|---|--|-----------------|---------------------|-----------------------|------------------|-------------------------------|--------------------------------------|------|
| PEDOT:PSS | Formic-acid | p | 1900 | 20.6 | 0.2 | 80.6×10^{-6} | 0.32 (RT) | [75] |
| PEDOT:PSS | EG | p | 640 | 21.4 | 0.18 | 29.3×10^{-6} | 0.13 (RT) | [75] |
| PEDOT:PSS | Methanol | p | 1300 | 21.1 | 0.19 | 58×10^{-6} | 0.25 (RT) | [75] |
| PEDOT | Tos-PPP (NaBH ₄ /DMSO) | p | 5.7 | 143.5 | 0.451 | 98.1×10^{-6} | 0.064 (RT) 0.155 (385 K) | [76] |
| Copolymer latex containing vinyl acetate and ethylene/CNT composites | Stabilizing agent | p | 400 | 25 | 0.4 | 25×10^{-6} | 0.02 (RT) | [77] |
| PEDOT:PSS/r GO composites (GO 3 wt%) | HI as reducing agent | p | 1160 | 12.5 | 0.3 | 32.6×10^{-6} | 0.03 (RT) | [78] |
| PEDOT | Spin coating + LLP | p | 380.7 \pm 33.5 | 14.7 \pm 0.1 | – | $8.3 \pm 0.7 \times 10^{-6}$ | – | [79] |
| PEDOT/rGO (rGO 17 wt%) | Spin coating + LLP | p | 516.0 \pm 4.3 | 16.5 | – | $14.1 \pm 0.3 \times 10^{-6}$ | – | [79] |
| PEDOT | (Spin coating) + VPP | p | 285.0 \pm 15.6 | 19.3 \pm 0.7 | – | $10.6 \pm 0.6 \times 10^{-6}$ | – | [79] |
| PEDOT/rGO (rGO 17 wt%) | (Spin coating)+ VPP | p | 398.3 \pm 28.5 | 18.9 \pm 0.4 | – | $14.2 \pm 1.0 \times 10^{-6}$ | – | [79] |
| PEDOT | In situ Poly + EG | p | 96.3 \pm 27.0 | 11.52 \pm 0.92 | – | $1.3 \pm 0.3 \times 10^{-6}$ | – | [79] |
| PEDOT/rGO (rGO 17 wt%) | In situ Poly + EG | p | 152.3 \pm 33.5 | 30.47 \pm 4.44 | – | $14.1 \pm 3.1 \times 10^{-6}$ | – | [79] |
| PEDOT:PSS/rGO:C ₆₀ | Nano-hybrid i.e. two phase fillers (21 wt%) and C ₆₀ :rGO = 3:7 | p | 630 | 22.9 | 0.2 | 32.4×10^{-6} | 6.7×10^{-2} (300 K) | [80] |
| PEDOT/Paper | – | p | 0.2 | 30.6 | 0.156 | – | – | [81] |
| PEDOT/Paper | EG treated | p | 54.1 (30%) | 25.4 (5%) | 0.164 (5%) | 3.0×10^{-6} | 5.5×10^{-3} (30% EG, 300 K) | [81] |
| PEDOT/Paper | DMSO treated | p | 56.9 (30%) | 26.7 (5%) | 0.160 (5%) | – | – | [81] |
| PEDOT (Clevios PH 1000) | DMSO (5%) | p | 945 | 22.2 | – | 46.57×10^{-6} | – | [82] |
| PEDOT (Clevios FET) | – | p | 320 | 30.3 | – | 29.39×10^{-6} | – | [82] |
| PEDOT Clevios PH1000/p-type Bi ₂ Te ₃ (10% volume of PEDOT) | HCl Rinsing of Bi ₂ Te ₃ | p | 59 | 149 | – | 131×10^{-6} | – | [82] |
| PEDOT Clevios PH1000/n-type Bi ₂ Te ₃ (10% volume of PEDOT) | HCl Rinsing of Bi ₂ Te ₃ | n | 58 | –125 | – | 91×10^{-6} | – | [82] |
| PEDOT Clevios FET/p-type Bi ₂ Te ₃ (30% volume of PEDOT) | HCl Rinsing of Bi ₂ Te ₃ | p | 65 | 110 | – | 70×10^{-6} | – | [82] |
| PEDOT Clevios FET/n-type Bi ₂ Te ₃ (30% volume of PEDOT) | HCl Rinsing of Bi ₂ Te ₃ | n | 60 | –80 | – | 40×10^{-6} | – | [82] |
| PEDOT:PSS/Te nano-composite | – | p | 19.3 \pm 2.3 | 163 \pm 4 | 0.22–0.30 | 70.9×10^{-6} | 0.1 (RT) | [83] |
| PEDOT:PSS/Sb ₂ Te ₃ composites | – | p | 130–110 (300–523 K) | 175 (523 K) | 0.15 (300–523 K) | – | 1.18 (523 K) | [84] |
| Bi ₂ Te ₃ /PEDOT:PSS/Bi ₂ Te ₃ composites | Electro-deposition on PEDOT: PSS electrode | p | 403.5 | 15.3–15.7 | 0.169–0.179 | – | 0.0172 (RT) | [85] |
| P(MeOPV-co-PV) | 4.4-fold stretched | p | 183.5 | 43.5 | – | 30×10^{-6} (313 K) | – | [88] |
| TTF-TCNQ/PVC | – | n | – | –48 | – | – | – | [89] |
| BEDT-TTF-TCNQ | – | p | – | 47.5 | – | – | – | [89] |
| Graphite-PVC Blends | – | p | – | 44 | – | – | – | [89] |
| P3HT/Te nanowire composite | – | p | – | 285 | – | – | – | [90] |
| Poly[Na _x (Ni-ett)] | – | n | 40 | –75 | 0.2 | 23×10^{-6} | 0.042 (300 K) 0.1 (440 K) | [91] |

Table 1 (continued)

| Polymer | Dopant | Conduction Type | σ (S/cm) | α (μ V/K) | κ (W/m K) | PF (W/m K ²) | ZT | Ref. |
|---|--|-----------------|-----------------|-------------------------------|-------------------------------------|--------------------------------|---------------------------------|-------|
| Poly[K _x (Ni-ett)] | – | n | 44 | –121.6 (RT) –151.7 (440 K) | 0.2 | 66×10^{-6} (300 K) | – 0.2 (440 K) | [91] |
| Poly[Cu _x (Cu-ett)] | – | p | 9.5 | 83 | 0.35 | 6.5×10^{-6} | 0.014 (380 K) | [91] |
| Poly[Na _x (Cu-ett)] | – | p | 0.2 | 79 | – | 0.12×10^{-6} | – | [91] |
| PP-PEDOT (SCP method & Applied potential \sim 0.5 V) | pristine | p | 1355 | 79.8 | 0.37 from report [66] | 862.9×10^{-6} | – | [93] |
| PP-PEDOT (SCP method & Applied potential \sim 0.1 V) | pristine | p | – | – | 0.37 from report [66] | 1270×10^{-6} | 1.02 (RT) | [93] |
| PEDOT/paper composite | – | p | 770 (298 K) | 18 | 0.42–0.52 from report [67] | 25×10^{-6} | 0.01 | [94] |
| PEDOT/paper composite | – | p | 550 (473 K) | 25 | 0.42–0.52 from report [67] | 34×10^{-6} | – | [94] |
| Poly[Cu _x (Cu-ett)] | – | p | 42.45 | 57.1 | – | 13.86×10^{-6} (300 K) | – | [95] |
| Poly[Cu _x (Cu-ett)]/PVDF/DMSO [mass ratio (2:1)] | – | p | 5.14 | 41.0 | – | 0.86×10^{-6} (300 K) | – | [95] |
| Poly[K _x (Ni-ett)] | – | n | 8.31 | –67.4 | – | 3.71×10^{-6} (300 K) | – | [95] |
| Poly[K _x (Ni-ett)]/PVDF/NMP (2:1) | – | n | 2.12 | –44.9 | – | 0.43×10^{-6} (300 K) | – | [95] |
| PEDOT:PSS/Bi ₂ Te ₃ (n-type) | – | n | 73 ± 0.04 | –137.8 \pm 2.8 | 0.25 ± 0.01 | – | 0.16 ± 0.01 | [96] |
| PEDOT:PSS/Sb ₂ Te ₃ (p-type) | – | p | 341 ± 0.15 | 92.6 ± 1.2 | 0.44 ± 0.01 | – | 0.20 ± 0.02 | [96] |
| PEDOT coated Fabric | – | p | 1.4 | 15.8 | 0.12 | – | 0.5 (300 K) | [97] |
| PVDF/Bi ₂ Se ₃ composites | – | n | 49 | –90 | 0.29 | 40.1×10^{-6} | 0.04 (290 K) | [98] |
| PFDF/Cu _{0.1} Bi ₂ Se ₃ composites | – | n | 146 | –84 | 0.32 | 103.2×10^{-6} | 0.10 (290 K) | [98] |
| PVDF/Te nanorods composites | – | p | 5.5 | 288 | – | 45.8×10^{-6} (300 K) | – | [99] |
| PEDOT:PSS/non-woven fabric composite | – | p | 13.59 | 18 | 0.10 | 0.44×10^{-6} | 0.0013 (in \perp dir) (295 K) | [101] |
| PEDOT:PSS/Te composites (70 wt%) | – | p | 650 | 26 | 0.197–0.218 | 51.4×10^{-6} | 0.076 (292 K) | [102] |
| PEDOT:PSS | H ₂ SO ₄ treated | p | 4839 | 10.35 | 0.20 | 51.85×10^{-6} | 0.08 (300 K) | [103] |
| PEDOT:PSS/Te composites | H ₂ SO ₄ treated | p | 214.86 | 114.97 | 0.22 | 284×10^{-6} | 0.39 (300 K) | [103] |
| PEDOT:PSS/PANI composites | – | p | 1585 | 17.5 | 0.24 (assuming for bulk PEDOT: PSS) | 49×10^{-6} | 0.08 | [113] |

cavity and electrochemical sensors. Solubility of highly conjugated 2,7-carbazole-based polymers in chloroform also drew attention for further investigation by making them deposit on various substrates and electrodes [31]. Good thermoelectric performance in case of PCz is well expected due to their highly polarized properties indicating well-ordered molecular structures which lead to intermolecular interactions such as heteroatom contacts or π - π interactions [34]. It was found that the oxidation of nitrogen atoms prior to backbone chain caused strong localization of charge in case of poly(2,7-carbazole) derivatives, thus making favourable for generation of large Seebeck voltages. But this charge carrier pinning may also lead to counter effect on conductivity [34]. As a result, introduction of vinylene unit (to form poly(2,7-carbazolylenevinylene) derivatives) can be done to enhance σ without reducing α . Also enhancement in solubility of N-substituted poly(2,7-carbazolylenevinylene)s can be obtained by adding alkyl substituents at the 3-,6-positions of the carbazole unit, thus making the polymer soluble in chloroform and tetrahydrofuran to be drop-casted for fabricating flexible films. The optimized doping resulted in maximum power factor of $7.5 \times 10^{-2} \mu\text{W}/\text{m K}^2$ [32]. Similarly introduction of alkyl side chains on the carbazole cycle and different side chains (alkyl or benzoyl) on the nitrogen atom of the backbone exhibited highest power factor of $10^{-1} \mu\text{W}/\text{m K}^2$ for copolymers consisting of thiophene units alternating with carbazole or indolocarbazole and having linkages in the positions meta to the nitrogen atom. The study reports the fabrication of ladder type oligomers and polymers derived from diindolocarbazoles and indolo-carbazoles which had high charge mobility and thermal stability because of their very rigid backbone. The introduction of different flexible side chains was meant to improve the solubility, whereas the benzoyl substituents were introduced to enhance the conductivity. At room temperature, assuming $\kappa \sim 0.1 \text{ W}/\text{m K}$ the power factor of $1.5 \times 10^{-1} \mu\text{W}/\text{m K}^2$ led to $ZT \sim 3 \times 10^{-4}$ because highly conductive moieties like bithiophene when introduced as co-monomer units, facilitated the doping process along with improvement in the organizational structure of the polymeric films [33]. Infact PCz demonstrated much earlier that how structure-property association can be manipulated to alter the TE properties in CPs. Also increase in mobility had already been reported with the introduction of benzothiadiazole unit in the backbone of poly(2,7-carbazole-alt-bithiophene) [34], so recently, while investigating for thermoelectric properties, FeCl_3 doped benzothiadiazole-containing molecules (PCDTBT) exhibited power factor of $19 \mu\text{W}/\text{m K}^2$ (shown in Fig. 6a and which is 130 times higher than $1.5 \times 10^{-1} \mu\text{W}/\text{m K}^2$ observed in case of poly(2,7-carbazolylenevinylene) [33]) and σ up to 500 S/cm and a relatively high $\alpha \sim 70 \mu\text{V}/\text{K}$. This can be considered as the best thermoelectric performance reported so far in case of carbazole-based copolymers. Moreover, after an initial decrease within the first few hours, the σ of PCDTBT reached a saturation value of $\sim 120 \text{ S}/\text{cm}$ while α showed a small increase, both of which ensured a relatively stable power factor ≈ 17 – $18 \mu\text{W}/\text{m K}^2$ in presence of air as well as argon environment (Fig. 6b) [35].

Since poly(2,7-carbazole), poly(indolo[3,2-*b*]carbazole) and polydiin-dolocarbazole derivatives exhibit good Seebeck coefficients, addition of substituent functional groups can be used as a methodology for enhancing electrical conductivity to improve their over-all thermoelectric performance.

3.3. Poly-pyrrole and its composites

Polypyrrole (PPy) is termed as quasi uni-dimensional polymer due to existence of cross linking and chain hopping [36]. Apart from the advantageous properties such as excellent environmental stability, bio-compatibility and good conductivity; the ability to attune in form of mechanically stable flexible films, makes PPy a good choice for thermoelectric applications. Many studies [37,38] have reported a number of ways to fabricate flexible conducting PPy films. Films grown by means of chemical or photo chemical polymerization exhibited high $\sigma \sim 2000 \text{ S}/\text{cm}$ [38] and have found their applications in gas-sensing [39]. However, poor adhesion of PPy layers to substrates and non-uniformity in thickness and morphology over large-area substrates restrict their use in thermoelectric applications. Buildout of free-standing films instead and use of intermediate silane or diazonium coupling agents can solve the problem of poor adhesion up to certain extent [39]. Recently Wu et al. investigated the thermoelectric properties of PPy films in the temperature range 290–370 K. They observed the

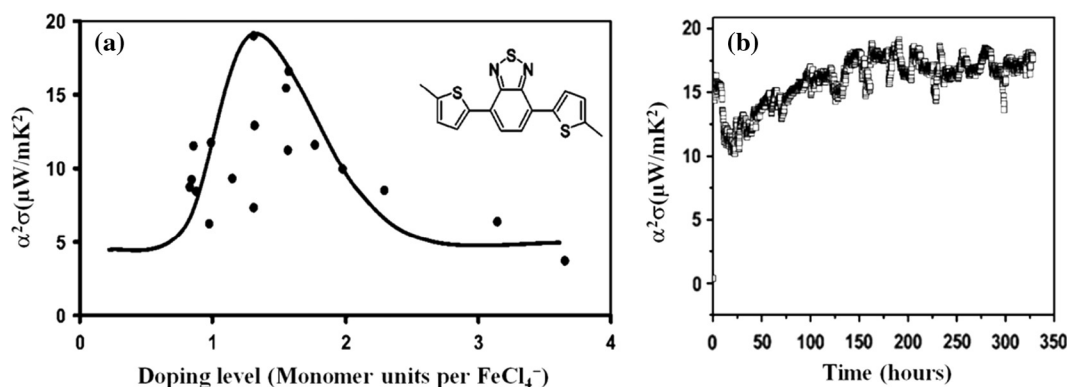


Fig. 6. (a) Power factor for FeCl_3 -doped PCDTBT films as a function of the doping level; (b) Stability study of the power factor of doped PCDTBT. Reproduced with the permission from Ref. [35].

power factor $\sim 4.1 \times 10^{-7}$ W/m K² that resulted in high *ZT* value of $\sim 7.84 \times 10^{-4}$ at 370 K [44]. While electro-polymerized free-standing PPy films exhibited power factor of $\sim 3.9 \mu\text{W/m K}^2$ and *ZT* was calculated as 6.8×10^{-3} [45]. To the best of our knowledge, these are the highest values of $\alpha^2\sigma$ and *ZT* reported so far, for pure PPy films [45]. Following the recent trends of research on polymer composites, PPy composites with multi-walled carbon nanotubes (MWCNT, content ranging from 0 to 20 wt% [46]) were prepared by chemical polymerization method using MWCNT as hard templates with *p*-toluenesulfonic acid (TSA) as a dopant and iron chloride (FeCl₃) as an oxidant. The power factor of the composite samples increased with the MWCNT content and the maximum power factor $\sim 2.08 \mu\text{W/m K}^2$ was approximately 26 times higher than that of pure PPy [46]. However recently, much higher value of power factor has been obtained by adopting a new design strategy, in which nanocomposites having 3D interconnected architecture (i.e. bulk samples consisting 2D reduced Graphene Oxide (rGO) nanolayers sandwiched by 1D PPy nanowires) were fabricated. With rGO:PPy ratio of 50 wt%, power factor for nanocomposite reached $8.56 \mu\text{W/m K}^2$ which was 476.1 times than that of pure PPy nanowires. This value of power factor was much better than $3.9 \mu\text{W/m K}^2$ obtained in case of free-standing PPy films [45] and also greater than $2.079 \mu\text{W/m K}^2$ of MWCNT-PPy [46] composite films. The improvement of power factor can be attributed to the effective interfacial contact among the rGO nanolayers (which provided fast conducting pathways for electron transport) and secondly to enhanced carrier mobility that was obtained as a result of expanded molecular conformation and ordered chain packing (which reduced the π - π conjugated defects in the polymer backbone and lowered the hopping barrier) [47].

3.4. Poly(3-hexylthiophene) (P3HT) and its composites

Regioregular (RR) poly(3-hexylthiophene) (P3HT) is an exemplary semiconducting polymer due to its ready availability, ease of solution processability and promising electrical properties [48,49]. In one of the few earlier studies, Crispin et al. [50] investigated the thermoelectric properties of drop-casted acetonitrile (NOPF₆) doped P3HT films. As a result, power factor increased to the three orders of magnitude (approximately from 10^{-10} W/m K² to 1.4×10^{-7} W/m K²) when the doping was between 20% and 31% [50]. Similarly, doping with a benign ferric dopant i.e. incorporating ferric salt of triflimide TFSI (with the formula (CF₃SO₂)₂N⁻) raised the power factor up to $20 \mu\text{W/m K}^2$ [51], the highest ever reported in P3HT films. *ZT* ~ 0.04 obtained for TFSI doped films at 340 K (assuming $\kappa \sim 0.2$ W/m K), illustrates that solution-processable CP after optimized doping treatment, can be a cost-effective choice for room-temperature flexible thermoelectrics [51]. Recently, energy filtering effect of organic-inorganic composites has been demonstrated as a strategy to enhance Seebeck coefficient and power factor [48]. Selective scattering of low energy charge carriers by the potential barrier of the P3HT/Bi₂Te₃ interface improved the power factor $\sim 13.6 \mu\text{W/m K}^2$ [48], much higher than that for pure P3HT ($\sim 3.9 \mu\text{W/m K}^2$). Whereas, Muller et al. [52] showed that the thermoelectric performance of CPs can be raised by collective approach of mixing them with CNTs and optimized *p*-doping. As a result, ferric chloride doped MWCNT/P3HT films exhibited much higher power factor $\sim 6 \pm 2 \mu\text{W/m K}^2$ (when $c_{\text{MWCNT}} \sim 10$ –40 wt%) as compared to $\sim 0.2 \pm 0.1 \mu\text{W/m K}^2$ of undoped composite films. Similar trends were observed for doped SWCNT/P3HT nanocomposite films, which exhibited power factors of $95 \pm 12 \mu\text{W/m K}^2$ and *ZT* ~ 0.015 (greater than *ZT* $\sim 7 \pm 2 \times 10^{-4}$ for undoped) at room temperature [52]. Rather than controlling doping levels like Muller et al. [52], improvement of thermoelectric properties of CNT/polymer nanocomposites can also be done by taking care of processing conditions such as coating method, SWCNT or ink concentration [53]. Wire-bar-coated (where a metal bar wound with a closely spaced fine wire is used for spreading the polymer solution) SWCNT/P3HT nanocomposite films consisting of well-dispersed networks of SWCNTs exhibited power factors up to $105 \mu\text{W/m K}^2$ at room temperature. This wire-bar coated method [53], though, resulted in power factor values comparable to that obtained in case of drop-casted FeCl₃ doped SWCNT/P3HT films [52], provided an additional advantage of elimination of doping from the processing technique [53]. Nanostructuring along with insitu control of dopant [54] also raised the power factor $\sim 6.84 \pm 0.64 \mu\text{W/m K}^2$ in case of silver percholate doped nanofibres of P3HT (nearly 50 times higher than the value $\sim 0.14 \mu\text{W/m K}^2$ reported [50] for PF₆⁻ doped P3HT films). This resulted in *ZT* value of 0.0026 at room temperature [54]. Apart from these studies, one recent paper has explored the potential of P3HT in developing the polymers based thermoelectric generators. The study [55] demonstrates the effect of photoexcitation to simultaneously increase the α and σ with increase in doping concentration and thus, improved the thermoelectric properties of P3HT:PCBM based devices. Improved thermoelectric parameters under illumination resulted in the maximum *ZT* ~ 0.5 at 147 °C, higher than that of Bi₂Te₃/Sb₂Te₃ superlattice devices at room temperature [55].

3.5. Polyaniline (PANI) and its composites

Besides having properties such as mechanical flexibility, solution processability, as well as being low-cost and light-weight like various other polymers, Polyaniline especially draws attraction due to its three distinct oxidation states and acid/base doping response. Moreover, its σ depends upon its oxidation states and lies between 10^{-7} S/cm to 3×10^2 S/cm [57,58] and crossover behaviour (change from *p*- to *n*-type) of Seebeck coefficient can also be obtained either by varying pH level of dopants or adding organic/inorganic groups [62–64]. Doping enhanced conductivity from 10^{-9} S/cm to 3.2 S/cm has also been observed in PANI nanotubes [60]. On the similar trend, Camphor sulphonic acid (CSA) doped PANI in semicrystalline nanostructured form displayed very large value of α which along with an intrinsically low σ and κ gave rise to the *ZT* of 0.77 and 2.17 at 45 K and 17 K [61] respectively (shown in Fig. 7). The huge value of maximum α (0.07–0.58 V/K) as well as peculiar thermal and electrical conductivities has been explained on the basis of phonon-drag effect [61]. Since

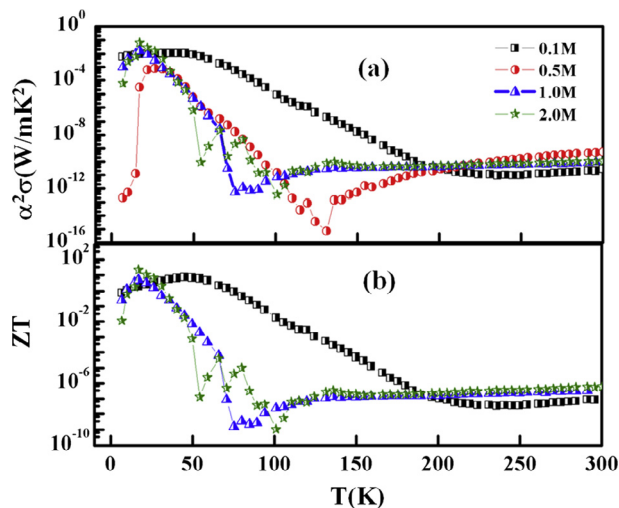


Fig. 7. Power factor $\alpha^2\sigma$ (a) and ZT (b) versus T plots for PANI doped with different concentrations of CSA. Reproduced with the permission from Ref. [61].

very few materials are available with $ZT \sim 1$ below room temperature, the outcome of this study can be used for low temperature applications such as Peltier coolers.

In addition, threefold increase in σ i.e. from 0.48 S/cm for pristine PANI to 123 S/cm in case of composites of PANI and graphite nanoplatelets (GNPs) with GNPs as filler materials provides insight to move towards hybrid materials for better thermoelectric performance [57]. Furthermore, transition from n-type to p-type of PANI with variation in GNP content changed the Seebeck coefficient from $-2.6 \mu\text{V/K}$ (for pure PANI) to $+33.8 \mu\text{V/K}$ (in case of composites) [57] to be utilized for device development.

3.6. Poly(3,4-ethylenedioxythiophene) (PEDOT) and its composites

Poly(3,4-ethylenedioxythiophene) (PEDOT), derivative of polythiophene, is one of best conducting polymer available in terms of conductivity, processability, and stability. PEDOT is doped with polystyrenesulphonic (PSS) acid to make it solution processable, and is widely used as hole-injection layers in organic electronics devices such as light emitting diodes and solar cells [2]. Further, commercial availability of highly conductive aqueous PEDOT:PSS dispersions and ease of doping to control the charge carrier concentration without much affecting Seebeck coefficient, make PEDOT an attractive candidate for thermoelectric applications [6]. It can be easily seen from Table 1, that the thermoelectric properties of PEDOT:PSS vary with the products and dopants/fillers.

The conductivity enhancement in PEDOT was reported way back in 2007 when vapour-phase polymerization resulted in ultra-thin polycrystalline conducting films of self-assembled monomers. PEDOT nanofilms prepared using FeCl_3 as oxidant were compared with those prepared using Fe(III) tosylate. The highest σ achieved for a thin film of PEDOT:tos was 4500 S/cm while $\sigma \sim 2000$ S/cm was obtained when FeCl_3 was used as oxidant [65]. The remarkable increase in conductivity from 0.3 S/cm to 3065 S/cm of PEDOT:PSS films [66] has also been observed on treatment with dilute sulphuric acid (H_2SO_4). Similarly, the concentrated H_2SO_4 treatment caused restructuring of PEDOT:PSS to give rise to highly crystalline nanofibrils which exhibited σ as high as 4380 S/cm [67]. The single-crystal PEDOT nanowires obtained from self-assembled and crystallized 3,4-ethylenedioxythiophene (EDOT) monomers also displayed ultra high conductivity with average value as 7619 S/cm to the highest ~ 8797 S/cm [68]. Such high value of conductivities, though, studied for optoelectronics only, can also find their productivity in thermoelectric applications. PEDOT films with high σ can also be obtained by doping with several counterions such as ClO_4^- , PF_6^- and bis(trifluoromethylsulfonyl)imide (BTfMSI) [69]. These counter-ions of different sizes when doped in the PEDOT, caused stretching of the polymer chains and brought three times enhancement in σ of PEDOT keeping α at the same order of magnitude (also discussed in Section 4.3.6) [69]. Addition of dielectric solvent dimethyl sulfoxide (DMSO) also improved the conductivity of polymeric PEDOT:PSS films without much affecting Seebeck coefficient and thermal conductivity [70]. As a result, $ZT \sim 9.2 \times 10^{-3}$ at room temperature was achieved when 5 vol% DMSO was added to both (PH750 and PH500) the PEDOT:PSS formulations [70]. A study reports that optimization of the power factor ($\alpha^2\sigma$) of PEDOT-Tos can be obtained by controlling its oxidation level [71]. Electrical conductivity (σ) for pristine doped PEDOT-Tos films was observed 300 S/cm with $\alpha \sim 40 \mu\text{V/K}$ and $\alpha^2\sigma \sim 38 \mu\text{W/m K}^2$. On exposure with tetrakis(dimethylamino)ethylene (TDAE), decrease in oxidation level resulted in six times improvement of power factor from $38 \mu\text{W/m K}^2$ to $324 \mu\text{W/m K}^2$ at 22% oxidation level. Thus, $ZT \sim 0.25$ [71] was obtained at room temperature (Fig. 8a). The study also investigated the effect of chemical reduction on power output of PEDOT-Tos films based devices. The power output of ink-jet printed single p-n leg measured by varying doses of TDAE at different load resistances (shown in Fig. 8b) clearly indicates that TDAE influenced the power output [71].

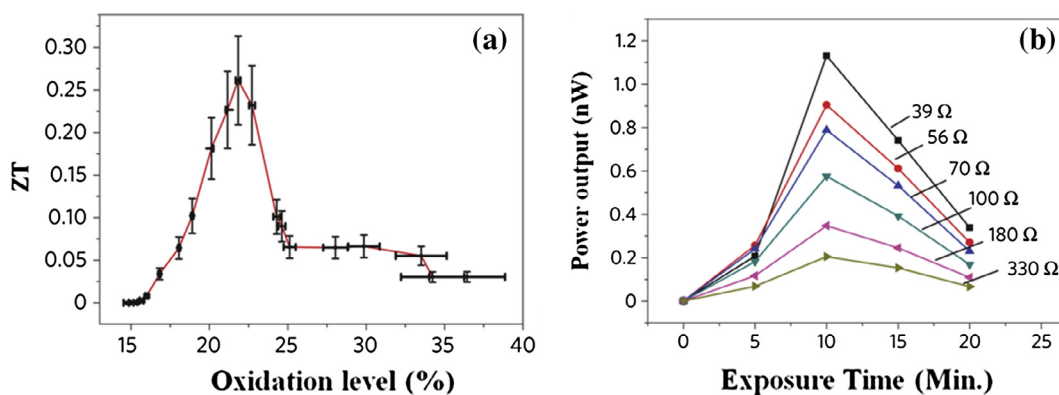


Fig. 8. (a) Values of ZT at room temperature for various oxidation levels assuming that the thermal conductivity of PEDOT-Tos is constant and equals 0.37 W/m K ; (b) the measured power output of a PEDOT-Tos/carbon thermocouple with different loads versus exposure time to the TDAE vapour. Reproduced with the permission from Ref. [71].

Though ZT of 2.17 at 17 K [61] and 0.5 at 420 K [55] has been achieved in PANI and P3HT:PCBM films respectively, yet the maximum ZT value of 0.42 reported by Kim et al. [72] for DMSO-mixed PEDOT:PSS, is the highest value achieved till now among CPs at room temperature. In this study, optimization of TE parameters was obtained through de-doping i.e. removal of non-ionized dopant atoms using hydrophilic solvent like Ethylene glycol (EG). EG treatment for about 100 min on EG/DMSO-mixed PEDOT:PSS maximized both α and σ while lowered down κ (values given in Table 1) and hence, resulted in ZT values ~ 0.28 for EG and ~ 0.42 in case of DMSO samples [72]. ZT enhancement from 0.25 [71] to 0.42 [72] can be attributed to ordered layered structure of polymer chains (shown in Fig. 9) due to addition of cosolvents EG or DMSO. Such an alignment of PEDOT chains is responsible for enhanced charge carrier mobility. Moreover this aligned geometry makes PEDOT more prone to the environmental oxygen which enhances charge carrier density. Thus, enhancement in both the charge carrier density and mobility leads to remarkable values of σ [6].

Similarly, addition of sorbitol into PEDOT:PSS [73] altered the morphology to enhance σ up to 722.06 S/cm which was higher by two orders of magnitude in comparison to pristine PEDOT:PSS (1.53 S/cm). While its addition slightly decreased α (that remained between 8.5 and $10.0 \mu\text{V/K}$ almost equal to $\sim 10.3 \mu\text{V/K}$ for pristine PEDOT:PSS), whereas power factor was raised to $7.26 \mu\text{W/m K}^2$ from value $\sim 0.016 \mu\text{W/m K}^2$ of pristine films [73]. Further treatment with tetrakis (dimethylamino) ethylene (TDAE) raised the power factor to $22.28 \mu\text{W/m K}^2$ displaying three fold enhancement from that $7.26 \mu\text{W/m K}^2$ of sorbitol mixed PEDOT:PSS. ZT estimated for the film having highest power factor was of the order 10^{-2} (0.013 – 0.039) [73]. However, conventional organic solvents used for doping/dedoping to improve TE performance have their own limitation of inherent toxicity. Therefore, deep eutectic solvents (DES) [74] can be used instead of conventional organic solvents to optimize TE parameters. It was found that using DES i.e. combined mixture of Choline chloride ($\text{C}_5\text{H}_{14}\text{ClNO}$) and Ethylene glycol (EG) led to a maximum α of $29.1 \mu\text{V/K}$ and σ of 620.6 S/cm in PEDOT:PSS films. Power factor obtained $\sim 24.08 \mu\text{W/m K}^2$ was approximately four orders of magnitude higher than the pure PEDOT:PSS and was explained on the synergistic effect of both the components on improvement of electrical conductivity [74]. Unlike many studies, where TE performance was improved by changing the oxidation levels, Mengistie et al. [75] emphasized that secondary solvents caused improvement in conductivity through enhancement of ordering, carrier mobility and concentrations and surprisingly did not affect oxidation levels. Treatment with ethylene glycol, polyethylene glycol, methanol, and formic acid respectively resulted in σ of 640 , 800 , 1300 , and 1900 S/cm as compared to 0.3 S/cm of pristine films [75]. On the other hand, not much significant change in α i.e. from value $\sim 32.3 \mu\text{V/K}$ of pristine films to $21.4 \mu\text{V/K}$ and $\sim 20.6 \mu\text{V/K}$ for ethylene glycol- and formic acid-treated thick films respectively, has been explained on the basis of unaffected oxidation levels. Selective removal of 'free PSS' i.e. non-ionized chains by formic acid [75] has been reported as a cause for $\sigma \sim 1900 \text{ S/cm}$ and power factor $\sim 80.6 \mu\text{W/m K}^2$

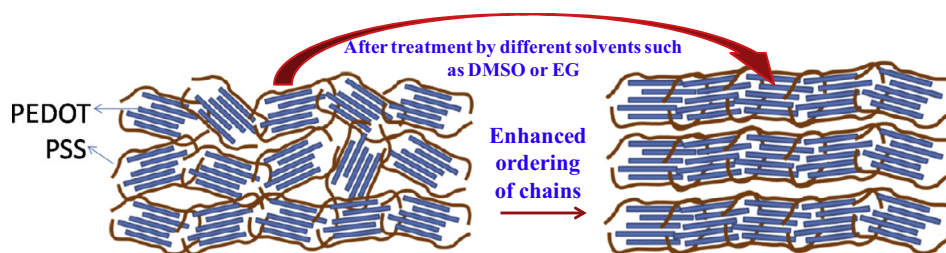


Fig. 9. Schematic showing extension of polymer chains due to removal of oxidants or addition of counter-ions. Reproduced with the permission from Ref. [6].

in case of formic acid treated films. This removal of PSS providing better conductive pathways due to extended alignment resulted in room temperature $ZT \sim 0.32$ [75]. Similarly, enhancement of TE properties was achieved by selective removal of PPP/Tos and increased alignment of PEDOT chains in case of PEDOT-Tos-PPP (where PPP stands for polyethylene glycol-polypropylene glycol-polyethylene glycol) films [76]. But here, mixture of NaBH_4 and DMSO was used to alter the oxidation level of PEDOT-Tos-PPP films [76] in contrast to the study [75] where it was considered that secondary solvents did not affect oxidation levels. Power factor $\sim 98.1 \mu\text{W}/\text{m K}^2$ of dedoped films ($\text{NaBH}_4/\text{DMSO}$ treated) was much higher than $34.4 \mu\text{W}/\text{m K}^2$ observed in case of pristine films [76]. Besides this improved power factor, significant reduction of κ from 0.501 to $0.451 \text{ W}/\text{m K}$ resulted in enhancement of room temperature ZT from 0.02 (before treatment) to 0.064 (de-doped films) which further rose to 0.155 at 385 K [76].

In addition to the treatment by dopants/co-solvents to enhance TE performance of PEDOT, various novel strategies are being continuously searched for further improvement. In this regard PEDOT-CNT composites are gaining much attention owing to the remarkable electronic, mechanical and adsorption properties of CNTs. CNTs forming bundles naturally, due to van der Waals forces, are difficult to disperse in solvents. In order to have proper connection between conjugated polymers and CNTs there is a need of stabilizing agents [11,77] which can alter the energy barrier for carriers flow [78] through the junctions. Therefore, while investigating the TE properties of CNT filled polymer composites, DMSO doped PEDOT:PSS and electrically non-conducting Gum Arabic (GA) were used as stabilizing agents [77]. In polymer composites prepared by dispersing CNTs in matrix of copolymer latex containing vinyl acetate and ethylene, it was found that composites with PEDOT:PSS (as stabilizing agent) showed higher electrical conductivity than those with GA [77]. As a result, maximum power factor $\sim 25 \mu\text{W}/\text{m K}^2$ was observed in case of samples with 35 wt% SWCNT and 35 wt% PEDOT:PSS as stabilizing agent. $ZT \sim 0.02$ obtained at room temperature (using $\kappa \sim 0.4 \text{ W}/\text{m K}$) due to being higher in magnitude by one order for most CPs and even higher than bulk Si, encouraged the use of CNTs for improving TE performance of CPs [77]. Improvement of TE properties has also been observed by dispersing Graphene oxide (GO) [78] in water soluble PEDOT:PSS and later reducing it to graphene (GN) by some reducing agent (i.e. Hydroiodic acid in this case). Maximum power factor $\sim 32.6 \mu\text{W}/\text{m K}^2$ obtained in case of reduced graphene and PEDOT:PSS (r-GO/PEDOT:PSS) composite films with GO ~ 3 wt% was found 1.5 times higher than that of a neat PEDOT:PSS film [78]. Similarly, enhancement of power factor has been reported in case of PEDOT/rGO nanocomposites prepared via three in situ chemical oxidative polymerization preparation routes [79]. Among various studies on polymer-CNT composites, a study deduced an important and unique result that instead of incorporating single type of nano-fillers, hybrid nanocarbon fillers would be more efficient in increasing the TE performance of CPs. Usually introduction of one type of fillers into the polymer matrix either improves the power factor or reduces thermal conductivity [80]. Therefore, the authors optimized the TE properties of PEDOT:PSS by introducing fullerene-functionalized graphene ($\text{rGO}_x\text{C}_{60(30-x)}$) into the polymer matrix [80]. It was observed that fullerene and graphene when added to PEDOT:PSS matrix in appropriate ratio, increased σ much faster than κ and caused four times increase in α . For instance, with the enhancement of σ from 100 S/cm to 700 S/cm, increase in κ has also been reported from $0.2 \text{ W}/\text{m K}$ to $2.3 \text{ W}/\text{m K}$ (i.e. still not so high) for loading of rGO from 3 to 30% in polymer composites [80]. As a result, $ZT \sim 0.067$ [80] obtained with $x = 21\%$ in $\text{rGO}_x\text{C}_{60(30-x)}$ nanohybrids-filled polymer composites (when the ratio of C60 to rGO was 3:7) was three times higher than 0.02 [77] reported in case of polymer/CNT composites with PEDOT:PSS as stabilizing agent. However in quest of novel approach to seek alternative of expensive CNTs, the study presented an easy, facile, low cost one step method to prepare PEDOT:PSS/paper composites by direct writing the solution on paper using Chinese calligraphy [81]. The $\alpha \sim 30.6 \mu\text{V}/\text{K}$ (at 300 K) of PEDOT:PSS/paper films [81] was found comparable to that observed in case of PEDOT:PSS/CNTs composites i.e. $15\text{--}30 \mu\text{V}/\text{K}$ [77]. These films on further treatment with EG/DMSO showed notable enhancement in σ from $0.2 \text{ S}/\text{cm}$ to $56.9 \text{ S}/\text{cm}$ (for DMSO-treated) and $54.1 \text{ S}/\text{cm}$ (for EG treated) PEDOT:PSS/paper films. In addition much lower $\kappa \sim 0.16 \text{ W}/\text{m K}$ of these films (attributed to low κ of paper $\sim 0.139 \text{ W}/\text{m K}$), resulted in $ZT \sim 5.5 \times 10^{-3}$. Use of paper as a substrate in this study suggests a way towards wearable flexible low-cost thermoelectric devices [81].

Apart from polymer/CNT composites, research is also being inclined towards developing composite materials [114] comprising both organic and inorganic entities so that combination of characteristics of both these entities can be used for optimizing TE performances. Hybrid materials have attained much importance because high power factors that have been made possible due to high σ of inorganic component along with poor κ of organic polymers can result in higher ZT . A study investigates that addition of Bi_2Te_3 [82] improved TE properties of PEDOT:PSS. Among all types of PEDOT, CLEVIOS PH1000 and FET displayed unexpectedly higher Seebeck coefficients leading to promising PFs of $\sim 47 \mu\text{W}/\text{m K}^2$ (with $\sigma = 900 \text{ S}/\text{cm}$ & $\alpha = 20 \mu\text{V}/\text{K}$) and $30 \mu\text{W}/\text{m K}^2$ respectively. In this study, it is very interesting to note that by adding n- and p-type Bi_2Te_3 into PEDOT:PSS, the composite material exhibit n- and p-type conduction with highly improved power factors in comparison to pristine PEDOT:PSS. Among all the types of PEDOT:PSS, Clevios PH1000 based p-type composites displayed the highest power factor of $120 \mu\text{W}/\text{m K}^2$ where as n-type exhibited PF of $80 \mu\text{W}/\text{m K}^2$ [82]. Similarly, composites of PEDOT:PSS and Tellurium nanostructures displayed high power factor ($\sim 70 \mu\text{W}/\text{m K}^2$) and low κ ($\sim 0.2 \text{ W}/\text{m K}$) resulting to ZT of 0.1. It is the highest value attained at room temperature in case of any aqueous processed material. The study provides a low cost synthesis method since the system was directly processed from water. PEDOT:PSS besides providing stronger interconnections between Te nanorods also prevented surface oxidation of Te, thus, conductivity of composites was higher than both PEDOT:PSS and Te nanorods individually [83]. Similar behaviour was reflected by the much higher power factor $\sim 51.4 \mu\text{W}/\text{m K}^2$ of PEDOT:PSS/Te nanorods composites (i.e. greater than $5 \times 10^{-3} \mu\text{W}/\text{m K}^2$ and $26.2 \mu\text{W}/\text{m K}^2$ in case of individual PEDOT:PSS and Te nanorods respectively) [102]. Moreover, these composites films were treated with H_2SO_4 to remove PSS by Bae et al. [103]. Table 1 shows that as a result, power factors $\sim 70.9 \mu\text{W}/\text{m K}^2$ [83] and $51.4 \mu\text{W}/\text{m K}^2$ [102] were improved to $284 \mu\text{W}/$

m K² in case of H₂SO₄ treated PEDOT:PSS/Te composites [103]. Although hybrid materials show better thermoelectric performance but dispersing medium can also affect thermoelectric performance of these films. For instance, in case of PEDOT and Au nanoparticles (NPs) composites, out of the two types of ligands—terthiophenethiol (TSH) and dodecanethiol (DT) as dispersing medium, it was observed that only hybrids with DT ligand displayed better TE performance than pristine PEDOT [59]. PEDOT/Au-DT hybrids displayed $\sigma \sim 240$ S/cm i.e. 2.4 times higher than that of solvents treated PEDOT. Therefore, study provided an important analysis by investigating that TE properties of CPs can be enhanced by adding metallic NPs; provided a proper method is selected for dispersion of nanoparticles inside the polymer matrix [59].

Keeping in view the advancements of TE properties ascertained by organic/inorganic composites, people are concerned to find that whether polymers can also serve for improving the properties of already established highly efficient inorganic thermoelectric materials. Recently, the study by Xiong et al. [84] reports dispersing of PEDOT as an embedment or inclusions in inorganic matrix of Sb₂Te₃ to fabricate p- type mingling composites rather than considering PEDOT as basic material and doping inorganic nanostructures in it. High value of $ZT \sim 1.18$ at 523 K (double than pristine Sb₂Te₃) provides an insight that high conductivity of Sb₂Te₃ has been supported by low value of κ of PEDOT. ZT value, though, reduced to 0.857 with 50 thermal cycles, but it remained higher than pure Sb₂Te₃ [84]. Similarly, flexible (free-standing) film of PEDOT:PSS was used as working electrode to electro-deposit Bi₂Te₃ resulting in Bi₂Te₃/PEDOT:PSS/Bi₂Te₃ composite films. Due to the high $\sigma \sim 403.5$ S/cm, much low $\kappa \sim 0.169$ – 0.179 W/m K (in comparison to 0.560 W/m K reported in case of other Bi₂Te₃/PEDOT composites [82]) and stable $\alpha \sim 15.3$ – 15.7 μ V/K, these films demonstrated ZT value of 1.67×10^{-2} at 300 K. The value reported here, is low in comparison to inorganic materials, but suggests that this facile technique of electrodeposition can be applied to various other materials such as chalcogenides, graphene or CNTs to prepare hybrid films with improved TE performance [85].

4. Key issues with conducting polymers

It can be envisioned from the overview of many CPs discussed in Table 1, that organic thermoelectrics has reached to a place that was previously unforeseen. Infact there are no generalized set of well-defined rules that can be applied to all the CPs for enhancing their TE performances [106]. We need to figure out specific approaches regarding to a particular CP depending upon many factors such as its chemical structure, feasibility of carrying out research with compatible dopants and choice of different types of appropriate substrates that will suit to the desirable device geometry (like in-plane and out of plane). Therefore, to make use of CPs in practical TE applications, key issues are categorized as: (1) Factors affecting thermoelectric properties; (2) Challenges encountered during research; and (3) Strategies required for optimizing thermoelectric performances.

4.1. Factors influencing thermoelectric properties

Electrical and thermal properties of CPs are determined by their structural and chemical designs. Moreover, inter-relationship between morphology, chain structure and charge transport has yet not been well-understood [106,114]. For practical applications, CPs need facile processability, but since, most of the CPs require oxidative doping, this can lead to infusibility as well as charged backbone having poor environmental stability [106]. Moreover, addition of substituent or functional groups to enhance solubility further complicates the synthesis process [106]. Factors which can influence TE performance are discussed as follow.

4.1.1. Polymer structure

Eminent reason behind different electrical conductivities, thermal conductivities, figure of merits and TE performances of various polymers like polyaniline (PANI), poly(*p*-phenylene vinylene) (PPV), polyacetylene (PA), poly(2,7-carbazolenevinylene), and poly(2,5-dimethoxy phenylenevinylene) (PMeOPV) can be understood as outcome of their respective structures. The molecular basis of conductive properties lies in the conjugation of their bonds. For instance, the polymers developed for organic FETs/photovoltaic owing to the π -stacking of conjugated bonds showed higher degree of ordering which reduced the number of grain boundaries, thus resulted in high charge-carrier mobilities [11,108–110]. Similarly, enhancement in electrical conductivity of PEDOT:Tos [105] has been reported due to structural ordering (i.e. due to enhanced mobility) rather than altered carrier concentration/doping, thus, resulting in an increase of the power factor from 25 to 78.5 μ W/m K² [105]. Impact of structure on TE properties is clearly exhibited in case of P3HT, where regioregularity $\sim 90\%$ is preferred to regiorandom P3HT for TE applications as latter fails to crystallize. Also high regioregularity $\sim 97\%$ is not preferred as it makes P3HT less soluble, thus leading to less promising electrical conductivities [52].

4.1.2. Polymer concentration

Polymer concentration during the synthesis determines the chain length/molecular weight which in turn influences solubility and viscosity of CPs [11]. Besides causing hindrance to facile processability of CPs through solution or melt, different molecular weights give rise to different size of nanostructures which further influence the charge transport in CPs. Muller et al. [52] have demonstrated that concentration of polymer and respective dopant affect the charge carrier mobility as well as the charge carrier density, thus influencing both Seebeck coefficient and electrical conductivity [48,52].

4.1.3. Polymer molecular weight and chain length

It has been well explained theoretically as well as experimentally that carrier mobility is influenced by molecular weights of the polymers. Polymers with low molecular weight have shorter chain lengths and are more crystalline in nature than high molecular weight polymers [2,49]. Even then, the mobility can be lower in these CPs due to obstructed connections by insulating boundaries [2,7]. Whereas in case of high molecular weight polymers longer side chains though interrupt the conjugation, but at the same time longer polymer (i.e. backbone) chains spreading through several material segments connect ordered regions more effectively with one another [2,49]. Moreover, thermal conductivity also shows an increase with the increase of polymer chain length. For example, a study [49] describes that variation in length of polymeric fibres occurs with the variation in the length of alkyl side chains. Study on P3ATs (where A = **M**-methyl, **B**-butyl, **H**-hexyl, **O**-octyl, **D**-dodecyl) reports that P3DT polymer with longer side chains resulted in very short nanofibres whereas length of nanofibres increased up to 1 μm in case of P3BT and P3HT having shorter alkyl side chains. As shown in Fig. 10, P3BT polymer having longer length of nanofibres exhibited higher σ of 35 S/cm than 0.77 S/cm in case of P3DT. Consequently, the highest value of power factor $\sim 10 \mu\text{W/m K}^2$ achieved in case of P3BT having shortest alkyl chain, was found to be 40 times higher than that obtained in case of polymer having longest alkyl side chain i.e. P3DT. Role of supramolecular structure (i.e. inter-chain distance here) is clearly emphasized by lowering down of the electrical conductivity with alkyl side-chain length [49] and should be taken care of while synthesizing organic thermoelectric materials.

4.1.4. Temperature

All thermoelectric parameters of CPs are also governed by operating temperature because it affects the carrier density through trapping/release of charge carriers as well as electron-phonon scattering [27,86]. For instance, it has been reported in case of polyacetylene that electrical conductivity displayed the non-metallic behaviour $\sigma \rightarrow 0$ as $T \rightarrow 0$ and exponential-like increase with increase in temperature at low doping levels [23]. This temperature dependent behaviour of thermoelectric properties provides an additional advantage to segment two or more CPs so that high conversion efficiency can be obtained through the superposition of their individual performances [13].

4.1.5. Humidity

Enhancement of power factor from 23 ± 5 to $225 \pm 130 \mu\text{W/m K}^2$ in case of PEDOT:PSS has been reported by Qingshuo Wei et al. in high-humidity conditions (Fig. 11a). Effect of water on the obtained results indicates the requirement of proper ambience i.e. humidity in this case, for adequate measurements of TE properties in CPs [6]. In a recent study, the temperature sensitivity as well as variation of the thermoelectric performance of P3HT samples with aging was investigated (Fig. 11b). The prevention of moisture during storage diminished the degradation effectively as the half-life of the power factor was elongated two fold [51].

4.1.6. Alignment of the polymer chains

Alignment of polymer chains is also known to cause effect on TE performance of CPs by increasing their electrical conductivity. As a result of stretching, it has been found that electrical conductivity can be increased two fold in stretched direction than in case of the perpendicular [88]. For instance, in case of PEDOT it has been reported that aligned chains enhance carrier mobility as well as provide ease for neutralization of the positive charges of PEDOT by the counter anions and hence, increased electrical conductivity [69,71]. Similarly, high values of electrical conductivity (80% greater than in case of perpendicular direction) and power factor along the oriented and aligned chains of PANI/CNT hybrids provide an insight to control TE performance by manipulating the alignment of polymer backbone [112]. Stretched P(MeOPV-co-PV) copolymers doped with Iodine [88] exhibited electrical conductivity $\sim 184 \text{ S/cm}$, Seebeck coefficient $\sim 44 \mu\text{V/K}$ and power factor $\sim 30 \mu\text{W/m}$

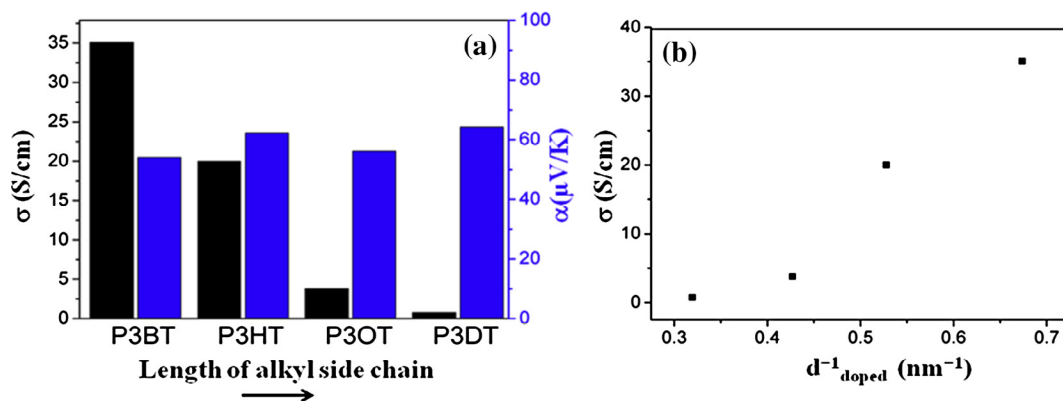


Fig. 10. (a) Electrical conductivity, Seebeck coefficient and power factor values for highly doped P3ATs; (b) Maximum electrical conductivity values as function of the reciprocal chain distance of the highly doped polymers. Reproduced with the permission from Ref. [49].

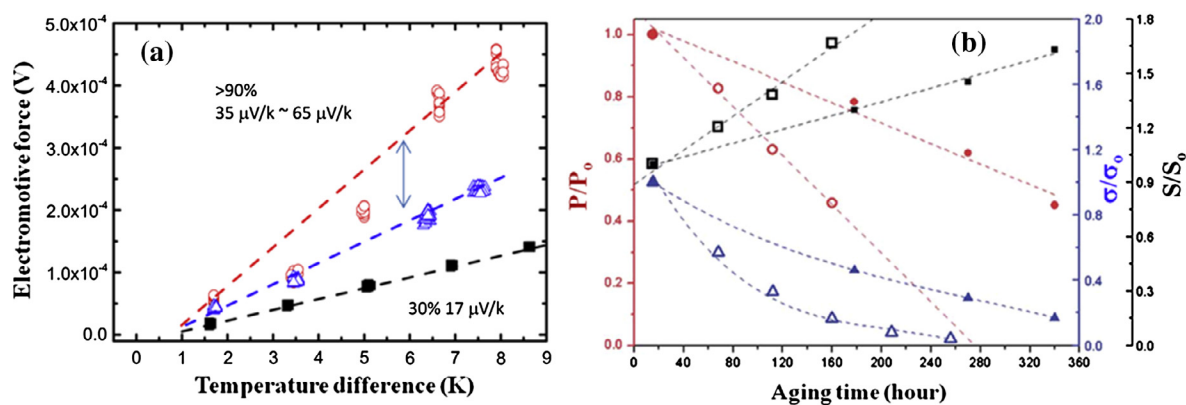


Fig. 11. (a) Seebeck coefficient measurements of PEDOT:PSS films: at humidity level of 30% (closed circles) and humidity level larger than 90% (open circles) (reproduced with the permission from Ref. [9]); (b) stability of the thermoelectric properties of P3HT-TFSI samples, filled and open symbols are for samples kept inside and outside the desiccator respectively (reproduced with the permission from Ref. [51]).

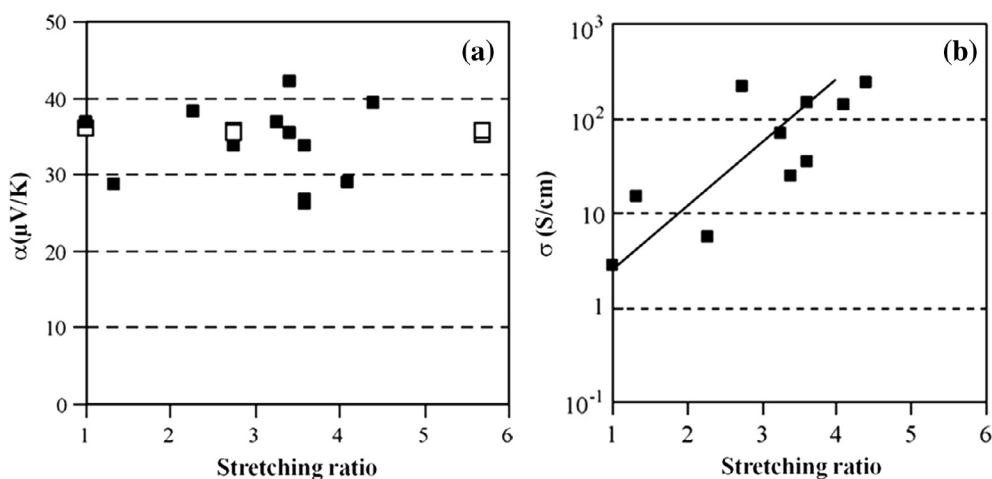


Fig. 12. (a) Seebeck coefficient α at 308 K as a function of stretching ratio for P(MeOPV-co-PV) with MeOPV content in the monomer feed: 10 mol% (■ filled squares) and 5 mol% (□ open squares); (b) electrical conductivity σ at 308 K as a function of stretching ratio for P(MeOPV-co-PV) with MeOPV content in the monomer feed: 10 mol%. Reproduced with the permission from Ref. [88].

K² at 313 K. Fig. 12 shows that preferable orientation by stretching alignment of P(MeOPV-co-PV) however, kept the Seebeck coefficient nearly same but caused enhancement of two orders in the electrical conductivity [88]. Infact, anisotropy in κ has been well studied in comparison to both σ , α in aligned CPs. Therefore, while optimizing ZT such anisotropy of TE parameters due to induced chain alignment [112] needs considerable attention. Recently Lipomi et al. [104] have investigated the electrical conductivity of PEDOT films on stretched substrates. These films retained sufficient electrical conductivity even when subjected to 188% strain and showed alignment in the direction of the strain [104]. Interestingly, bi-axial alignment in PEDOT:PSS/cotton cellulose composites [101] have shown that anisotropic materials can also give rise to isotropic electrical conductivity (discussed later in Section 5).

4.2. Challenges with the organic materials for thermoelectric applications

4.2.1. Long term stability

Majority of the CPs remain stable up to 150 °C of temperature only, hence, thermal stability of these materials is a matter of serious concern for practical use. Moreover, addition of dopants for enhancing electrical conductivity can lead to poor processability as well as low environmental stability due to the charged backbone [11,106]. In addition to this, very poor stability of n-type polymers (due to oxidizing nature of the environment) poses a limitation to complete the essentials of a thermoelectric module. Doping of CPs to get efficient n-type nature is also not so easy due to their low electron affinity [98]; most of the CPs are p-type in nature. However, in literature it has been reported [82] that n-type polymer composites can be obtained through addition of already existing n-type inorganic materials to polymers. Blending of n-type inorganic

material influences (or gets influenced by) the positive Seebeck coefficient of the polymer matrix. For instance, Zhang et al. [82] reports that due to mutual cancellation of Seebeck coefficients of opposite nature, mixture of PEDOT with n-type Bi_2Te_3 shows less value of Seebeck coefficient than observed in the mixture with the same content of p-type Bi_2Te_3 . Therefore, initially when concentration of n-type Bi_2Te_3 was low than overall Seebeck coefficient of the blend was positive, it approached to zero when PEDOT was 42% of the volume ratio and when ratio of PEDOT was further reduced to 10–30%, mixture behaved as n-type. Infact, the study [82] suggests a way to develop stable n-type polymer composites by integrating high conductivity and high Seebeck coefficient n-type powders into a low Seebeck coefficient p-type conducting polymers which will also inherit the flexibility of these CPs. But for depositing environmentally-stable polymeric films through solution processable techniques, a suitable solvent that will not affect stability is also required.

4.2.2. Sample preparations and measurement techniques

Conventional methods such as ball milling and hot pressing used for preparing inorganic thermoelectric materials, are still not appropriate for solution processed organic thermoelectric materials. Spin-coating and drop-casting methods are usually used to deposit organic-thermoelectric films but most effective fabrication methods for large-area deposition are still being developed. For fabricating organic/inorganic TE composites, techniques particularly in situ oxidative/interfacial polymerization/intercalation are preferred [48,53,87]. Further, the efficiency of a real device can be much lowered than that of fabricated in the lab because synthesis is not reproducible and also, there lies a large variation among different batches of materials [87]. Precise electrical measurements demand that the resistance of the organic samples must be several orders of magnitude smaller than that of the substrates to prevent flow of current through the substrates. The four-probe techniques should be used preferably to abolish contributions of the current leads or the contacts, while making voltage measurements [2]. However, free-standing films of CPs are usually preferred for measuring TE parameters like Seebeck coefficient and thermal conductivity. Therefore, development of home-made characterization setups with customized controls is highly needed for reliable and accurate thermoelectric measurements of organic films deposited on substrates [10].

4.2.3. Adherence of films to substrates

To have a flexible device, films must be either adherent to the substrate or should be free-standing. Due to amorphous/semi-crystalline nature of organic materials, films of various otherwise stable polymers like poly-pyrrole do not remain adhered to the substrates. This issue has been tried to be solved by using various binding agents. Interfacial polymerization technique is also being used for growing free-standing films which provide more feasibility of thermoelectric measurements [37,44,45]. Addition of a dopant, to increase electrical conductivity, also enhances brittleness [52,102]. So, concentration of the dopant needs to be optimized to have better thermoelectric performance as well as good mechanical strength. For example, to synthesize PEDOT:PSS and Bi_2Te_3 composites [82], aqueous dispersion of PEDOT/PSS was mixed with binder resins and functional additives to have better processability and good quality films [82].

4.2.4. Good electrical contacts between the organic/inorganic interface at active thermoelectric region and as well as between the polymer and metallic interconnect for device application

Lack of good electrical contact between organic/inorganic interface in active composite thermoelectric material and as well as between active thermoelectric material (i.e. pure CP or composite) and metal interconnects (for devices) is a challenging issue in organic thermoelectrics [114]. In case of organic-inorganic composites, the contact resistance from interfaces can be a reason behind low electrical conductivity [82]. The contact resistance was found to be $0.004 \Omega \text{ cm}^2$ for the composite of PEDOT:PSS (CLEVIOS P) and Bi_2Te_3 and $0.0025 \Omega \text{ cm}^2$ when type CLEVIOS PH1000 was used to make the composite with Bi_2Te_3 [82]. Thus, we need to reduce the contact resistance; one way is to introduce nanostructures (for example sometimes CNTs) into the polymer matrix to have better connectivity [82]. But inspite of the fact that CNTs have good mechanical strength and high electrical conductivity, their incorporation into the polymer matrix does not solve this problem. For example, in case of P3HT/CNT blends [52], P3HT being a semiconductor prevents good electrical contact by maintaining separation between adjacent CNTs. This issue was resolved by trying further doping of the polymer matrix by using anhydrous FeCl_3 in nitromethane as the dopant for P3HT/CNT composites [52]. It was found that electrical properties could be severely altered by varying dopant concentration as well as doping time. Electrical conductivity in case of the composite with $c_{\text{MW-CNT}} \sim 10 \text{ wt} \%$, though increased with the increase in dopant concentration and doping time, showed opposite behaviour at very high doping levels [52]. In addition, excessive doping may lead to increase in friability which may introduce fractures during sample handling and thus, can lower down electrical conductivity [52,102]. Doping parameters, therefore, require proper estimation in order to offer good electrical performance of a device. Similarly for device applications, the specific contact resistance between metallic interconnects and TE element should be low ($10^{-6} \sim 10^{-7} \Omega \text{ cm}^2$). Importance of the interface between the polymer and metallic interconnect has been shown in the study [94] where conductance measurements of the (silver paste/PEDOT:PSS/silver paste) device displayed decrease to about 70% of its initial value after 100 h and similar decrease was confirmed by the power output of the TE modules. This degradation was observed even when separate electrical conductivity measurements of both PEDOT:PSS and silver paste indicated their thermal stability [94]. Therefore, it can be concluded that device efficiency can be influenced by degradation of interface and proper care should be taken while designing CP based TEGs.

4.3. Strategies required for optimizing thermoelectric properties in conducting polymers

Development of smart devices which can compete with future trends needs novel strategies for optimization of thermoelectric properties. ZT values ~ 0.4 , achieved in case of most fertile CPs till date i.e. PEDOT-tosylate and PEDOT-PSS, are mostly enabled by their metallic (semi-metallic) electrical conductivity. Contrastingly P3HT, though exhibit high Seebeck coefficient [54], has not created its niche in practical applications due to its low electrical conductivity. Therefore, different strategies that can be employed to find a solution for the strict co-dependency of the thermoelectric parameters and enhance thermoelectric performance of CPs are given below.

4.3.1. Doping of polymers

The electric conductivity in CPs has been improved by doping the polymers with adequate amount of properly chosen dopants. Infact, interplay between polymer concentration and dopant is used to optimize the thermoelectric performance. Increase in the concentration of charge carriers brings improvement in electrical conductivity. But with increase in the electrical conductivity, Seebeck coefficient reduces rapidly while there occurs a slight enhancement in thermal conductivity. Thus, charge carrier density lays contrasting influence on behavioural pattern of these TE parameters [54]. Therefore, to achieve maximum ZT , optimum doping level has to be adjusted in such a way that CPs should be in an insulating or critical regime. Since in insulating/critical regime, charge transport is thermally activated, therefore, the coupling between chains through the wave functions of counter ions is very important for inter-chain transport. In this context, packing of chains along with position of counter ions is essential for electrical conductivity. Olga et al. [71], achieved a maximum ZT of 0.25 at room temperature, by doping Tos in PEDOT polymer and controlling the doping level through tetrakis(dimethylamino) ethylene (TDAE) exposure afterwards. Fig. 13a displays the variation of TE properties with oxidation level in case of PEDOT-Tos [71]. Similarly, Kim et al. recently optimized the ZT of the PEDOT: PSS mixture by de-doping the portion of unionized PSS dopant using different solvents, thus achieved a record value of $ZT = 0.42$ at room temperature shown in Fig. 13b [72].

4.3.2. Polymers - carbon nanotubes blends

CNTs that are known for their stable one-dimensional nanostructures and excellent electrical and mechanical properties, when are incorporated into a polymer matrix, alter the thermoelectric properties of the materials. CNT-polymer interaction has been well exploited for alignment of polymers at the molecular level to enhance TE performance [112]. PANI-CNT interaction after being subjected to electric field of electro-spinning caused orientation of PANI/CNT composites in parallel direction [112] which not only reduced the π - π conjugated defects but also decreased localization of charge carriers. This enhanced the mobility by lowering the hopping barrier. Similarly, simultaneous enhancement of electrical conductivity and Seebeck coefficient in case of composites of PEDOT:PSS with graphene oxide (GO) [78] after reduction with hydroiodic acid (HI), has been ascribed to the interaction between r-GO and polymer matrix and removal of some PSS from the film. The interaction provided a channel for carriers transport and made the PEDOT:PSS chains pack more ordered. This fact that introduction of carbon nanostructures into the polymer matrix can enhance thermoelectric properties has also been well evidenced by the unique study made by Kun Zhang et al. [80]. After incorporating the fullerene functionalized grapheme ($rGO_xC_{60(30-x)}$) into the PEDOT:PSS it was examined that addition of rGO improved electrical conductivity by increasing the carrier mobility, while C_{60} enhanced the Seebeck coefficient and reduced the thermal conductivity. This enhancement of Seebeck coefficient due to insertion of C_{60} has been explained in three ways [80]; firstly there may be possibility of shifting of Fermi level away from valence band; and secondly, C_{60} nanoparticles that were assembled on rGO surfaces, due to energy filtering effect selectively allowed passage to high energy carriers by obstructing cold-energy carriers. This resulted in increase of mean carrier energy leading to the improvement of Seebeck coefficient. Moreover, C_{60} due to having zero-

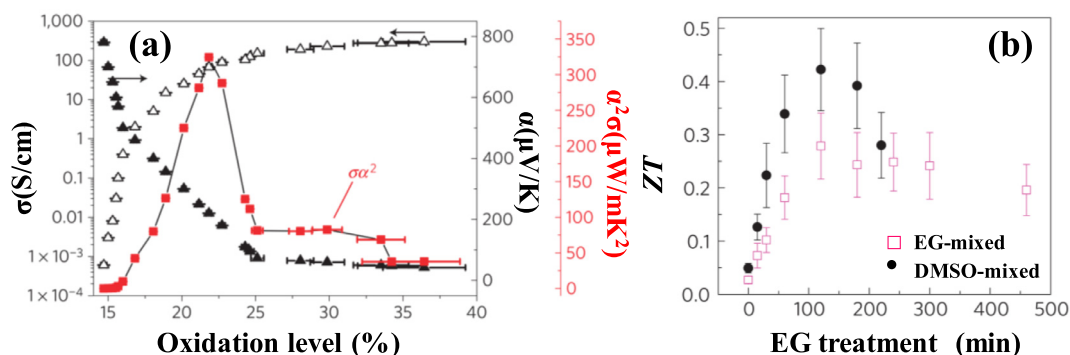


Fig. 13. (a) Thermoelectric properties: Seebeck coefficient (filled triangles), electrical conductivity (open triangles) and corresponding power factor (red squares) versus oxidation level (reproduced with the permission from Ref. [71]); (b) ZT optimization of EG-mixed (pink squares) and DMSO-mixed PEDOT (black circles) by EG treatment (dedoping process) (reproduced with the permission from Ref. [72]).

dimension structural form perhaps caused quantum confinement during carrier transport and thus, enhanced the Seebeck coefficient. Therefore, these nano hybrids-based polymer composites displayed $ZT \sim 6.7 \times 10^{-2}$, higher than the $ZT \sim 10^{-3}$ achieved with the single-phase filler-based polymer composites [80].

4.3.3. Organic-Inorganic composites

Introduction of inorganic materials in polymer matrix improved thermoelectric properties of CPs due to their relatively higher Seebeck coefficient values. Zhang et al. [82] illustrated that power factor for both n- and p-type composite materials increased after integration of n- and p-type Bi_2Te_3 ball milled powders with PEDOT:PSS. Power factor $47 \mu\text{W}/\text{m K}^2$ achieved in case of PEDOT:PSS (CLEVIOS PH1000) was enhanced to $131 \mu\text{W}/\text{m K}^2$ after insertion of ball milled Bi_2Te_3 particles in the PEDOT:PSS matrix. Further, incorporation of p- and n-type Bi_2Te_3 particles can be used for developing the two different types of thermoelements that are essential for a TEG. Similarly, Te nanorods when dispersed into a PEDOT matrix not only enhanced σ but also restricted κ to retain its polymeric value. As a result, $ZT \sim 0.1$ was obtained at room temperature [83]. The high ZT obtained in case of composites can be used to fabricate an OTEG, for example recently Cai et al. developed a PEDOT:PSS/Te nanorods based TEG that resulted in an output of 2.5 mV at ΔT of 13.4 K [102]. Yang et al. also used Te-nanowire/poly(3-hexyl thiophene) (P3HT) polymer composite to develop a flexible thermoelectric nanogenerator (TENG) discussed later in detail [90].

4.3.4. Nanoscaled organic/inorganic materials

It has been verified both experimentally and theoretically, that if nanostructured materials are incorporated into the polymer matrix, interfacial resistance can be decreased. The nanoparticles forming proper band alignments with the matrix expedite the flow of carriers from the nanoparticles into the matrix. Room temperature $ZT \sim 0.0026$ [54] was obtained when P3HT in form of nanonet was doped with Ag^+ . Better thermoelectric performance of P3HT nanonet than its bulk form as a function of varied dopant concentration has been manifested in Fig. 14. High ordering and intimate contact among nanofibers caused enhancement of electrical conductivity and in addition, provided enough porosity for dopant percolation [54]. Therefore, thermoelectric performance can be improved by incorporating nanostructures into the composites of CPs with CNTs/inorganic materials, because benefits of the nanoscale will add up the already amplified strength of the organic/CNT or organic/inorganic hybrid systems.

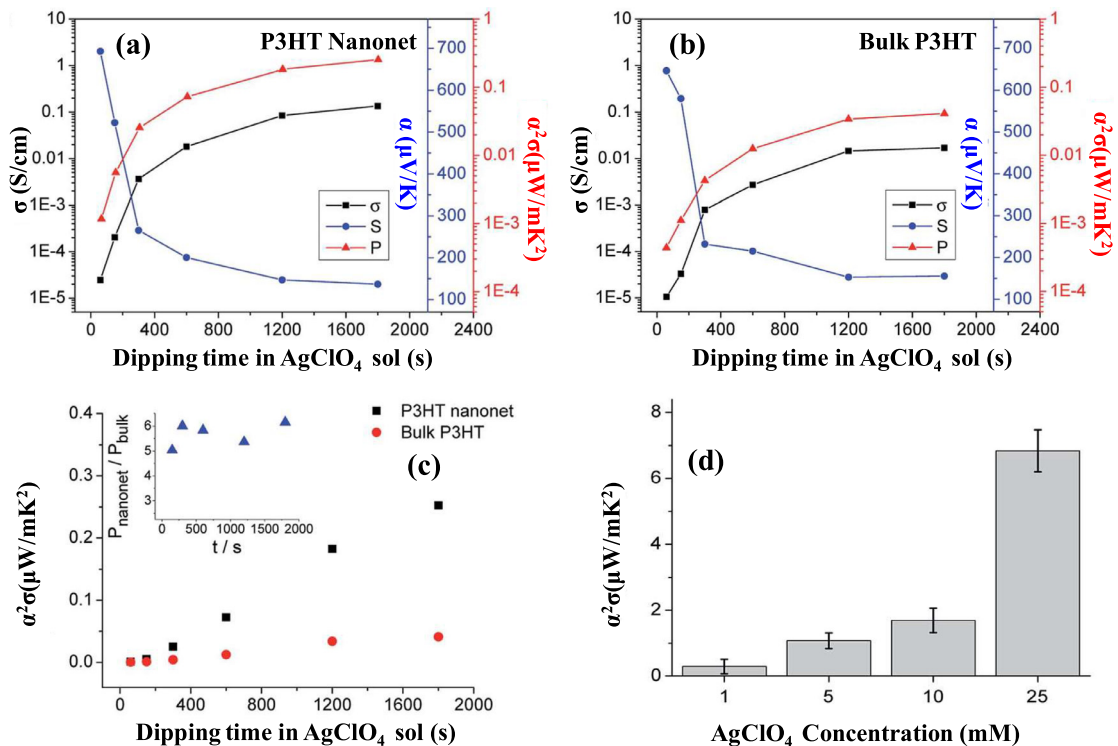


Fig. 14. Doping level dependent thermoelectric properties of (a) P3HT nanonet, (b) Bulk P3HT; (c) comparison of the power factors measured for the bulk and nanonet structured P3HT doped with 1 mM AgClO_4 solution; (d) maximum power factor of the P3HT nanonet at different oxidant concentrations. Reproduced with the permission from Ref. [54].

4.3.5. Energy filtering effect

It is pertinent to mention that the energy-filtering approach though suggested earlier for superlattices only in which alternately existing energy barrier layers served as energy filters; now being expanded to bulk inorganics too. We have already discussed the organic-inorganic composites yet energy filtering effect of the organic-inorganic interface that scatters the low energy carriers needs to be emphasized distinctly as a tool to enhance power factor, particularly through Seebeck coefficient without much affecting electrical conductivity. For instance, in a recent study on P3HT and Bi_2Te_3 composites energy filtering effect has been demonstrated as the cause behind enhancement of Seebeck coefficient/power factor [48]. Similarly, enhanced power factor of PEDOT/rGO composites $\sim 32.6 \mu\text{W}/\text{m K}^2$ (for 3% GO) after reduction had been attributed to size-dependent energy-filtering effect that was created due to coating of nanostructured PEDOT:PSS on the r-GO [78].

4.3.6. Bilayer/multilayer approach

Recently, a novel strategy [113] for optimizing TE performance through multilayer approach in case of PEDOT:PSS/PANI-CSA composites has been reported. Multilayer deposition in these polymer hybrids enhanced electrical conductivity in two ways: firstly via stretching of PEDOT layer due to underneath PANI-CSA chains and secondly, because of hole diffusion from PANI-CSA layer to the PEDOT:PSS layer [113]. Moreover, non-variation of Seebeck coefficient was also observed due to difference in the orbital energy of two polymers which altered the symmetry of the density of states around Fermi level. This bilayer/multilayer approach can be extended to other combination of polymer systems for improving TE performance.

4.3.7. Externally controlled factors such as device structure, electrode potential during electro polymerization, size of counter-ions, technique of polymerization, calibration of oxidation level

Photoexcitation can generate excited states in a device and thus, can control electrical transport similar to doping. Phonon-electron coupling effect due to these generated excited states improved the thermoelectric properties [55]. Such an optimization of transport properties of organic thermoelectric materials leading to increase of thermoelectric efficiency has been reported; where illumination increased the concentration of electrons and holes while the phonon component of the heat flux was reduced by phonon scattering [55]. Fig. 15 illustrates the increase in value of ZT up to 0.5 at 147 °C, the highest ever shown for CPs at such temperatures under illumination [55].

Similarly, electronic structure of polymers was altered through doping to have a favourable density of states and Fermi level [79]. For example, doped poly(alkylthiophene) blends having defined density of states showed simultaneous increase in Seebeck coefficient and electrical conductivity [79]. Improvement in thermoelectric performance has also been obtained by varying electrode potential during electropolymerization. Alteration of electrical conductivity and Seebeck coefficient in case of free standing PPy films on application of varying potential differences, suggests the method to control and optimize the ZT [45]. Besides varying the potential, variation in the counter-ion size during electro-polymerization [69] can also bring enhancement in the thermoelectric efficiency; as observed in case of PEDOT derivatives obtained via doping with several counter-ions such as ClO_4 , PF_6 and bis(trifluoromethylsulfonyl)imide (BTfMSI). It has been well reported that an extended chain besides enhancing carrier mobility becomes more favourable for the neutralization of the positive charges of PEDOT (by the counter anions) and hence, increases electrical conductivity [69,71]. Moreover, techniques employed for polymerization such as solution processed crystallization or vapour-phase deposited polymerization also influence the thermoelectric performance of CPs [67]. Optimization of ZT can be done by controlling the oxidation levels. This is well illustrated by the increase of electrical conductivity of PP-PEDOT up to 2120 S/cm with the increase of applied potential from 0.5 to 1.1 V, which resulted in the highest power factor ($\sim 1270 \mu\text{W}/\text{m K}^2$) ever achieved [93]. Whereas, oxidation level in Tos doped PEDOT was altered by tetrakis(dimethylamino)ethylene (TDAE) exposure to optimize the power factor [71]. Similarly, PEDOT-Tos-PPP films [76] were dedoped using mixture of NaBH_4 and DMSO to manipulate the oxidation level to have better thermoelectric performance.

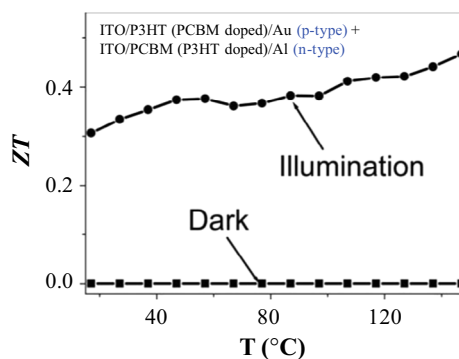


Fig. 15. Figure of merit (ZT) of p-type and n-type structure of thin-film device (p-type is 30% PCBM-doped P3HT, n-type is 30% P3HT-doped PCBM) under different temperatures with dark and illumination. Reproduced with the permission from Ref. [55].

5. Designing and development of an organic thermoelectric module

Measurements and optimization of thermoelectric parameters such as electrical conductivity, Seebeck coefficient and thermal conductivity of CPs do not end the process. It, rather, sets up the need to develop an efficient TEG for practical applications. From the graph (shown in Fig. 16) that summarizes year wise progress in thermoelectric figure-of-merit of the promising CPs, we are of the view that PEDOT and P3HT can exhibit remarkable performances for room temperature TE device applications. Chain structure of polymers such as P3HT or PEDOT having π - π interactions can be exploited for alignment in a desirable plane (i.e. in-plane or out of plane) as per device geometry. Moreover, π - π interactions among the chains of P3HT/PEDOT besides causing enhancement of electrical conductivity (due to chain alignment) [2,11] interact with inorganic components and thus, make these CPs best suited for composites. For instance, it has been reported recently [102] that the interaction between the van der Waals force from the Te atom layer and π interaction from the PEDOT:PSS chains at the interface resulted in a good interfacial adhesion between the two phases [102]. However, the CP like polypyrrole having relatively good stability has not been studied too much because of its low ZT . We, in this section, have compiled detailed report on promising CPs (graphical summary shown in Fig. 16) that have been reported so far by various research groups for providing insight to future technology of smart devices.

Extraction of the electrical power from an efficient thermoelectric material primarily depends upon the design engineering of a TEG [13]. CPs based TEG, now onwards will be referred as an 'Organic Thermoelectric Power Generator' i.e. OTEG, shown in Fig. 17a, usually consists of a large number of p-type and n-type thermoelements alternately connected electrically in series and thermally in parallel [13]. Availability of a p-type CP is not an issue as mostly stable CPs are p-type but for ease in designing, n-type CP is also required. Not so many n-type CPs are available till date and those exist have poor air stability. However, even in case of unavailability of a compatible and stable n-type material, one can design an OTEG using only p-type material as per the schematic shown in Fig. 17b. It may be noted, that designing with a single type of material (Fig. 17b) can have some issues due to transfer of heat from hot end of one thermoelement to the cold end of next thermoelement via metallic interconnect. Such a heat transfer can eventually reduce the temperature difference across the device which in turn will cause degradation of the device efficiency and power output. Also, thermal contact resistance between heat source and device needs to be minimized so that efficient transfer of heat can be done from source to the hot end of the device. This part is most crucial in case of wearable electronics or self powered sensors, where heat is to be supplied to the devices attached on the curved surfaces. Electrically insulating and thermally conducting adhesives based on Al_2O_3 or AlN can be used to provide a good thermal contact.

In context of the discussion made here, Table 2 summarizes the CPs based thermoelectric generators (OTEGs) developed so far.

From the Table 2, it may be noted that although many CPs have been employed for fabrication of TEGs by various research groups, but so far, a few groups have taken care about the estimation of conversion efficiency. The detailed description of the studies on OTEGs (compiled in the Table 2) is as follows.

The study [89] reports one of the few early developed OTEGs to realize the concept of energy autarkic operation by demonstrating TEGs consisting of 3p-n legs (length = 2 cm, width = 0.5 cm and thickness = 70 μm) screen printed on flexible

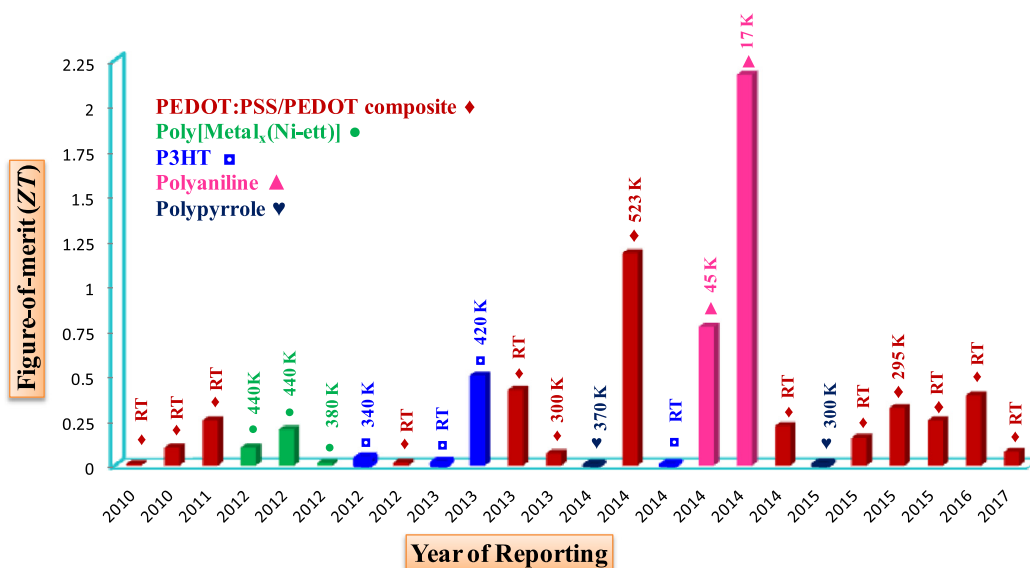


Fig. 16. Graph showing year wise progress in ZT of various conducting polymers.

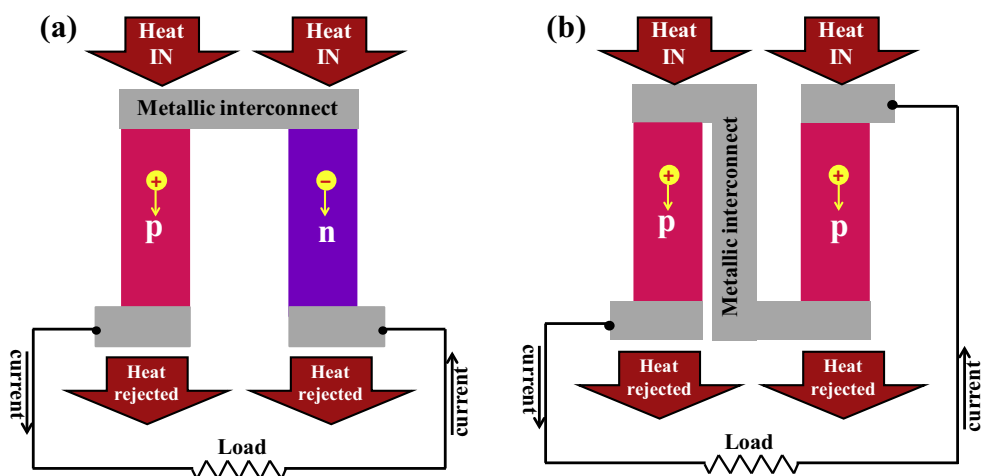


Fig. 17. Schematic shows the organic thermoelectric power generator consisting of (a) A single p-n leg. (b) A single p-p leg.

substrates (Fig. 18). Various organic charge transfer salts such as tetrathiafulvalene–tetracyanoquinodimethane (TTF–TCNQ) which showed a negative Seebeck coefficient along with iodine doped salt bis(ethylen-dithiolo)tetrathiofulvalene (BEDT–TTF) derived by substitution of TTF by BEDT having p-type conduction were thoroughly investigated. Polyvinylchloride (PVC) with graphite formed the p-leg of thermoelectric module while a blend of PVC and the organic charge transfer salt TTF–TCNQ was used to make the n-leg of the TE module. Though value of Seebeck voltage was obtained $\sim 120 \mu\text{V/K}$, yet individual Seebeck coefficients measured in case of PVC–graphite composites $\sim 44 \mu\text{V/K}$ and TTF–TCNQ–PVC $\sim -48 \mu\text{V/K}$ suggest that theoretical value of Seebeck coefficient could reach up to $\sim 136 \mu\text{V/K}$ i.e. 15% higher than the experimental value. The author proposed that module of dimension $6 \times 6 \text{ cm}^2$ could exhibit low power output of $\sim 1.5 \mu\text{W}$ (for $\Delta T \sim 5 \text{ K}$) with internal resistance $\sim 250 \text{ K}\Omega$ [89].

Another prototype of an OTEG consisting of 55 legs in a vertical architecture has been demonstrated by Xavier et al. [71]. To develop a single thermocouple, both p- and n-legs were ink-jet printed on pre-deposited Au electrodes on silicon substrate. EDOT monomer with oxidant $\text{Fe}(\text{Tos})_3$ was polymerized to make p-leg of PEDOT–Tos while carbon black ink was used as n-type leg. On exposure by reducing agent (TDAE) for 10 min, maximum power output of the thermocouple reached to 1.13 nW at $\Delta T = 1.5 \text{ }^\circ\text{C}$ for load resistance of 39Ω . To fabricate another TE module [71], photolithography was used to pattern cavities upon the bottom Au electrodes. Fig. 19a shows the legs having $1 \times 1.5 \text{ mm}^2$ area and 30 mm length, fabricated by filling the cavities with precursor solutions. The n-legs and p-legs of TE module were synthesized using TTF–TCNQ–PVC composites and PEDOT–Tos respectively. The power $\sim 0.128 \mu\text{W}$ shown in Fig. 19b was obtained at $\Delta T = 10 \text{ K}$. Here, thickness of the device provided hindrance for ΔT , so to achieve high power legs that had long dimensions and higher packing density were required. The expected power generated per unit area was extrapolated to $0.27 \mu\text{W/cm}^2$ at $\Delta T = 30 \text{ K}$ [71].

In another study, significant finding about TE properties of a series of metal coordination n- and p-type polymers containing 1,1,2,2-ethenetetrathiolate (ett) linking bridge: $\text{poly}[\text{A}_x(\text{M}-\text{ett})]$ ($\text{A} = \text{tetradecyltrimethyl ammonium}$, $\text{tetrabutyl ammonium}$, Na^+ , K^+ , Ni^{2+} , Cu^{2+} , $\text{M} = \text{Ni}$, Cu) has been reported [91]. The n-type materials $\text{poly}[\text{Na}_x(\text{Ni}-\text{ett})]$ and $\text{poly}[\text{K}_x(\text{Ni}-\text{ett})]$ exhibited excellent TE characteristics (they are among best organic TE materials reported yet). $ZT \sim 0.042$ at 300 K was obtained in case of $\text{poly}[\text{Na}_x(\text{Ni}-\text{ett})]$ which reached to 0.10 at 440 K whereas $\text{poly}[\text{K}_x(\text{Ni}-\text{ett})]$ displayed $ZT \sim 0.2$ at 440 K . The ZT value of $\text{poly}[\text{Cu}_x(\text{Cu}-\text{ett})]$ varied between 0.002 and 0.014 from 230 to 400 K . These ZT values prompted for the development of a TE module to be used for power generation. The legs of the module were prepared by pressing the polymer powder into pellets having $5 \times 2 \text{ mm}^2$ as base area and 0.9 mm as length. Thin Au layer was coated on both sides of the pellets to make better contact with interconnects while assembling the module (Fig. 20a). TE module consisting of 35 n-p single couples (each fabricated using n-type $\text{poly}[\text{Na}_x(\text{Ni}-\text{ett})]$ and p-type $\text{poly}[\text{Cu}_x(\text{Cu}-\text{ett})]$) generated a $V_{\text{OC}} = 0.26 \text{ V}$ and $I_{\text{SC}} = 10.1 \text{ mA}$ at $\Delta T = 82 \text{ K}$ (Fig. 20b). This maximum power output of $750 \mu\text{W}$ (shown in Fig. 20c) that has been obtained with a load resistance of 33Ω for ΔT of 82 K and T_h of 423 K , is the highest value reported so far, for organic materials [91].

From the studies discussed here, it seems that n-type element is a pre-requisite for development of a thermoelectric module. However, recently an important study by Krebs et al. [92] demonstrating Roll-to-roll (R2R) technique suggests that the compulsion of the presence of n-type element for fabrication of a TE module can be overcome. Also, this novel R2R method can provide additional advantage of fabricating OTEGs that can cover large surface area for practical applications. OTEG was fabricated by connecting 18,000 thermoelectric junctions in series in three steps which included: (1) Flexoprinting of a nanoparticle silver ink as the bottom electrode; (2) Rotary screen printing of PEDOT:PSS; and (3) Flexoprinting of a silver paste for the back electrode [92]. Alignment of prints was done in a manner (displayed in Fig. 21a) so that an infinite connection could be created along the network by serially connecting each junction to the two adjacent ones. Two different kind of rolled-up devices were fabricated: one by using a pressure sensitive adhesive ($60 \mu\text{m}$) on the back side of the whole foil to

Table 2

Summary of the OTEGs developed so far.

| Thermoelements | Device configuration | Output | Comments | Application demonstrated | Ref. |
|---|---|---|---|---|------|
| <i>n</i> -TTF-TCNQ/PVC, <i>p</i> -Graphite/PVC blend | 3 <i>p</i> - <i>n</i> legs, Active area of the device: $6 \times 6 \text{ cm}^2$, $\Delta T = 3 \text{ K}$ | Voltage: 1.5 V, Power: $1.5 \mu\text{W}$ (Estimated theoretically) | Screen printed on polyester foils of thickness $\sim 0.18 \text{ mm}$, graphite interconnects, Device resistance: $250 \text{ k}\Omega$ | – | [89] |
| <i>n</i> -TTF-TCNQ/PVC blend, <i>p</i> -PEDOT-Tos | 54 <i>p</i> - <i>n</i> legs, $\Delta T = 10 \text{ K}$ | Output Power: $0.128 \mu\text{W}$ | Drop casted on patterned substrate with gold electrode | As a power generator | [71] |
| <i>p</i> -Te nanowire with P3HT | Connecting two <i>p</i> -type layers in series, $\Delta T = 55 \text{ K}$ | Voltage: 38 mV, Current: 120 nA | Drop casted films on fabric and kapton, Ag as interconnects, Device resistance: $79 \text{ k}\Omega$ | Flexible power generator and Sensing of temperature of air exhaled by lungs | [90] |
| <i>n</i> -poly[Na _x (Ni-ett)], <i>p</i> -poly[Cu _x (Ni-ett)] | 35 <i>p</i> - <i>n</i> legs, $\Delta T = 82 \text{ K}$, $T_h = 423 \text{ K}$ | Voltage: 0.26 V, Current: 10.1 mA, Power: $750 \mu\text{W}$, load resistance: 33Ω | Pellets mounted on AlN substrate, Ag/Al as interconnects on Au coated <i>p</i> - and <i>n</i> -pellets, Stability found up to 300 h | As a power generator | [91] |
| <i>p</i> -PEDOT:PSS | $\Delta T = 70 \text{ K}$, 10 windings of 576 junctions without any adhesive with heater at the centre | Output: 50–60 pW | Screen printing, Roll to roll on PET substrate, silver ink used to form interconnects | Only one single type of thermoelement i.e. either <i>p</i> or <i>n</i> can be used to fabricate a TE device | [92] |
| <i>p</i> -PP-PEDOT | $\Delta T = 5.3 \text{ K}$ | Output: $590 \mu\text{W}$ | By solution casting polymerization on PET substrate with gold electrodes | As a power generator using body heat | [93] |
| <i>p</i> -PEDOT:PSS/paper composite | 70 Series connected paper i.e. 385 thermocouples (M1) 70 Parallel connected paper i.e. 14 thermocouples (M2) | Output of M1 at $\Delta T = 50 \text{ K}$ (0.2 V, 4 μA) Output of M2 at $\Delta T = 50 \text{ K}$ (0.012 V, 1.4 mA), Load Resistance = 7Ω | Screen printed of PEDOT:PSS on paper as substrate and connected by silver paste | Power Efficiency estimated at $100 \text{ K} \sim 0.1\%$, Module tested at $100 \text{ }^\circ\text{C}$ for 100 h, DC to DC convertor was used to boost the output voltage obtained from TE module to 2.2 V (sufficient to light an LED), Device performance depends on interfacial contact between PEDOT:PSS and silver paste | [94] |
| <i>n</i> -Poly[K _x (Ni-ett)]/PVDF/DMSO composite, <i>p</i> -poly[Cu _x (Cu-ett)]/PVDF/DMSO composite | 300 pieces parallel connected paper (10 in parallel, 30 in series, each piece contain 11 PEDOT arrays) 6 <i>p</i> - <i>n</i> legs, $\Delta T = 25 \text{ K}$, $T_h = 293 \text{ K}$ | Output in case of 300 pieces in parallel at $\Delta T = 100 \text{ K}$ (40 mV, $50 \mu\text{W}$), $R < 10 \Omega$ Output: 15 mV, 3 μA , Power: 45 nW, Device resistance: 5000Ω | <i>p</i> - and <i>n</i> -layers of Poly[A _x (M-ett)]/PVDF composites obtained via ball milling were inkjet printed on PET substrate with gold electrodes | Solution processed Flexible TEG | [95] |
| <i>n</i> -Bi ₂ Te ₃ /PEDOT: PSS composite, <i>p</i> -Sb ₂ Te ₃ /PEDOT:PSS composite | 15 <i>p</i> - <i>n</i> legs at $\Delta T = 5 \text{ K}$ and $T_h = 293 \text{ K}$ 7 TE couples at $\Delta T = 50 \text{ K}$ and $T_h = 333 \text{ K}$ | Output: 12.1 mV Output for 7 TE couples: 85.2 mV, Power: $1.2 \text{ mW}/\text{cm}^2$ | Screen printing of inorganic <i>p</i> and <i>n</i> -layer on flexible polyimide films subsequently coated with PEDOT:PSS, with Ag electrodes | Low power wearable electronics & TEG for harvesting body heat | [96] |
| <i>p</i> -PEDOT:PSS | $\Delta T = 75.2 \text{ K}$ | Output: 4.3 mV, Power: 12.29 nW | Dip coating on polyester fabric, 5 elements (fabric stripes) mounted on commercial fabric using silver paint and connected by silver wire and silver paint | Fabric based thermoelectric power generator | [97] |
| <i>n</i> -Cu _{0.1} Bi ₂ Se ₃ /PVDF composite | $\Delta T = 15 \text{ K}$ | Output: 1.3 mV | Drop casted films of solution containing Cu doped Bi ₂ Se ₃ nanoplates and PVDF were peeled of the glass substrates | Self powered wearable electronics and wearable thermal sensors | [98] |

Table 2 (continued)

| Thermoelements | Device configuration | Output | Comments | Application demonstrated | Ref. |
|---|---|---|--|---|-------|
| <i>p</i> -PEDOT:PSS/non woven fabric composite | Connecting 54 pieces in series, $\Delta T = 55$ K | Power: 34 μ W | Dipped cotton cellulose fibres with PEDOT:PSS solution connected by Nickel foil and silver paint | Fabric based thermoelectric power generator | [101] |
| <i>p</i> -PEDOT:PSS/functionalized Te composite | $\Delta T = 13.4$ K | Output: 2.5 mV | Composite films of Te nanorods and PEDOT:PSS collected on PVDF membrane were pasted on polyimide substrates using Ag paste as interconnect | Flexible thermoelectric power generator | [102] |
| <i>p</i> -PEDOT:PSS/functionalized Te composite | 16 p-n legs, $\Delta T = 5$ K (deg cel) | Output: 12.75 mV, Power: 10.59 nW, Device resistance: 5000 Ω | Solution of Te nanorods and PEDOT:PSS printed on flexible PET substrates using Ag as interconnect | Flexible thermoelectric power generator | [103] |

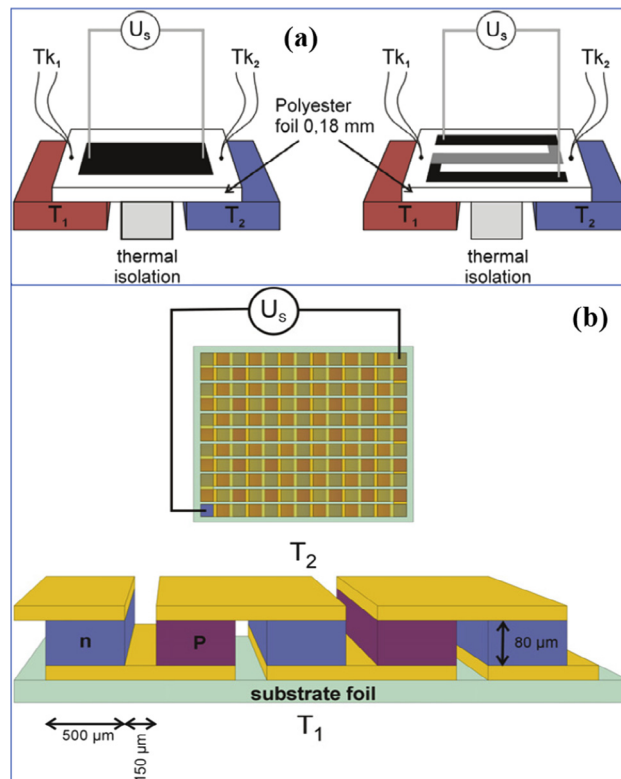


Fig. 18. (a) Schematic of the experimental set up; (b) design of a TEG with two dimensional arrangement of a meander of p-n junctions. Reproduced with the permission from Ref. [89].

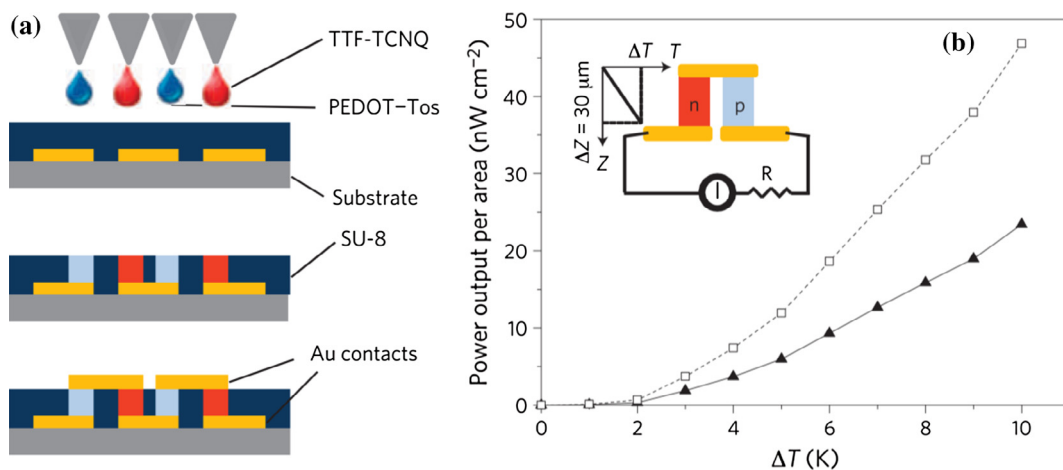


Fig. 19. (a) Thermogenerator fabrication process steps; (b) maximum power output per area of the PEDOT-Tos/TTF-TCNQ TEGs consisting of 54 thermocouples with the following leg dimensions: 25 mm × 25 mm × 30 μm. Reproduced with the permission from Ref. [71].

ensure good thermal contact between the layers when foil was wrapped on the cylinder and secondly, without any adhesive by directly winding the foil onto the cylinder. Influence of number of windings on power output of a rolled-up structure was also estimated by fabricating two serial devices (Fig. 21b) with 10 windings (576 junctions, ~1 m²) and 106 windings (7000 junctions). Though, the determined average Seebeck coefficients shown in Fig. 21c were all quite low (i.e. ~nV/K), but they represented Seebeck coefficient of the whole device including for substrate, adhesive, and all printed layers. Considering the effect of thermoelectric material only, average Seebeck coefficients were estimated from 0.7 to 3.5 μV/K, which were found comparable to the values determined for PEDOT:PSS pellets. The study clearly illustrates the emphasis of the relative thickness of the TE material and the substrate in the processing of OTEG and presents a quick method to process polymer based

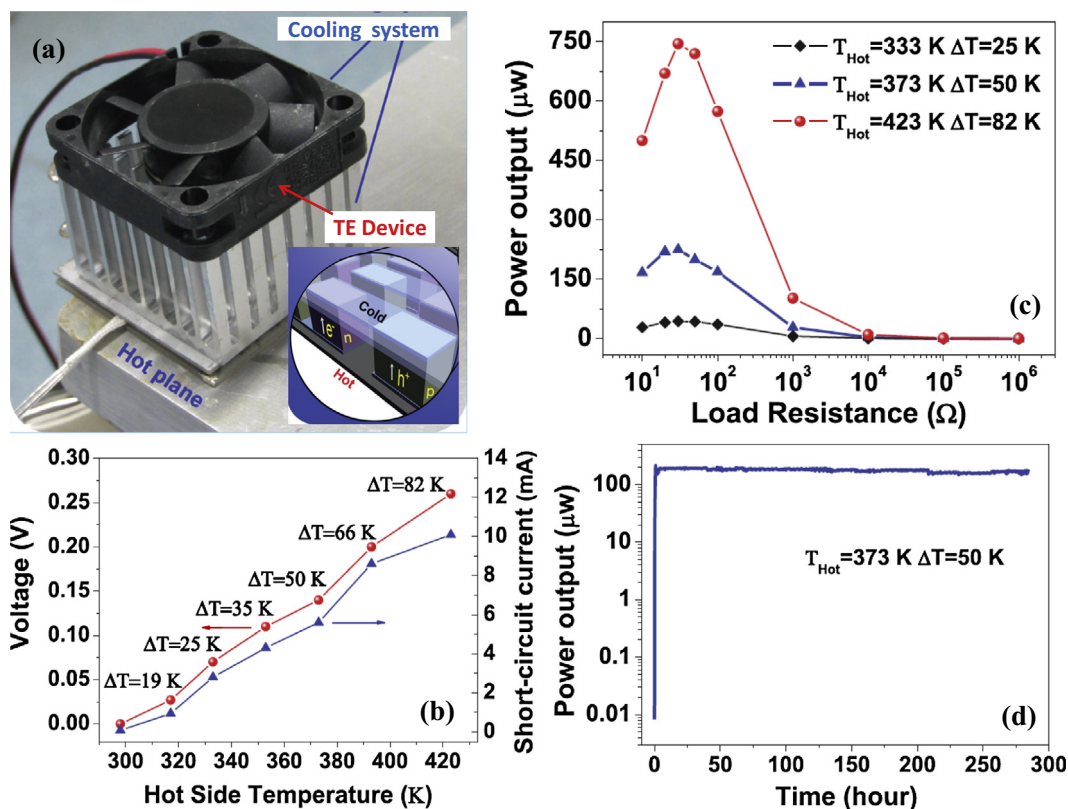


Fig. 20. (a) Photograph of thermoelectric module consisting of 35 thermocouples (Inset showing module structure); (b) the output voltage and short-circuit current at various T_h and ΔT ; (c) power output of the module with different load; (d) power output stability of the module operating with $T_h = 373$ K and $\Delta T = 50$ K. Reproduced with the permission from Ref. [91].

thermoelectric devices in series through R2R printing techniques. However, certain limitations of R2R method such as loss of thermal gradient through the carrier substrate as well as need and development of thin substrates must be looked upon for improvement [92].

To overcome these limitations of R2R technique, recently, a study reports solution casting polymerization (SCP) technique which can be applied to large area film processing as well as to conventional film processes of roll-to-roll/printing, thus, being not limited to the size of the chamber or substrate. Flexible and cuttable PEDOT films obtained by SCP [93] were used to generate Seebeck voltage by the touch of fingertips to harness human body's heat energy. These PP-PEDOT films exhibited high conductivity of 2120 S/cm at 1.1 V, where as maximum Seebeck coefficient ~ 190 $\mu\text{V/K}$ was obtained at -2 V. Enhancement of power factor to 1270 $\mu\text{W/m K}^2$ (at 0.1 V), the highest ever achieved, can be attributed to the optimized polymerization solution PP-PEDOT in which mixture of pyridine and PP-PEDOT [i.e. Poly(ethylene glycol)-*block*-poly(propylene glycol)-*block*-poly(ethylene glycol) triblock copolymer (PEPG) with PEDOT] caused higher degree of polymerization and much denser polymer films [93]. These PP-PEDOT flexible films deposited on PET substrate generated an output voltage of 8–10 μV by the touch of fingertips at room temperature (Fig. 22a), and when connected to Peltier's cooler at the opposite end generated a high Seebeck voltage of 584–590 mV (at temperature difference of 5.3 K); which dropped rapidly when finger was detached (Fig. 22b). High power factor ~ 1140 $\mu\text{W/m K}^2$ and $ZT \sim 1.02$ (estimated using κ reported [71] by Crispin et al.) show good possibility of device fabrication based on these films.

Fabrication of OTEG using only p-type element but with paper as a substrate (Fig. 23) has also been reported [94]. 5% ethylene glycol in aqueous solution of PEDOT:PSS was used to screen print the PEDOT:PSS layer (having 2.5 mm width, 40 mm length and about 20 mm thickness) on a 300 mm thick piece of paper. Eleven PEDOT:PSS arrays with 8 mm distance in between them, were printed on one piece of paper. Though high density of the arrays caused cracks in PEDOT:PSS films during drying but paper provided better thermal stability and better wettability to PEDOT:PSS ink than any other plastic substrates. Module 1 consisting of 385 thermocouples (70 pieces of series connected paper, 2 in parallel, 35 in series) resulted in an open circuit voltage of 0.2 V and a short-circuit current of 4 μA at $\Delta T = 50$ K, while module 2 containing 14 thermocouples (70 pieces of parallel connected paper, 5 in parallel, 14 in series) provided a lower open circuit voltage of 0.012 V and a higher short circuit current of 1.4 mA. Maximum output power ~ 4 μW obtained with a load resistance of about 7 Ω in case of module 2, can be used to power practical devices and was demonstrated by fabricating a larger area module containing 300 pieces of parallel connected paper (10 in parallel, 30 in series; Fig. 23d). Since the power ~ 50 μW and open circuit volt-

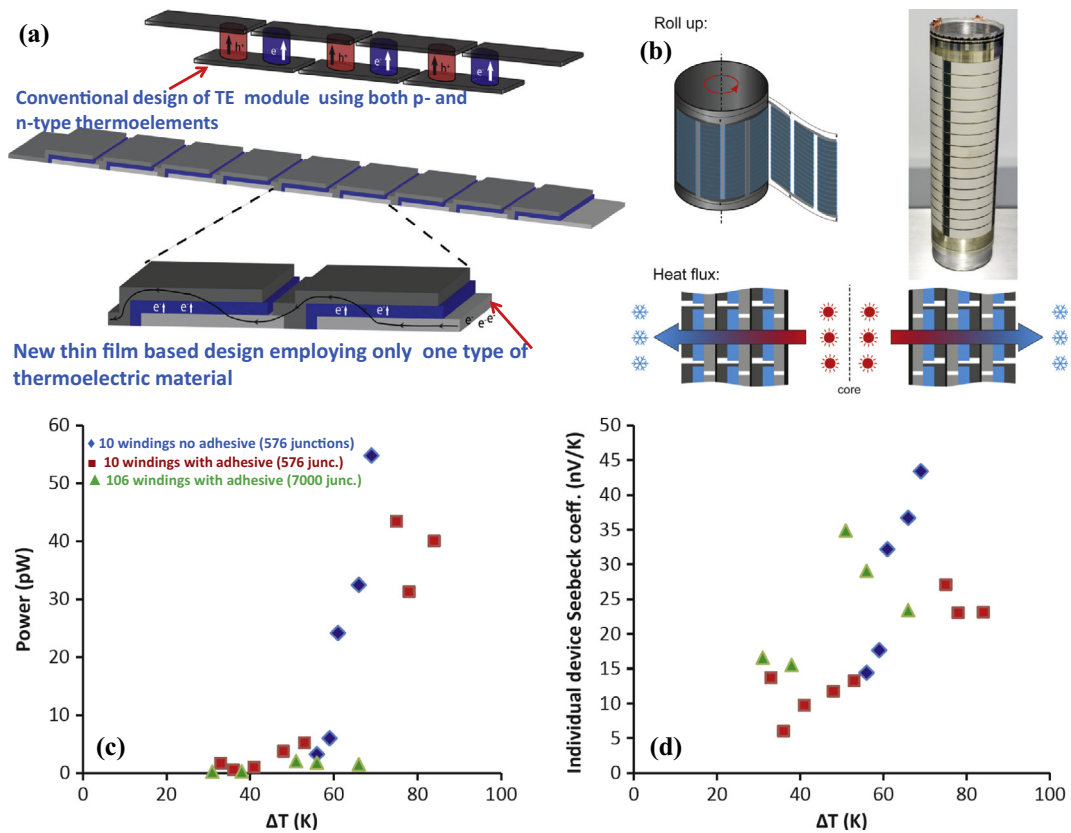


Fig. 21. (a) Traditional thermoelectric design employing complementary p- and n-type materials in order to avoid charge build up in the series connected system and new thin-film-based design employing only one type of thermoelectric material for series connection. When printing the top electrode of a junction this is simultaneously connected with the adjacent bottom electrode, thus allowing for directional charge transport without charge build up (the arrow tracing through the stacks show the flow of electrons); (b) Top: Illustration of and picture of the rolled-up final device, Bottom: Illustration of the heat transport in the final setup; (c) power factors and (d) seebeck coefficients obtained with the three different rolled-up structures [blue diamonds - 10 windings with no adhesive (576 junctions), red squares - 10 windings with adhesive (576 junctions), green triangles - 106 windings with adhesive (7000 junctions)]. Reproduced with the permission from Ref. [92].

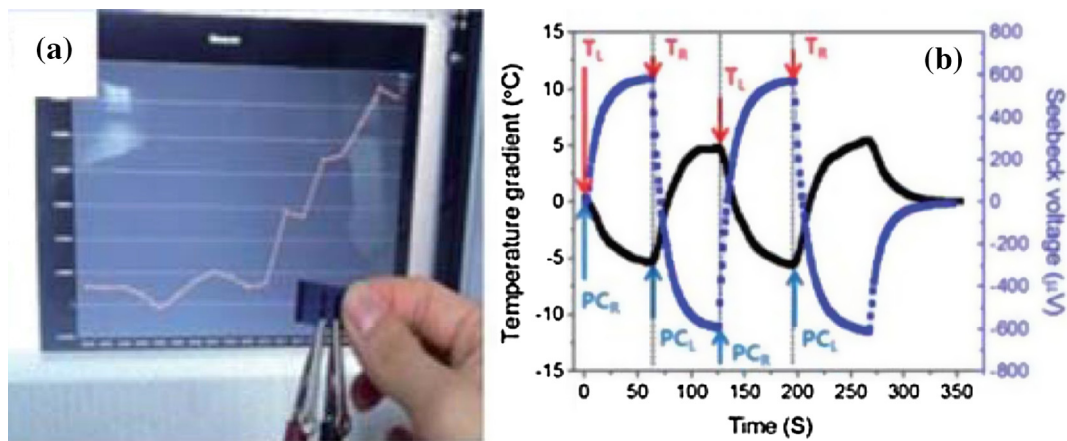


Fig. 22. (a) Electricity generation by fingertip touch at one side with air; (b) electricity generation (blue square) and the corresponding temperature gradient (black square) measured from Peltier module reference (TL: touch left side, TR: touch right side with fingertips, PCR: a right side Peltier device cooling, and PCL: a left side Peltier device cooling to generate the temperature difference). Reproduced with the permission from Ref. [93].

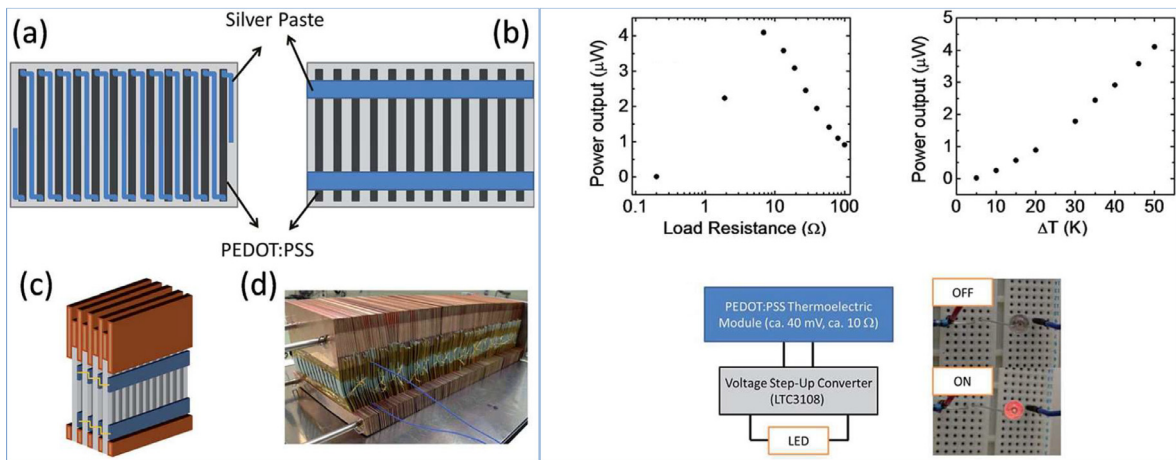


Fig. 23. Schematic representation of the (a) Series and (b) parallel PEDOT:PSS array; (c) schematic and (d) photograph of the PEDOT:PSS modules sandwiched between copper plates; (e) power output of parallel connected module (M2) at different load resistances; (f) maximum power output at different temperature differences; (g) schematic of the circuit for powering an LED and photograph of the LED driven by the PEDOT:PSS thermoelectric module. Reproduced with the permission from Ref. [94].

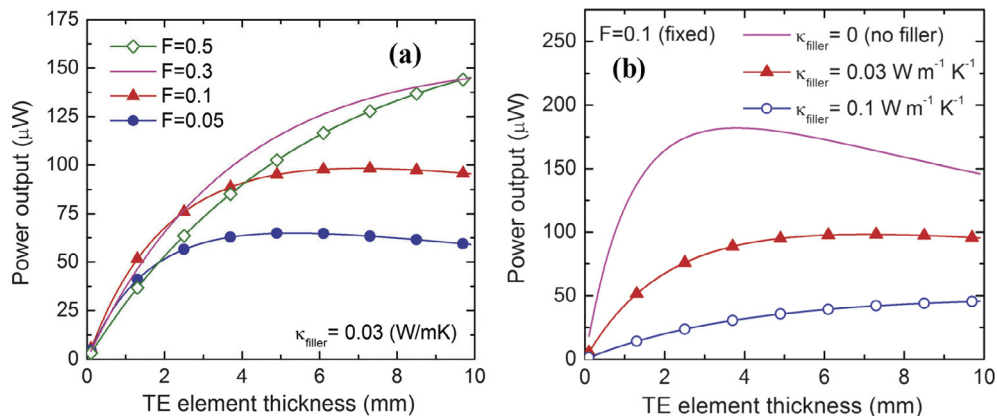


Fig. 24. (a) Calculated power output for the inorganic-polymer hybrid material PEDOT/Bi₂Te₃ composites reported by Zhang et al. [82] as a function of TE element thickness, the module size is 3 cm × 15 cm (wrist-band type), and the cross-sectional area of each TE element is 0.5 × 0.5 cm². The number of TE elements was determined by the fill factor and the thermal conductivity of the gap filler is 0.03 W/m K; (b) Power output with varying gap filler's thermal conductivity for the same inorganic-polymer hybrid material as a function of TE element thickness when the fill factor was fixed to 0.1. Reproduced with the permission from Ref. [9].

age ~40 mV achieved in this case was low, therefore a DC to DC convertor was used to boost the output voltage to ~2.2 V (i.e. sufficient to illuminate an LED) [94].

However, power generation for practical applications (>100 mW) requires millimetre-level thickness of TE materials and a large size of the device [9]. Variation of power output as a function of thermoelement's thickness (by considering different values of fill factor (i.e. amount of space covered by thermoelements in a module) and gap fillers) has been demonstrated [9] and is shown in Fig. 24. Therefore, while optimization for TE performance of a device due attention should be given to fill factor and as well as to gap filler materials.

Apart from these studies, few groups have also focussed on the development of OTEGs which were prepared from organic/CNTs or organic/inorganic composites in order to improve TE performance by integrating the advantages of each component. Recently, Wanq et al. [90] have demonstrated a flexible thermoelectric nanogenerator (TENG) both as a temperature sensor and energy harvester based on Te nanowire/P3HT composites. These composites exhibited $\alpha \sim 285 \mu\text{V/K}$, though much smaller than $\alpha \sim 408 \mu\text{V/K}$ of Te materials (reported by He et al. [48]), but greater than α (about $24 \mu\text{V/K}$) of pristine P3HT [83]. Two TENGs provided an output voltage of 38 mV in serial connection and a current density exceeding 32 nA/mm² in parallel connection when the temperature gradient was 55 K (Fig. 25). The output voltage ~2.5 mV and current ~16nA of the flexible device when attached to human body (with cooler attached to outer surface) indicated its use as a wearable energy harvester. Whereas, TENG as self-powered temperature sensor had output voltage of 0.8 mV with response time

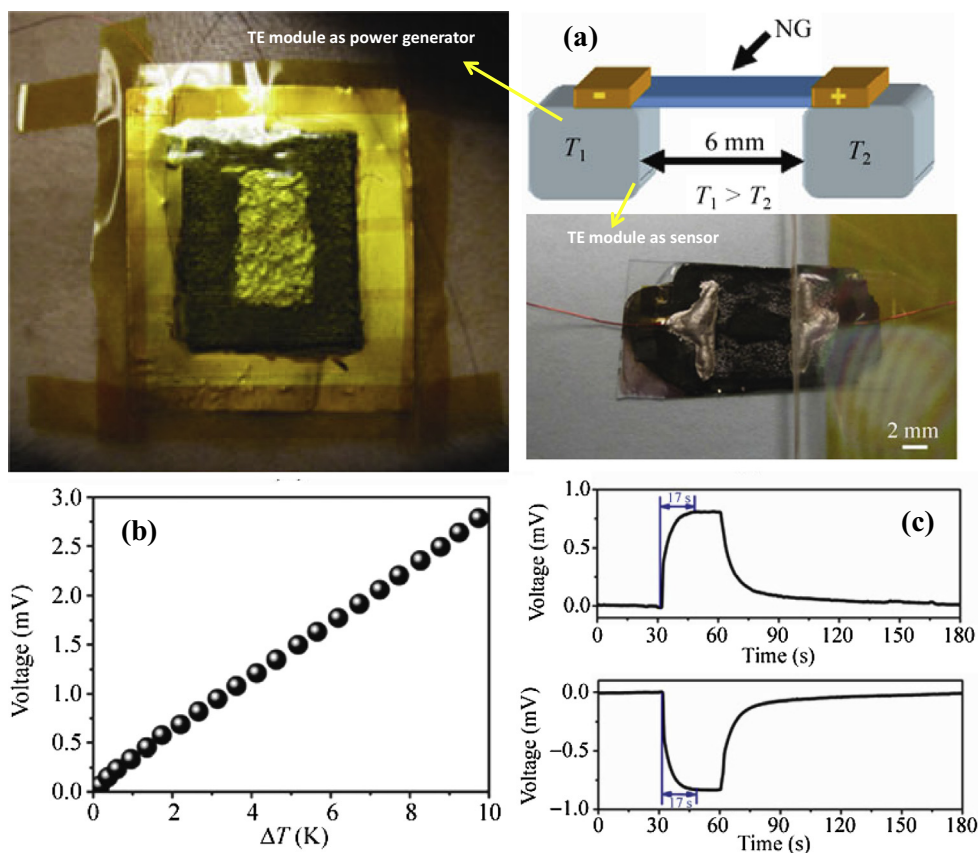


Fig. 25. (a) Schematic diagram showing measurements of the device attached on the human body and as a self-powered temperature sensor (photographs of a Te-nanowire/P3HT-polymer composite device on a fabric attached with Kapton substrate); (b) the output voltage of the TENG as a function of change in temperature difference across the device; (c) electrical output voltage of the sensor when it was contacted with a heat source at a temperature of 298 K in forward connection and reversed connection conditions. Reproduced with the permission from Ref. [90].

and reset time of about 17 s and 9 s respectively and was used to measure the temperature of exhaled air from lungs. The study also compares Te nanowire/PEDOT:PSS composites with Te nanowire/P3HT and observed better flexibility in case of P3HT polymer [90].

Following the similar trends on hybrids materials, recently Cai et al. [102] developed a flexible OTEG as shown in Fig. 26a using eight strips of PEDOT/Te composite pasted on a polyimide substrate with Ag interconnect. It gave an output voltage of 2.5 mV (shown in Fig. 26b) when temperature difference between body and environment was 13.4 K.

Similarly Te/PEDOT:PSS (H_2SO_4 treated) hybrids were used to fabricate an OTEG (device geometry shown in Fig. 27a) [103]. Printed module had 32 legs (each having dimensions of 1 mm \times 1 cm) with overall size of TEG as 5 cm \times 3 cm with Ag as metallic interconnect (Fig. 27b). Fig. 27c shows the output of TE module with varying number of p-n legs. Whereas, Fig. 27d shows the maximum output voltage \sim 12.75 mV and output power \sim 10.59 nW of 16p-n legs when ΔT was 5 $^\circ\text{C}$ and internal resistance was 5 k Ω . Moreover, consistent voltage response of 2 ± 0.2 mV for $\Delta T = 0.5$ K (shown in Fig. 27e) developed between the middle (air) and edge (hot plate) part established the use of TEG as thermal sensor also [103].

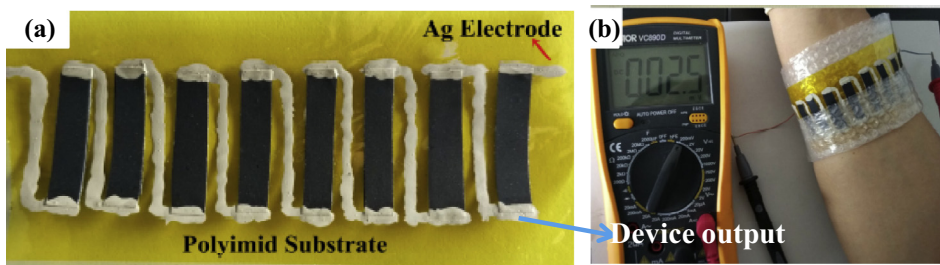


Fig. 26. (a) Photograph of a flexible device consisting of eight (PEDOT:PSS/PF-Te)-Ag thermocouples on a polyimide substrate; (b) output performance of the device due to the temperature difference between a fore arm (\sim 305.4 K) and the ambient (\sim 292 K). Reproduced with the permission from Ref. [102].

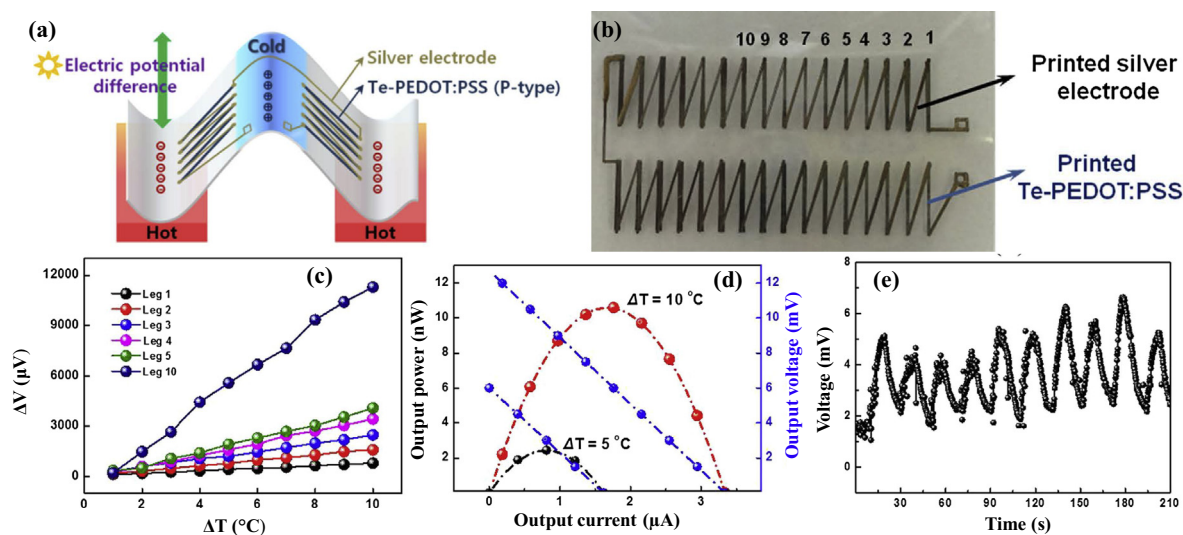


Fig. 27. (a) Schematic diagram of geometry of the reported thermoelectric generator and the generation of electricity; (b) image of the planar thermoelectric generator consisting of 32 legs arranged in two rows; (c) open circuit thermoelectric voltage (V_{OC}) vs. temperature difference (ΔT) according to the number of TE legs; (d) output power curves depending on the output voltage and output current at $\Delta T = 5$ and 10°C ; (e) variation of output thermoelectric voltage with the cyclic change in temperature difference. Reproduced with the permission from Ref. [103].

OTEGs can also be fabricated by making composites of insoluble co-ordination polymers with other polymers that easily exist in form of solutions. For instance, the study [95] makes use of poly[Cu_x(Cu-ett)] and poly[K_x(Ni-ett)] respectively as p- and n-type metal coordination polymers that were ball-milled with other polymeric solutions, which enabled these infusible polymers to be deposited as films. The power factors reached to 1.92 and 1.58 $\mu\text{W}/\text{m}^2\text{K}^2$ at 400 K respectively for n- and p-type composites with mass ratio of 2:1 of coordination polymer to PVDF. The p- and n-type composite films (of thickness $\sim 2\text{--}5\ \mu\text{m}$) were deposited onto PET substrate by inkjet printing and dried at 363 K for 10 h. Later, a 100 nm gold electrode was thermally evaporated to connect each p- and n-type leg for the module fabrication. The voltage output reached 15 mV at the temperature gradient of 25°C . In the module, the contact resistance at the TE material and device electrode interface was quite high ($\sim 51\ \Omega$) in comparison to resistance of the TE leg ($\sim 3.1\ \Omega$), hence, caused hindrance to the current/power output. The maximum output power of 45 nW was obtained for load resistance of $5000\ \Omega$ [95].

Another study also reports fabrication of flexible TEG modules by making use of composite of screen-printed inorganic thick film and organic CP [96]. Initially, n-type legs were screen-printed on polyimide (PI) substrate using Bi_2Te_3 film and subsequently Sb_2Te_3 film was printed on the same PI film to form p-type legs with thickness of 40 nm for each leg. These screen-printed films were annealed in a nitrogen ambient and coated with DMSO mixed PEDOT:PSS solution afterwards. Ag film (thickness $\sim 10\ \text{nm}$) was deposited as metallic interconnect and was annealed at 200°C for 20 min in a vacuum ambient. The module having 7 TE couples gave output voltage of 85.2 mV and the output power density of $1.2\ \text{mW}/\text{cm}^2$ at $\Delta T = 50\ \text{K}$ with hot end temperature $\sim 333\ \text{K}$. Such TEG module (shown in Fig. 28) can be used to power various wearable devices. The study also illustrates the performance of TEG module consisting of 15 TE couples by using the difference between the body temperature and the ambient temperature. The output voltage of the module was $\sim 12.1\ \text{mV}$ for temperature difference $\sim 5\ \text{K}$ [96].

In pursuit of wearable TEGs, recently a study has demonstrated an interesting fabric-based OTEG [97]. PEDOT:PSS coated commercial fabric was cut into thin strips (each with dimensions $40\ \text{mm} \times 5\ \text{mm}$) and those strips were mounted on another piece of commercial fabric (used as the substrate) by using silver paint (keeping distance between two strips $\sim 5\text{--}6\ \text{mm}$). Silver wires of diameter 0.2 mm were used as interconnect along with fine layer of conductive silver paint (applied between silver wire and PEDOT:PSS coated fabric) to reduce the contact resistance. The increased air permeability of the coated polyester fabric from $30.70 \pm 1.10\ \text{cm}^3/\text{cm}^2/\text{s}$ to $47.67 \pm 1.73\ \text{cm}^3/\text{cm}^2/\text{s}$ showed that the PEDOT:PSS coating had no negative effect on the breathable aspect of the fabric and flexibility of the fabric was maintained as such. The fabric-based TE module consisting of 5 PEDOT:PSS coated strips resulted in output voltage of $\sim 4.3\ \text{mV}$ at a temperature difference (ΔT) of $75.2\ \text{K}$ and when the load resistance matched the internal fabric resistance, the maximum power (P_{max}) was $12.29\ \text{nW}$ (Fig. 29). ZT value of the PEDOT:PSS coated fabric (average taken after 5 times measurements) increased from 9.5×10^{-5} (using in-plane thermal conductivity of PEDOT:PSS coated fabric as $0.12\ \text{W}/\text{K}$) to 0.5 at 300 K (greater than ZT of 0.42 for PEDOT:PSS reported [72] by K.P. Pipe research group), and the device efficiency (η_{TE}) was found to increase from 7.8×10^{-7} to 3.3×10^{-3} assuming the environmental and human body temperatures at 300 K and 310 K respectively [97].

Similarly, a recent study [101] has demonstrated an OTEG using non-woven fabric as substrate rather than paper/woven fabric. Cotton cellulose fibre when soaked with PEDOT:PSS solution exhibited very less κ ($0.10\ \text{W}/\text{m}\ \text{K}$) [101] even less than both PEDOT/paper composites [81] and PEDOT/woven fabric [97] due to excess porosity in case of non-woven fibre than

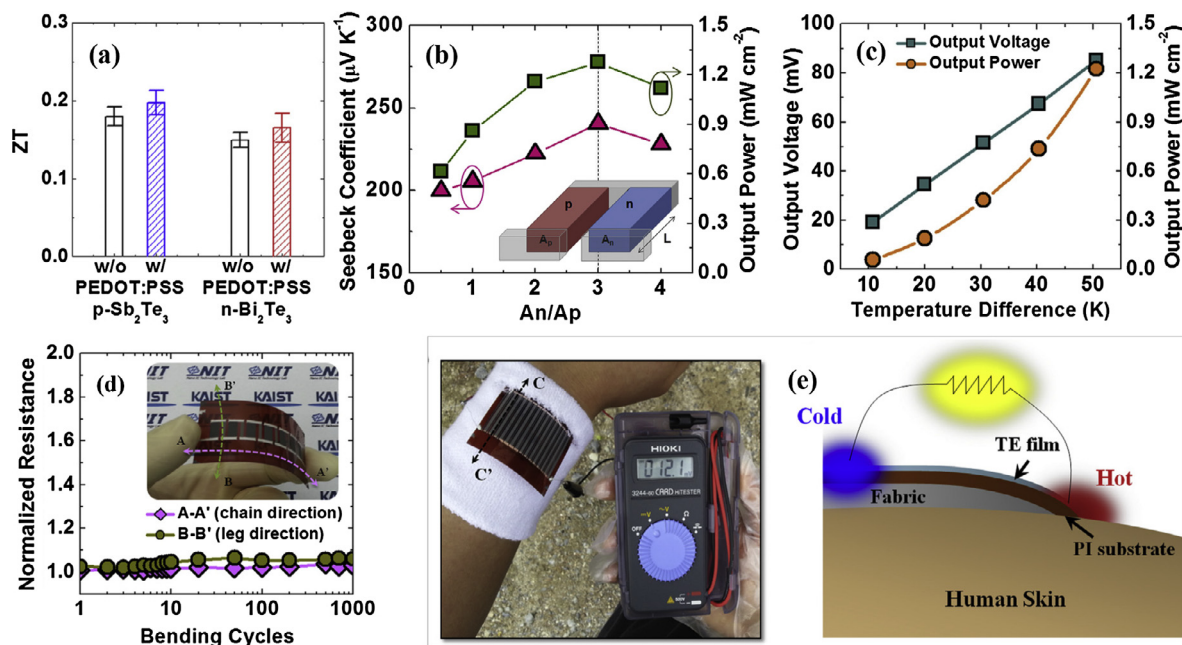


Fig. 28. (a) Figure-of-merit (ZT) of the samples with (w/) or without (w/o) PEDOT:PSS infiltration; (b) the Seebeck coefficient (filled triangles) and output power density (filled squares) of the TEG module as a function of different area ratio (A_n/A_p); (c) output voltage (filled squares) and output power density (filled circles) as a function of temperature difference of a fabricated flexible thermoelectric power generator (TEG) module; (d) resistance changes of the module as a function of the number of bending cycles with bending radius of 4 cm (the internal resistance of the unbent (flat) TEG module was 145.2 Ω); (e) performance demonstration of a flexible TEG module exploiting body heat and cross section along with C–C' (The output voltage of the module with 15 TE couples and the length of 30 mm, using the temperature difference between the body temperature and the ambient air temperature was 12.1 mV at a temperature difference of about 5 K). Reproduced with the permission from Ref. [96].

paper. Alignment of cotton fabric (acting as the substrate) in both perpendicular and in-plane directions with increasing PEDOT:PSS content resulted in isotropic electrical conductivity and emphasized the structure-property interplay in determination of TE properties. While, Seebeck coefficient was nearly independent of PEDOT:PSS concentration and did not show strong isotropy. Six uni-leg of fabric were connected using Ni foil and Ag paste as TE module (shown in Fig. 30) and it has been observed that contact resistance between PEDOT and metal electrode was also reduced due to enhanced area of wavy fibres. As a result, fabric elements gave power output of 34 μW at ΔT equals to 55 K [101].

In quest of stable n-type flexible films, multi-phase thermoelectric materials (showing n-type conduction) when mixed with polymers showed good thermoelectric performance. Cu doped Bi₂Se₃ nanoplates and Polyvinylidene Fluoride (PVDF) composite films exhibited power factor of 103 $\mu\text{W}/\text{m}^2\text{K}^2$ and $ZT \sim 0.1$ at 290 K [98]. Such improved thermoelectric performance for n-type organic materials can be attributed to the decoupled Seebeck coefficient and electrical conductivity due to energy filtering effect at organic/inorganic interface. Output voltage of 1.3 mV at $\Delta T = 15$ K (shown in Fig. 31), upon fingertip touch, demonstrates the use of n-type flexible composite films for self powered wearable electronics and sensors. The mechanism used in the study can be extended to other conductive-inorganic-nanocrystal/non-conductive-polymer composites [98]. Dun et al. [99] also investigated the finger tip touch response in case of Te nanorod/PVDF composites in which output voltage of 1 mV was obtained at temperature difference of about 4 K. In spite of the low value of electrical conductivity ~ 5 S/cm, significantly high value of Seebeck coefficient ~ 288 $\mu\text{V}/\text{K}$ resulted in room-temperature power factor of 45.8 $\mu\text{W}/\text{m}^2\text{K}^2$ for these flexible composite films. It has also been estimated that with coverable area of thermal radiation (which equals to 2 m and 100 W in case of a human body) ZT value of 0.005 can give power output ~ 4 mW, which can be sufficient enough to power wearable electronics [99].

6. Unrealized potential in the field of organic thermoelectric power-generation

CP-based thermoelectric devices can make use of the low temperature gradients (up to 10–12 $^\circ\text{C}$) lying in natural resources such as oceans, geo-thermal sources etc. for energy-harvesting. In addition, for low power applications, human body's temperature can also serve to create thermal difference with the ambience to be used in thermoelectric power generation. So far, the investigation of various CPs in the context of thermoelectric applications suggests that low power factor is the main hurdle in achieving high efficiency. The tuning of doping level in a CP (in such a way that critical regime of transport can be achieved) may be the best strategy for power factor optimization. In organic thermoelectrics, most of the studies for improving power factors are focussed on improving electrical conductivity (either by doping or mobility enhancement) without much attention on Seebeck coefficient. For a real practical application such as powering any electronic equipment,

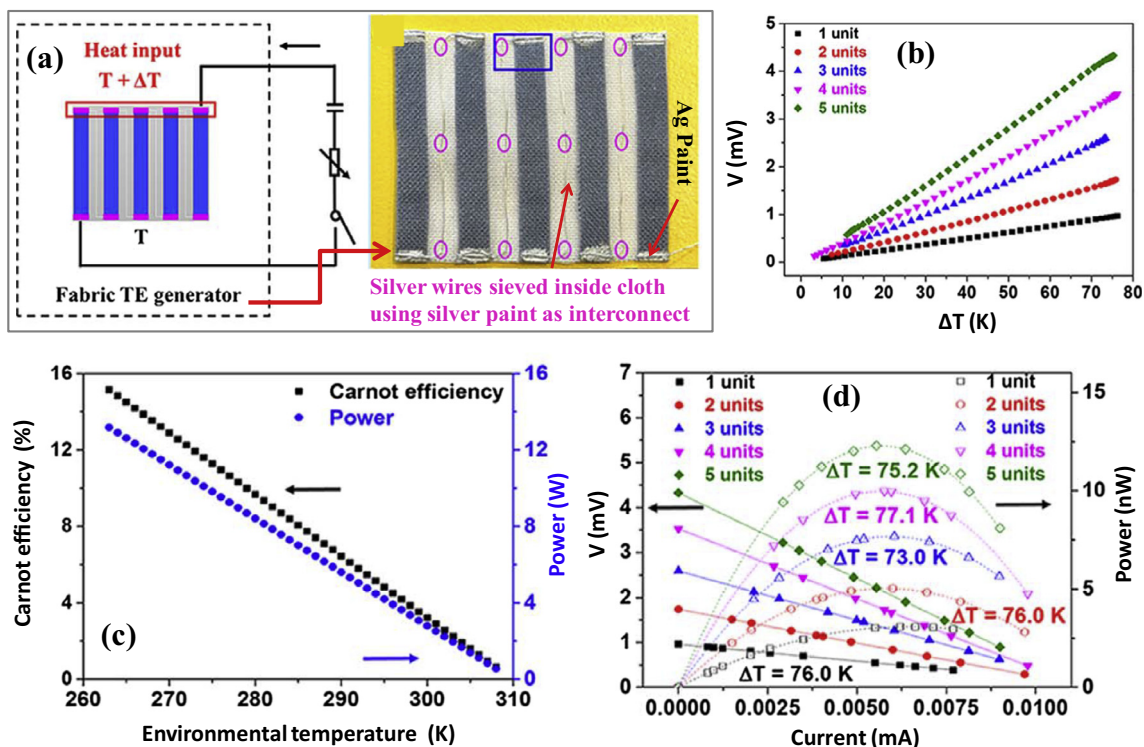


Fig. 29. (a) Schematic illustration of a fabric TE power generating unit made of multiple PEDOT:PSS coated strips and photograph of the positive face of the TE generator device; (b) TE voltage generated by the prepared devices versus ΔT ; (c) calculated Carnot efficiency and available power versus environmental temperature (assuming the human body temperature is 310 K); (d) output voltage and power as a function of current for the prepared devices. Reproduced with the permission from Ref. [97].

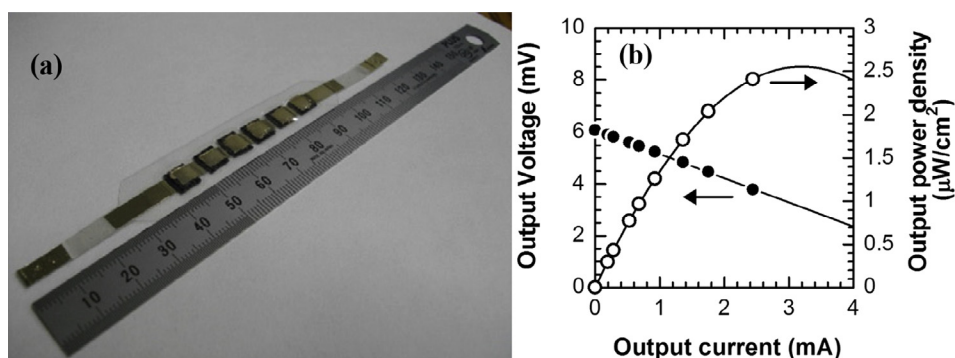


Fig. 30. (a) Photograph of the TE module; (b) Measured TE output voltage and power density of the module consisting of six fabric elements connected in series as a function of TE output current. Reproduced with the permission from Ref. [101].

one needs a sufficient voltage (~ 1.5 V) and current of a few mA (~ 10 mA). Therefore, to achieve such high output-voltage from organic thermoelectric devices, the Seebeck coefficient of the organic thermoelements must be high. Hence, for power factor enhancement, emphasis should be placed on optimization of both electrical conductivity and Seebeck coefficient. But the improvement of Seebeck coefficient in CPs requires the knowledge of different contributing factors such as electronic and phonon drag, and electron-phonon scattering. As seen from many previous studies, enhancement of the power factor has been realized in many organic-inorganic composites. But while designing such composites, care has to be taken that the conducting paths should have both organic and inorganic components with weighted average of Seebeck coefficients [114]. Also, to have a facile transport of charge-carriers, Fermi levels of organic and inorganic components need to be matched in such composites [11,114]. Moreover, the energy-filtering phenomenon in composites enhances Seebeck coefficient but requires a careful design of organic/inorganic interface, such that high electrical conductivity is maintained.

Till now, to enhance the thermoelectric properties of a particular CP, several innovative routes have been applied separately. We need to adopt a cumulative approach by merging these strategies (mentioned in the schematic shown in Fig. 33)

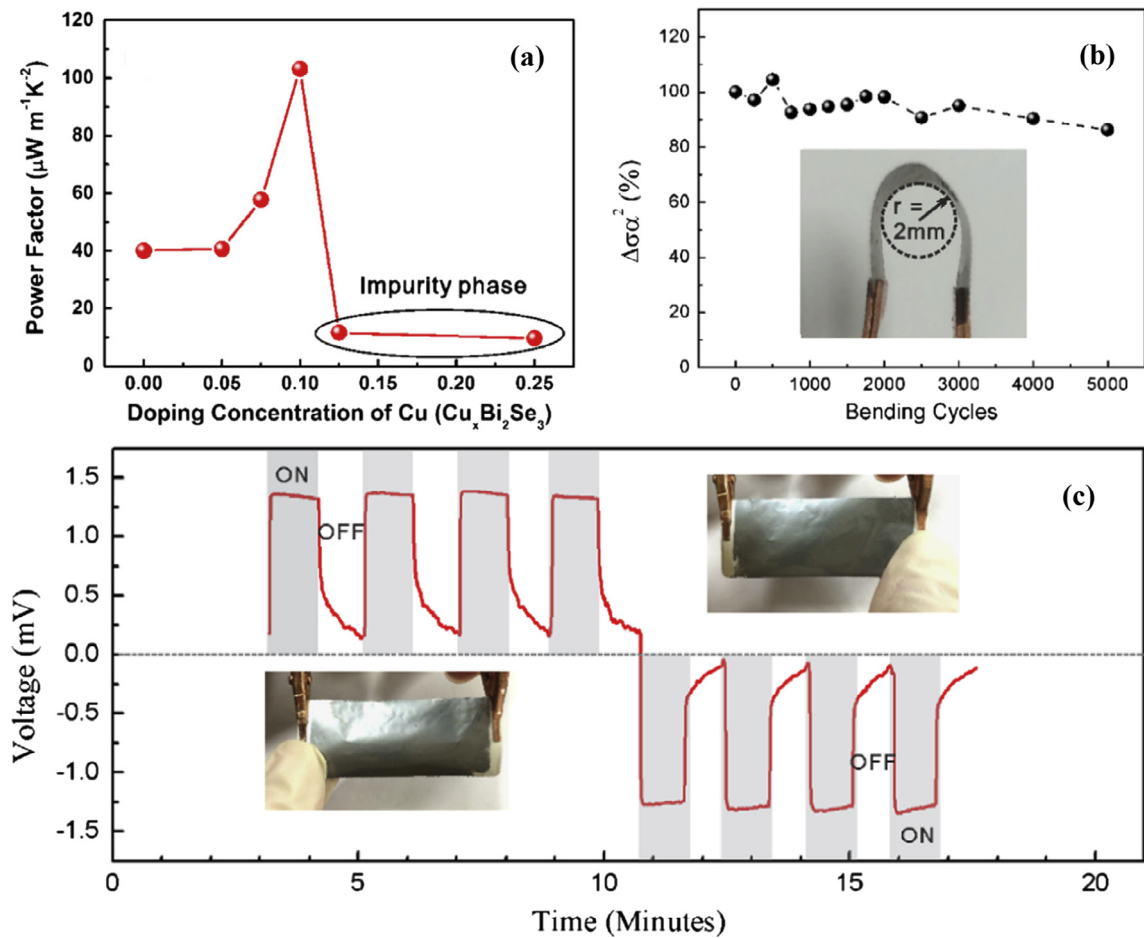


Fig. 31. (a) Room temperature power factors of Cu-doped Bi_2Se_3 nanoplates based thermoelectric films as a function of Cu doping concentrations; (b) reliability of the thermoelectric power factor over numerous bending cycles with the inset image demonstrating a bending test, where the bending radius is 2 mm; (c) fingertip touch response of the $\text{Cu}_{0.1}\text{Bi}_2\text{Se}_3$ nanoplate based flexible thermoelectric films, which shows the thermoelectric films could continuously convert the body heat into electricity. Reproduced with the permission from Ref. [98].

to strengthen the thermoelectric performance of a specific CP. Recently, a study reporting chemical treatment of hybrids-films of PEDOT:PSS and Te by H_2SO_4 is an apt illustration of combining two individual approaches for optimizing the TE performance [103]. Similarly in another report, PEDOT films exhibited a much higher $\sigma \sim 5400$ S/cm due to a combined approach in which controlled ordering of chains is followed by doping. The study shows the use of iron(III) trifluoromethanesulfonate as oxidant, N-methyl pyrrolidone as polymerization rate-controller and sulphuric acid as dopant, and illustrates that structural alignment together with carrier enhancement resulted in high conductivity of PEDOT films [111].

Following the synthesis stage, attempts should be made for precise ZT estimation. Mostly home-built customized set-ups used in measurement techniques emphasize the need for developing some standard measurement-tools/apparatus. Though this seems a matter of distant concern at such an initial stage of organic thermoelectrics, we think that the establishment of some standards like those existing in the field of photovoltaics is really a significant issue to be looked upon.

With the design and synthesis of high ZT organic materials, there comes the challenge of their translation in terms of smart and flexible wearable devices. Fabrication of such devices needs CPs which can exhibit both p and n-type conduction. At present, there are many options available for stable CPs with p-type conduction, but on the other hand n-type developed so far (by doping of two polymers or from co-ordination compounds of metal ligands) do not exhibit enough electrical conductivity as well as good environmental stability. However, a recent news has shown that the n-type conductive polymer (shown in Fig. 32), designed by the team "Printing Technology" at the Fraunhofer IWS Dresden [100], displayed electrical conductivity varying from 60 S/cm to 120 S/cm (i.e. one order higher as compared to the traditional n-type polymer) when temperature was raised from 40 °C to 200 °C [100].

Similarly, a recent study reports that n-type flexible films of PVDF- Bi_2Se_3 (Cu doped) nano-platelets have shown $ZT \sim 0.1$ [98]. Thus, these multi-phase thermoelectric materials can be used to synthesize n-type elements for thermoelectric modules.

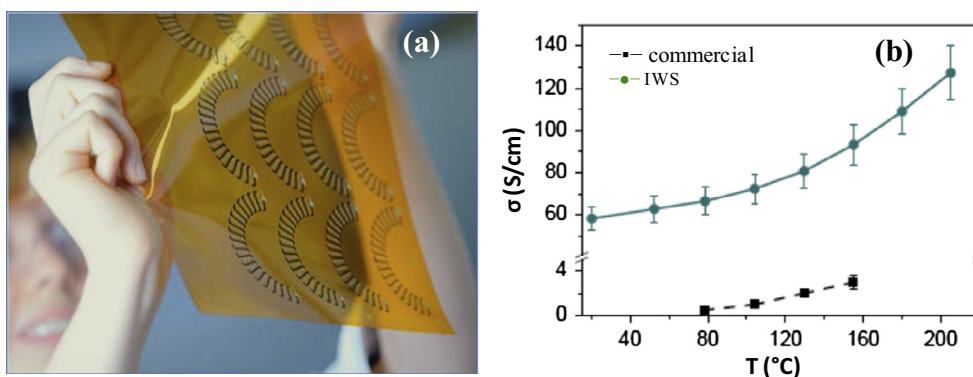


Fig. 32. (a) Photograph of polymer-based flexible thermoelectric generator; (b) Temperature dependence of electrical conductivity of n-type conducting polymer (non-doped) compared to a commercially available polymer. Reproduced with the permission from Ref. [100].

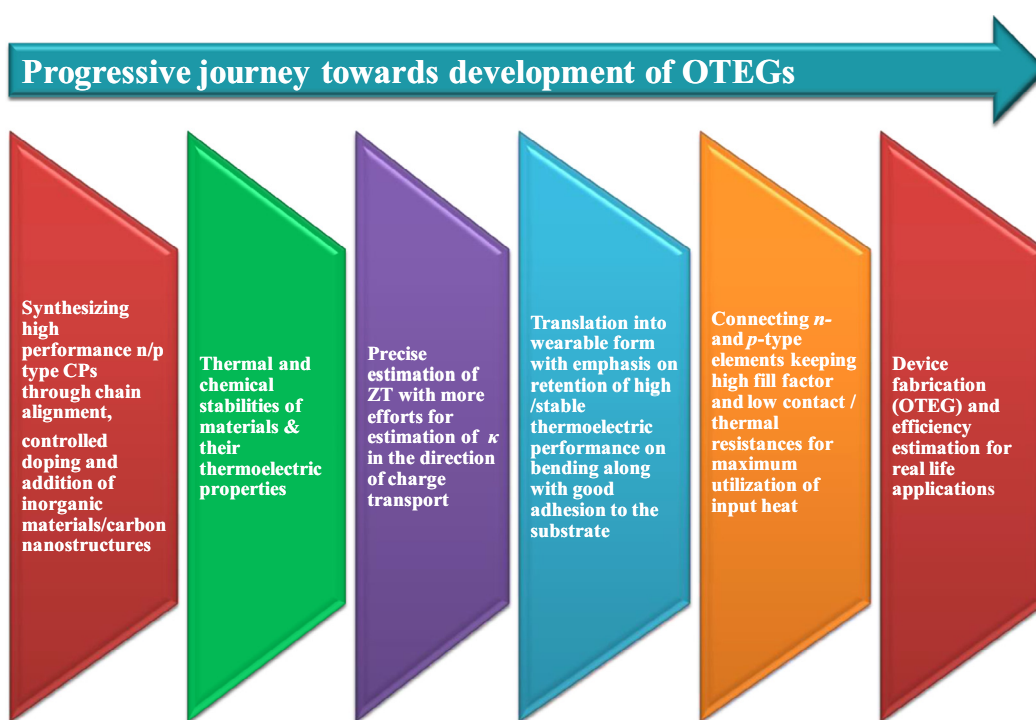


Fig. 33. Schematic revealing various stages of organic thermoelectric power generation.

CPs are easily processable due to solution-growth techniques. However, an inexpensive technique that can lead to enormous production on a large scale is yet to be discovered. In this regard, we need to integrate the available tools of large-area electronic displays, photovoltaics etc. that can be transferred to the field of flexible thermoelectrics [11]. Recently, roll to roll (R2R) method [92] for fabricating a large-area OTEG using only one type of (i.e. p-type) element has been reported. Therefore, device-design and structure make the most significant part to realize the concept of organic-thermoelectric wearable-devices. Also, decrease in thermoelectric performance due to the degradation of interfacial contact [94] needs to be taken care of and proper techniques must be developed to have better interconnects. Moreover, in-plane and out-of-plane measurements of thermoelectric parameters also play a role in finalizing the device-geometry due to anisotropy exhibited by both electrical and thermal conductivities. The commercial use of these wearable TE devices (having different device geometries) may not only be limited by their low efficiency but also by the level of comfort in using them. Schematic shown in Fig. 33 summarizes the main areas that need attention to move forward in the field of organic thermoelectrics. Regardless of so many challenges, the ongoing research in this field clearly ensures that CPs based thermoelectric power generators (i.e. OTEGs) can be made viable for practical use. Although the presently demonstrated OTEGs have exhibited low efficiency/low power-output, still their deployment can be thought of by charging supercapacitors or energy-storage cells. Such hybrid

devices can provide high output-power for a flash of time (i.e. by the discharging of supercapacitor) and it can be used to turn on sensors, transducers, etc.

7. Conclusion

In this review, we have discussed exciting studies exploring the role of CPs for thermoelectric applications (from materials to the device status). The efficiency of polymeric thermoelectric materials is limited by their relatively low power-factors. Therefore, in the case of CPs which possess the additional advantage of low thermal conductivity, to achieve high ZT ; we just need to concentrate on the improvement of power-factor. However, structure-property dependence requires careful attention while optimizing for power-factors. Also, numerous strategies such as addition of inorganic materials/carbon nano-structures as fillers, controlled doping, and enhancement of ordering and crystallinity in polymer matrices need to be merged together rather than applying them individually for amplification of thermoelectric properties of CPs. Till date, the maximum ZT of p-type polymer at room temperature (i.e. 0.42 at RT) has been obtained in DMSO treated PEDOT:PSS. However, feasible n-type polymers that are available at present have been made possible with metal co-ordination compounds or hybrid materials only. So far, for n-type organic materials, the best reported $ZT \sim 0.2$ (at 167 °C) has been observed for coordination organic compound poly[K_x(Ni-ett)]. Despite the several reports that have confirmed improvement in the thermoelectric properties of CPs, the development of efficient polymer based thermoelectric devices still lies at its initial stage. In the light of this, the present article summarizes the strategies required for the development of efficient organic thermoelectric devices as well as the challenges that arise due to complex structure-property relationship of CPs. However, inherent features like low cost, flexibility, non-toxicity, solution processability of CPs along with promising outcome of ongoing research grant us enough valour to search their applications in low-heat recovery programmes. That time does not seem far when the collective approach of diversified fields of polymer engineering and device fabrication will make us capable of harnessing each and every bit of thermal gradient that exists in our surroundings.

Acknowledgement

Meetu Bharti would like to acknowledge University Grants Commission (UGC), Delhi, India and Directorate of Higher Education (DHE), Haryana, India for their support under the Faculty Improvement Programme of Plan-XII. The author would also like to thank her colleagues Dr. Ramnik Mohan (Retd. Associate Professor & Head) and Sh. Raminder Hooda (Associate Professor) from Department of English, A.I.J.H.M. College, Rohtak for their support and willingness to edit the manuscript.

References

- [1] Dubey N, Leclerc M. Conducting polymers: efficient thermoelectric materials. *J Polym Sci Part B: Polym Phys* 2011;49:467–75.
- [2] Bubnova O. Thermoelectric properties of conducting polymers. Ph.D. Thesis. Sweden: Linköping University; 2013.
- [3] Han C, Li Z, Dou SX. Recent progress in thermoelectric materials. *Chin Sci Bull* 2014;59:2073–91.
- [4] Pichanusakorn P, Bandaru P. Nanostructured thermoelectrics. *Mat Sci Eng R* 2010;67:19–63.
- [5] Aswal DK, Yakhmi JV. Molecular and organic electronic devices. Nova Sciences Publishers; 2010.
- [6] Wei Q, Mukaida M, Kirihara K, Naitoh Y, Ishida T. Recent progress on PEDOT-based thermoelectric materials. *Materials* 2015;8:732–50.
- [7] Bubnova O, Crispin X. Towards polymer-based organic thermoelectric generators. *Energy Environ Sci* 2012;5:9345–62.
- [8] He M, Qiu F, Lin Z. Towards high-performance polymer based thermoelectric materials. *Energy Environ Sci* 2013;6:1352–61.
- [9] Bahk JH, Fang H, Yazawa K, Shakouri A. Flexible thermoelectric materials and device optimization for wearable energy harvesting. *J Mater Chem C* 2015;10:1039–51.
- [10] Chen Y, Zhao Y, Liang Z. Solution processed organic thermoelectrics: towards flexible thermoelectric modules. *Energy Environ Sci* 2015;8:401–22.
- [11] Kroon R, Mengistie DA, Kiefer D, Hynynen J, Ryan JD, Yu L, et al. Thermoelectric plastics: from design to synthesis, processing and structure–property relationships. *Chem Soc Rev* 2016;45:6147–64.
- [12] Russ B, Glaudell A, Urban JJ, Chabinyk ML, Segalman RA. Organic thermoelectric materials for energy harvesting and temperature control. *Nat Rev Mater* 2016;1:1–13.
- [13] Aswal DK, Basu R, Singh A. Key issues in development of thermoelectric power generators: High figure-of-merit materials and their highly conducting interfaces with metallic interconnects. *Energy Convers Manage* 2016;114:50–67.
- [14] Snyder GJ, Toberer ES. Complex thermoelectric materials. *Nat Mater* 2008;7:105–14.
- [15] DiSalvo FJ. Thermoelectric cooling and power generation. *Science* 1999;285:703–6.
- [16] Zhou Y, Wang L, Zhang H, Bai Y, Niu Y, Wang H. Enhanced high thermal conductivity and low permittivity of polyimide based composites by core-shell Ag@SiO₂ nanoparticle fillers. *Appl Phys Lett* 2012;101:012903–12904.
- [17] Han Z, Fina A. Thermal conductivity of carbon nanotubes and their polymer nanocomposites: a review. *Prog Polym Sci* 2010;36:914–44.
- [18] Kurabayashi K. Anisotropic thermal properties of solid polymers. *Int J Thermophys* 2001;22:277–88.
- [19] Choy CL. Thermal conductivity of polymers. *Polymer* 1977;18:984–1004.
- [20] Zhang Y, Boer B, Blom Paul WM. Trap-free electron transport in poly(p-phenylene vinylene) by deactivation of traps with n-type doping. *Phys Rev B* 2010;81:085201–85205.
- [21] Lee JM, Park JS, Lee SH, Kim H, Yoo S, Kim SO. Selective electron- or hole-transport enhancement in bulk-heterojunction organic solar cells with n- or b-doped carbon nanotubes. *Adv Mater* 2011;23:629–33.
- [22] Bredas JL, Street GB. Polarons, bipolarons and solitons in conducting polymers. *Acc Chem Res* 1985;18:309–15.
- [23] Chiang CK, Fincher Jr CB, Park YW, Heeger AJ, Shirakawa H, Louis EJ, et al. Electrical conductivity in doped polyacetylene. *Phys Rev Lett* 1977;39:1098–101.
- [24] Jiang Q, Yan H, Khaliq J, Ning H, Grasso S, Simpson K, et al. Large ZT enhancement in hot forged nanostructured p-type Bi_{0.5}Sb_{1.5}Te₃ bulk alloys. *J Mater Chem A* 2014;2:5785–90.
- [25] Basescu N, Liu ZX, Moses D, Heeger AJ. High electrical conductivity in doped polyacetylene. *Nature* 1987;327:403–5.
- [26] Zuzok R, Kaiser AB, Pukachi W, Roth S. Thermoelectric power and conductivity of iodine-doped “new” polyacetylene. *J Chem Phys* 1991;95:1270–5.

- [27] Yoon CO, Na BC, Park YW. Thermoelectric power and conductivity of the stretch-oriented polyacetylene film doped with MoCl₅. *Synth Met* 1991;41:125–8.
- [28] Park YW, Yoon CO, Na BC. Metallic properties of transition metal halides doped poly-acetylene: the soliton liquid state. *Synth Met* 1991;41:27–32.
- [29] Kaneko H, Ishiguro T. Magneto-resistance and thermoelectric power studies of metal-nonmetal transition in iodine-doped polyacetylene. *Synth Met* 1993;57:4900–5.
- [30] Pukachi W, Plocharski J, Roth S. Anisotropy of thermoelectric power of stretch-oriented new polyacetylene. *Synth Met* 1994;62:253–6.
- [31] Zotti G, Schiavon G, Zecchin S, Morin JF, Leclerc M. Electrochemical, conductive, and magnetic properties of 2,7-Carbazole-based conjugated polymers. *Macromolecules* 2002;35:2122–8.
- [32] Levesque I, Gao X, Klug DD, Tse JS, Ratcliffe CI, Leclerc M. Highly soluble poly(2,7-carbazolenevinylene) for thermoelectrical applications: From theory to experiment. *React Funct Polym* 2005;65:23–36.
- [33] Levesque I, Bertrand PO, Blouin N, Leclerc M, Zecchin S, Zotti G, et al. Synthesis and thermoelectric properties of polycarbazole, polyindolocarbazole, and polydiindolocarbazole derivatives. *Chem Mater* 2007;19:2128–38.
- [34] Wakim S, Aich BR, Tao Y, Leclerc M. Charge transport, photovoltaic, and thermoelectric properties of poly(2,7-carbazole) and poly(indolo[3,2-b]carbazole) derivatives. *Polym Rev* 2008;48:432–62.
- [35] Aich RB, Blouin N, Bouchard A, Leclerc M. Electrical and thermoelectric properties of poly(2,7-carbazole) derivatives. *Chem Mater* 2009;21:751–7.
- [36] Wang LX, Li XG, Yang YL. Preparation, properties and applications of polypyrroles. *React Funct Polym* 2001;47:125–39.
- [37] Jha P, Koiry SP, Saxena V, Veerender P, Chauhan AK, Aswal DK, et al. Growth of free-standing polypyrrole nanosheets at air/liquid interface using J-aggregate of porphyrin derivative as in-situ template. *Macromolecules* 2011;44:4583–5.
- [38] Qi G, Huang L, Wang H. Highly conductive free standing polypyrrole films prepared by freezing interfacial polymerization. *Chem Commun* 2012;48:8246–8.
- [39] Singh A, Salmi Z, Joshi N, Jha P, Kumar A, Lecoq H, et al. Photo-induced synthesis of polypyrrole-silver nanocomposite films on n-(3-trimethoxysilylpropyl)pyrrole-modified biaxially oriented polyethylene terephthalate flexible substrates. *RSC Adv* 2013;3:5506–23.
- [40] Bender K, Gogu E, Hennig I, Schweitzer D. Electric conductivity and thermoelectric power of various polypyrroles. *Synth Met* 1987;18:85–8.
- [41] Maddison DS, Unsworth J, Roberts RB. Electrical conductivity and thermoelectric power of polypyrrole with different doping levels. *Synth Met* 1988;26:99–108.
- [42] Maddison DS, Roberts RB, Unsworth J. Thermoelectric power of polypyrrole. *Synth Met* 1989;33:281–7.
- [43] Lee WP, Park YW, Choi YS. Metallic electrical transport of PF₆⁻-doped polypyrrole: DC conductivity and thermoelectric power. *Synth Met* 1997;84:841–2.
- [44] Wu J, Sun Y, Pei WB, Huang L, Xu W, Zhang Q. Polypyrrole nanotube film for flexible thermoelectric application. *Synth Met* 2014;196:173–7.
- [45] Culebras M, Uriol B, Gomez CM, Cantarero A. Controlling the thermoelectric properties of polymers: application to PEDOT and polypyrrole. *Phys Chem Chem Phys* 2015;17:15140–5.
- [46] Wang J, Cai K, Shen S, Yin J. Preparation and thermoelectric properties of multi-walled carbonnanotubes/polypyrrole composites. *Synth Met* 2014;195:132–6.
- [47] Zhang Z, Chen G, Wang H, Zhai W. Enhanced thermoelectric property by the construction of a nanocomposite 3d interconnected architecture consisting of graphene nanolayers sandwiched by polypyrrole nanowires. *J Mater Chem C* 2015;3:1649–54.
- [48] He M, Ge J, Lin Z, Feng X, Wang X, Lu H, et al. Thermopower enhancement in conducting polymer nanocomposites via carrier energy scattering at the organic–inorganic semiconductor interface. *Energy Environ Sci* 2012;5:8351–8.
- [49] Endrői B, Mellár J, Gingl Z, Visy C, Janaky C. Molecular and supramolecular parameters dictating the thermoelectric performance of conducting polymers: a case study using poly(3-alkylthiophene). *J Phys Chem C* 2015;119:8472–9.
- [50] Xuan Y, Liu X, Desbief S, Leclerc P, Fahlman M, Lazzaroni R, et al. Thermoelectric properties of conducting polymers: the case of poly(3-hexylthiophene). *Phys Rev B* 2010;82:115454–9.
- [51] Zhang Q, Sun Y, Xu W, Zhu D. Thermoelectric energy from flexible P3HT films doped with a ferric salt of triflimide anions. *Energy Environ Sci* 2012;5:9639–44.
- [52] Bounioux C, Pablo DC, Mariano CQ, Marisol SM-G, Goni AR, Rachel YR, et al. Thermoelectric composites of poly(3-hexylthiophene) and carbon nanotubes with a large power factor. *Energy Environ Sci* 2013;6:918–25.
- [53] Lee W, Hong CT, Kwon OH, Yoo Y, Kang YH, Lee JY, et al. Enhanced thermoelectric performance of bar-coated SWCNT/P3HT thin films. *ACS Appl Mater Interfaces* 2015;7:6550–6.
- [54] Endrői B, Mellár J, Gingl Z, Visya C, Janaky C. Reasons behind the improved thermoelectric properties of poly(3-hexylthiophene) nanofiber networks. *RSC Adv* 2014;4:55328–33.
- [55] Xu L, Liu Y, Chen B, Zhao C, Lu K. Enhancement in thermoelectric properties using a p-type and n-type thin-film device structure. *Polym Compos* 2013;34:1728–34.
- [56] Wang D, Su Y, Chen D, Wang L, Xiang X, Zhu D. Preparation and characterization of poly(3-octylthiophene)/carbon fiber thermoelectric composite materials. *Composites Part B* 2015;69:467–71.
- [57] Abad B, Alda I, Pablo D-C, Kawakami H, Almarza A, Amantia A, et al. Improved power factor of polyaniline nanocomposites with exfoliated graphene nanoplatelets (GNPs). *J Mater Chem A* 2013;1:10450–7.
- [58] Yan H, Sada N, Toshima N. Thermal transporting properties of electrically conductive polyaniline films as organic thermoelectric materials. *J Therm Anal Calorim* 2002;69:881–7.
- [59] Toshima N, Jiravanichanun N, Marutani H. Organic thermoelectric materials composed of conducting polymers and metal nanoparticles. *J Electron Mater* 2012;41:1735–42.
- [60] Khalid M, Tumelero MA, Brandt IS, Zoldan VC, Acuna JJS, Pasa AA. Electrical conductivity studies of polyaniline nanotubes doped with different sulfonic acids. *Indian J Mater Sci* 2013. <https://doi.org/10.1155/2013/718304>.
- [61] Nath C, Kumar A, Kuo Y-K, Okram GS. High thermoelectric figure of merit in nanocrystalline polyaniline at low temperatures. *Appl Phys Lett* 2014;105:133108–5.
- [62] Park YW, Lee YS, Park C, Shacklette LW, Baughman RH. Thermopower and conductivity of metallic polyaniline. *Solid State Commun* 1987;63:1063–6.
- [63] Park YW, Moon JS, Bak MK, Jin J-I. Electrical properties of polyaniline and substituted polyaniline derivatives. *Synth Met* 1989;29:389–94.
- [64] Dalas E, Sakkopoulos S, Vitoratos E. Chemical preparation, direct-current conductivity and thermopower of polyaniline and polypyrrole composites. *J Mater Sci* 1994;29:4131–3.
- [65] Kim JY, Kwon MH, Min YK, Kwon S, Ihm DW. Self-assembly and crystalline growth of poly(3,4-ethylenedioxythiophene) nanofilms. *Adv Mater* 2007;19:3501–6.
- [66] Xia Y, Sun K, Ouyang J. Solution-processed metallic conducting polymer films as transparent electrode of optoelectronic devices. *Adv Mater* 2012;24:2436–40.
- [67] Kim N, Kee S, Lee SH, Lee BH, Kahng YH, Jo YR, et al. Highly conductive PEDOT:PSS nanofibrils induced by solution-processed crystallization. *Adv Mater* 2014;26:2268–72.
- [68] Cho B, Park KS, Baek J, Oh HS, Lee Y-EK, Sung MM. Single crystal poly(3,4-ethylenedioxythiophene) nanowires with ultrahigh conductivity. *Nano Lett* 2014;4:3321–7.
- [69] Culebras M, Gomez CM, Cantarero A. Enhanced thermoelectric performance of PEDOT with different counter-ions optimized by chemical reduction. *J Mater Chem A* 2014;2:10109–15.
- [70] Scholdt M, Do H, Lang J, Gall A, Colsmann A, Lemmer U, et al. Organic semiconductors for thermoelectric applications. *J Electron Mater* 2010;39:1589–92.

- [71] Bubnova O, Khan ZU, Malti A, Braun S, Fahlman M, Berggren M, et al. Optimization of the thermoelectric figure of merit in the conducting polymer poly(3,4-ethylenedioxythiophene). *Nat Mater* 2011;10:429–33.
- [72] Kim G-H, Shao L, Zhang K, Pipe KP. Engineered doping of organic semiconductors for enhanced thermoelectric efficiency. *Nat Mater* 2013;12:719–23.
- [73] Yang E, Kim J, Jung BJ, Kwak J. Enhanced thermoelectric properties of sorbitol-mixed PEDOT:PSS thin films by chemical reduction. *J Mater Sci Mater Electron* 2015;26:2838–43.
- [74] Zhu Z, Liu C, Shi H, Jiang Q, Xu J, Jiang F, et al. An effective approach to enhanced thermoelectric properties of pedot:pss films by a DES post-treatment. *J Polym Sci Pol Phys* 2015;53:885–92.
- [75] Mengistie DA, Chen C-H, Boopathi KM, Pranoto FW, Li L-J, Chu C-W. Enhanced thermoelectric performance of PEDOT:PSS flexible bulky papers by treatment with secondary dopants. *ACS Appl Mater Interfaces* 2015;7:94–100.
- [76] Wang J, Cai K, Shen S. A facile chemical reduction approach for effectively tuning thermoelectric properties of PEDOT films. *Org Electron* 2015;17:151–8.
- [77] Kim D, Kim Y, Choi K, Grunlan JC, Yu C. Improved thermoelectric behaviour of nanotube-filled polymer composites with poly(3,4-ethylenedioxythiophene) poly(styrenesulfonate). *ACS Nano* 2010;4:513–23.
- [78] Li F, Cai K, Shen S, Chen S. Preparation and thermoelectric properties of reduced graphene oxide/PEDOT:PSS composite films. *Synth Met* 2014;197:58–61.
- [79] Xu K, Chen G, Qiu D. In situ chemical oxidative polymerization preparation of poly(3,4-ethylenedioxythiophene)/graphene nanocomposites with enhanced thermoelectric performance. *Chem Asian J* 2015;10:1225–31.
- [80] Zhang K, Zhang Y, Wang S. Enhancing thermoelectric properties of organic composites through hierarchical nanostructures. *Sci Rep* 2013;3: 3448-7.
- [81] Jiang Q, Liu C, Xu J, Lu B, Song H, Shi H, et al. An effective substrate for the enhancement of thermoelectric properties in PEDOT:PSS. *J Polym Sci Pol Phys* 2014;52:737–42.
- [82] Zhang B, Sun J, Katz HE, Fang F, Opila RL. Promising thermoelectric properties of commercial PEDOT:PSS materials and their Bi₂Te₃ powder composites. *ACS Appl Mater Interfaces* 2010;2:3170–8.
- [83] See KC, Feser JP, Chen CE, Majumdar A, Urban JJ, Segalman RA. Water-processable polymer-nanocrystal hybrids for thermoelectrics. *Nano Lett* 2010;10:4664–7.
- [84] Zheng W, Bi P, Kang H, Wei W, Liu F, Shi J, et al. Low thermal conductivity and high thermoelectric figure of merit in p-type Sb₂Te₃/Poly(3,4-ethylenedioxythiophene) thermoelectric composites. *Appl Phys Lett* 2014;105:023901–23904.
- [85] Jiang Q, Liu C, Song H, Xu J, Mo D, Shi H, et al. Free-standing PEDOT:PSS film as electrode for the electrodeposition of bismuth telluride and its thermoelectric performance. *Int J Electrochem Sci* 2014;9:7540–51.
- [86] Kaiser AB. Systematic conductivity behaviour in conducting polymers: effects of heterogeneous disorder. *Adv Mater* 2001;13:927–41.
- [87] Kamarudin MA, Sahamir SR, Datta RS, Long BD, Sabri MFM, Said SM. A review on the fabrication of polymer-based thermoelectric materials and fabrication methods. *Sci World J* 2013. <https://doi.org/10.1155/2013/713640-56>.
- [88] Hiroshige Y, Ookawa M, Toshima N. High thermoelectric performance of poly(2,5-dimethoxyphenylenevinylene) and its derivatives. *Synth Met* 2006;156:1341–7.
- [89] Wusten J, Karin PK. Organic thermogenerators for energy autarkic systems on flexible substrates. *J Phys D Appl Phys* 2008;41:135113–20.
- [90] Yang Y, Lin ZH, Hou T, Zhang F, Wang ZL. Nanowire-composite based flexible thermoelectric nanogenerators and self-powered temperature sensors. *Nano Res* 2012;5:888–95.
- [91] Sun Y, Sheng P, Di C, Jiao F, Xu W, Qiu D, et al. Organic thermoelectric materials and devices based on p- and n-type poly(metal 1,1,2,2-ethenetetrathiolate)s. *Adv Mater* 2012;24:932–7.
- [92] Søndergaard RR, Hosel M, Espinosa N, Jorgensen M, Krebs FC. Practical evaluation of organic polymer thermoelectrics by large-area R2R processing on flexible substrates. *Energy Sci Eng* 2013;1:81–8.
- [93] Park T, Park C, Kim B, Shin H, Kim E. Flexible PEDOT electrodes with large thermoelectric power factors to generate electricity by the touch of fingertips. *Energy Environ Sci* 2013;6:788–92.
- [94] Wei Q, Mukaida M, Kirihara K, Naitoh Y, Ishida T. Polymer thermoelectric modules screen-printed on paper. *RSC Adv* 2014;4:28802–6.
- [95] Jiao F, Di C, Sun Y, Sheng P, Xu W, Zhu D. Inkjet-printed flexible organic thin-film thermoelectric devices based on p- and n-type poly(metal1,1,2,2-ethenetetrathiolate)s/polymer composites through ball-milling. *Philos Trans R Soc A* 2013;372:1–8.
- [96] We JH, Kim SJ, Cho BJ. Hybrid composite of screen-printed inorganic thermoelectric film and organic conducting polymer for flexible thermoelectric power generator. *Energy* 2014;73:506–12.
- [97] Du Y, Cai K, Chen S, Wang H, Shen SZ, Donelson R, et al. Thermoelectric fabrics: toward power generating clothing. *Sci Rep* 2015;5:6411–6.
- [98] Dun C, Hewitt CA, Huang H, Xu J, Zhou C, Huang W, et al. Flexible n-type thermoelectric films based on Cu-doped Bi₂Se₃ nanoplate and polyvinylidene fluoride composite with decoupled seebeck coefficient and electrical conductivity. *Nano Energy* 2015;18:306–14.
- [99] Dun C, Hewitt CA, Huang H, Montgomery DS, Xua J, Carroll DL. Flexible thermoelectric fabrics based on self-assembled tellurium nanorods with a large power factor. *Phys Chem Chem Phys* 2015;17:8591–5.
- [100] Press release XIX/2015, n-Type conductive polymers as electrical conductor of future printed electronics, <<http://www.iws.fraunhofer.de/en.htm>> and <http://www.iws.fraunhofer.de/en/pressandmedia/press_releases.html>.
- [101] Kirihara K, Wei Q, Mukaida M, Ishida T. Thermoelectric power generation using nonwoven fabric module impregnated with conducting polymer PEDOT:PSS. *Synth Met* 2017. <https://doi.org/10.1016/j.synthmet.2017.01.001>.
- [102] Song H, Cai K. Preparation and properties of PEDOT:PSS/Te nanorod composite films for flexible thermoelectric power generator. *Energy* 2017. <https://doi.org/10.1016/j.energy.2017.01.037>.
- [103] Bae EJ, Kang YH, Jang K-S, Cho SY. Enhancement of thermoelectric properties of PEDOT:PSS and Tellurium-PEDOT:PSS hybrid composites by simple chemical treatment. *Sci Rep* 2016;6:18805–14.
- [104] Lipomi DJ, Lee JA, Vosgueritchian M, Tee BC-K, Bolander JA, Bao Z. Electronic properties of transparent conductive films of PEDOT:PSS on stretchable substrates. *Chem Mater* 2012;24:373–82.
- [105] Petsagkourakis I, Pavlopoulou E, Portale G, Kuropatwa BA, Dilhaire S, Fleury G, et al. Structurally-driven enhancement of thermoelectric properties within poly(3,4-ethylenedioxythiophene) thin films. *Sci Rep* 2016;6:30501–8.
- [106] Skotheim T, Elsenbaumer R, Reynolds J. *Handbook of conducting polymers*. 2nd ed. New York (NY, USA): Marcel Dekker Inc; 1998.
- [107] Lee K, Cho S, Park SH, Heeger AJ, Lee C-W, Lee S-H. Metallic transport in polyaniline. *Nature* 2006;441:65–8.
- [108] Crossland EJ, Tremel K, Fischer F, Rahimi K, Reiter G, Steiner U, et al. Anisotropic charge transport in spherulitic poly(3-hexylthiophene) films. *Adv Mater* 2012;24:839–44.
- [109] McCulloch I, Heeney M, Bailey C, Genevicius K, Macdonald I, Shkunov M, et al. Liquid-crystalline semiconducting polymers with high charge-carrier mobility. *Nat Mater* 2006;5:328–33.
- [110] Noriega R, Rivnay J, Vandewal K, Koch FP, Stingelin N, Smith P, et al. A general relationship between disorder, aggregation and charge transport in conjugated polymers. *Nat Mater* 2013;12:1038–44.
- [111] Gueye MN, Carella A, Massonnet N, Yvenou E, Brenet S, Faure-Vincent J, et al. Structure and dopant engineering in PEDOT thin films: practical tools for a dramatic conductivity enhancement. *Chem Mater* 2016;28:3462–8.
- [112] Wang Q, Yao Q, Chang J, Chen L. Enhanced thermoelectric properties of CNT/PANI composite nanofibers by highly orienting the arrangement of polymer chains. *J Mater Chem* 2012;22:17612–8.
- [113] Lee HJ, Anoop G, Lee HJ, Kim C, Park J-W, Choi J, et al. Enhanced thermoelectric performance of PEDOT:PSS/PANI-CSA polymer multilayer structures. *Energy Environ Sci* 2016;9:2806–11.
- [114] McGrail BT, Sehirlioglu A, Pentzer E. Polymer composites for thermoelectric applications. *Angew Chem Int Ed* 2014;53:2–16.